

Simen Bjerkemyr Magnussen

NTNU
Norwegian University of
Science and Technology
Faculty of Engineering
Department of Civil and Environmental Engineering

Simen Bjerkemyr Magnussen

Rate effects in Halden silt

June 2020



Norwegian University of
Science and Technology

Rate effects in Halden silt

Simen Bjerkemyr Magnussen

Geotechnics and Geohazards

Submission date: June 2020

Supervisor: Steinar Nordal

Co-supervisor: Ana Priscilla Paniagua López

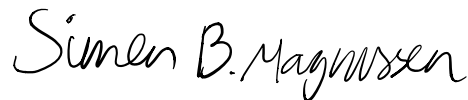
Norwegian University of Science and Technology
Department of Civil and Environmental Engineering

Preface

This master thesis in geotechnics is written in the course TBA 4900 - Geotechnical Engineering, Master Thesis which is part of the MSc Geotechnics and Geohazards program at NTNU. The thesis is carried out during the spring semester of 2020, and is executed in cooperation with NGI-Norwegian Geotechnical Institute. Before this thesis could get started, I had to learn my way around the labs and how the triaxial apparatus worked. I had to start from scratch and learn all the practical parts of running a triaxial test by experimenting with dummy samples over a few weeks with help from the geotechnical staff, in addition to how to process the data.

This thesis was originally planned with lab experiments and interpretation only. However, due to the fact that the university had to close down due to recent events, some changes had to be made. I was unfortunately unable to finish all the tests in the laboratory, which lead to the investigation of rate effects in the CPTU soundings from the same test site where the block samples were retrieved. A total of 7 tests were ran over the fall- and spring semester, when the total tests was originally planned to be 9. CPTU interpretations were conducted instead, an the goal here is to compare results obtained in the laboratory with field tests from Halden, and investigate the rate effects from the CPTU soundings. The CPTU data were provided by my supervisor from NGI.

Trondheim, June 2020

A handwritten signature in black ink that reads "Simen B. Magnussen". The script is cursive and fluid, with the first letters of each word being capitalized and prominent.

Simen Bjerkemyr Magnussen

Acknowledgment

I would like to thank Professor Steinar Nordal at NTNU for overseeing this thesis. I am very thankful for my supervisor Dr. Ana Priscilla Paniagua Lopez at NGI for her encouragement, guidance and patience during the writing of this thesis. A special thanks to Karl Ivar Volden Kvisvik for being patient when he showed me how to use the lab equipment in the early stages of this thesis.

S.B.M

Summary

The Halden test site has been used for different geotechnical purposes in silt. Here, CPTU soundings and extraction of high quality block samples have been performed. This thesis aims to investigate the effects of different rates during testing in the laboratory and in the field. Previous research shows that silty materials often result in different results with regards to undrained shear strength by varying the rate, which is why the silt from this test site is investigated. The drainage conditions in the selected focus intervals were also examined. Usually, the drainage conditions change when the rate is increased or decreased.

Seven triaxial tests were performed at three different rates, in addition to five CPTU soundings. Three different methods for evaluating the undrained shear strength for the triaxial tests were carried out, which lead to the decision of using one combined with one of the other for a more fitting determination of the strength. The triaxial tests showed little significant rate effects in the silt, which were confirmed with the results from the CPTU estimates as well.

The CPTU soundings showed the same response. No clear trend in the undrained shear strength at the chosen interval. However, the depth interval for the CPTU soundings might have been influenced by a coarser layer just above.

However, all the tests measured in the field occurred under partial drainage conditions, even at the highest rates. Usually, high penetration rate with CPTU results in drained conditions, standard rate results in partial drainage and slow rates results in undrained conditions. The resulting undrained shear strength becomes more complicated due to the partial drainage, and the results should be evaluated more carefully.

Sammendrag

Testområdet i Halden har blitt brukt til flere forskjellige geotekniske undersøkelser i silt. CPTU sonderinger og prøvetaking av blokkprøver av høy kvalitet har blitt utført på området. Denne masteroppgaven ser nærmere på effekten av hastighet på tester i felt og i laboratoriet som brukes for å estimere den udrenerte skjærstyrken. Tidligere forskning tilsier at effekt av hastighet påvirker resultatet i siltmaterialer. Dreneringsforholdene i området blir også undersøkt. Vanligvis vil dreneringsforholdene endre seg ved høyere eller lavere hastighet, men dette var ikke tilfellet.

Totalt syv treaksialforsøk ble utført med tre forskjellige hastigheter, i tillegg til tolkning av fem CPTUer med forskjellige hastigheter. Tre forskjellige metoder for å estimere den udrenerte skjærstyrken, som førte til beslutningen av å benytte en metode kombinert med annen for å få best mulig resultat. Treaksialforsøkene var lite påvirket av de forskjellige hastighetene, som tilsier at det ikke er en effekt av hastighet i Halden silten. Dette ble bekreftet av estimatene fra CPTU sonderingene.

CPTU sonderingene viste den samme responsen. Det var ingen tydelig trend for den udrenerte skjærstyrken over de forskjellige hastighetene. Intervallet som ble valgt for tolkning av CPTU kan ha blitt påvirket av laget over silten, som er av et grovere materiale.

Videre så viste det seg at dreneringsforholdet der CPTU og treaksialforsøkene ble utført var delvis drenering, selv ved de hurtigste hastighetene. Vanligvis fører høy hastighet til drenerte forhold, standard hastighet til delvis drenering og lav hastighet til udrenerte forhold. Dette var ikke tilfellet for noen av de undersøkte hastighetene i denne oppgaven. Delvis drenering fører til en mer komplisert tolkning av den udrenerte skjærstyrken, og resultatene bør derfor evalueres med stor forsiktighet.

Contents

Preface	i
Acknowledgment	iii
Summary	v
Sammendrag	vii
1 Introduction	1
1.1 Background	1
1.2 The Test Site	2
1.3 Previous Study	2
1.4 Problem Formulation	3
1.5 Objectives	4
1.6 Limitations	4
1.7 Structure of the Report	5
2 Literature Review	6
2.1 Block Samples	6
2.1.1 Sampling Methods	6
2.1.2 Water Content in Block Samples	8
2.2 Sample Disturbance	8
2.3 Triaxial Testing	9
2.3.1 Back Pressure	10
2.3.2 Triaxial Test Parameters	11
2.3.3 Standards and Guidelines	11
2.4 CPTU Field Testing	11
2.4.1 CPTU Parameters	12

2.5	Undrained Shear Strength	14
2.5.1	Undrained Shear Strength in Triaxial Testing	14
2.5.2	Undrained Shear Strength in CPTU Sounding	19
2.6	Rate Effects in CPTU Soundings	20
2.7	Carbon Dating of Shell Fragment	21
3	Laboratory Testing	22
3.1	The Test Material	22
3.2	The Block Sample	24
3.2.1	Inspection of the Block Sample	24
3.2.2	Cutting the Block Sample	25
3.2.3	Trimming the Block Sample	27
3.3	The Triaxial Apparatus	28
3.3.1	Preparing the Triaxial Apparatus	28
3.3.2	Building the Sample into the Triaxial Apparatus	28
3.3.3	Final Preparations of the Triaxial Apparatus	30
3.4	Start of Test	31
3.4.1	Saturation of the Sample	31
3.4.2	B-value Check	31
3.5	Consolidation of Sample	31
3.6	Shearing of Sample	32
3.7	Test Plan	34
4	Processing the Test Data	36
4.1	Triaxial Test Data Processing	36
4.2	Data from the Field	37
4.2.1	Establishing Necessary Parameters	37
4.2.2	Processing Data from CPTU Tests	39
5	Results	42
5.1	Triaxial Tests	42
5.2	CPTU Soundings	44
5.2.1	Rate Effects in CPTU Soundings	47
5.3	Results from Water Content Measurements	49

5.4	Result from Carbon Dating of Shell Fragment	50
6	Discussion	51
6.1	Sample Quality	51
6.2	Water Content	51
6.3	Triaxial Tests	52
6.3.1	Methods of Interpreting the Undrained Shear Strength	52
6.3.2	Friction Angle	53
6.3.3	Rate Effects in Triaxial Tests	53
6.4	CPTU Soundings	53
6.4.1	CPTU with Triaxial Results	53
6.4.2	Rate Effects in CPTU Soundings	53
7	Conclusion and Further Work	55
7.1	Conclusions	55
7.2	Recommendations for Further Work	57
	Bibliography	58
A	Report-Carbon Dating of Shell	61
B	Triaxial Results	63
C	CPTU Soundings with Triaxial Results Included	70
D	Drainage Conditions at Depth Interval 5.2-5.6 meters	86
E	Drainage Conditions for Focus Interval 14.5-15.5 meters	89
F	Acronyms	97

List of Figures

1.1	Location of the Halden test site in Norway	2
2.1	Sherbrooke block sampler. Borrowed from [1]	7
2.2	Conventional setup of a triaxial apparatus. Borrowed from [2]	10
2.3	CPTU probe principle. Borrowed from [3].	12
2.4	Soil classification charts. Borrowed from [4].	14
2.5	Different ways of interpreting S_u . Borrowed from [5].	15
2.6	p',q -plot example, from test sample S1B	18
2.7	S, t -plot example, from test sample S1B	19
3.1	Grain size distribution. Borrowed from [6]	23
3.2	Soil classification after [4]. Borrowed from [6]	23
3.3	The block sample used in the tests	25
3.4	The block sample after trimming at the top	26
3.5	Piece cut out from the block	27
3.6	Sample after trimming on the sides	27
3.7	The sample prepared for testing	30
3.8	The sample after complete shearing	33
4.1	In situ stress conditions (u_0, σ_{v0}).	39
4.2	CPTU interpretation, from test HALC01	40
4.3	Drainage conditions in HALC13 at 14.5-15.5 meters.	41
5.1	The different plots, here from S1B.	43
5.2	Location of CPTU soundings with the interval 14.5-15.5 meters.	44
5.3	S_u plotted with depth, and the triaxial results at U_{max} is added.	45

5.4 S_u plotted with depth, and the triaxial results at 4% strain (left) and $\bar{A} = 0$ (right) is added. . . 46

5.5 Drainage conditions in the focus interval at 14.5-15.5m. Figure after [7]. 47

5.6 Rate vs. corrected tip resistance. 48

5.7 Corresponding pore pressure. 48

5.8 Trend line for rate vs. corrected tip resistance. 48

5.9 Corresponding trend line for the pore pressure. 48

5.10 Drainage conditions in the focus interval at 5.2-5.6m for HALC07 with 2.2 mm/s rate. Figure
after [7]. 48

5.11 Average S_u plotted for each rate. 49

5.12 Corresponding trend line for the S_u 49

List of Tables

- 1.1 Different rates used in the laboratory 3

- 3.1 Test plan for triaxial testing 34

- 5.1 Results from triaxial testing 42
- 5.2 Results from triaxial testing in [6] 43
- 5.3 Results from interpretation of rate effects from CPTU soundings at depth interval 5.2-5.6
meter. 47
- 5.4 Results from water content measurements 49
- 5.5 Results from water content measurements in [6]. 49

Chapter 1

Introduction

1.1 Background

In Halden, Norway there is a geotechnical test site which is used for silt measurements in situ and sample collecting. The test site is one of five national test sites in the NGTS-project (Norwegian Geo Test Sites). Each test site focus on different materials, ranging from silt, sand, soft clay, quick clay and permafrost. These test sites are meant to provide valuable information for public authorities, industries and research organizations. The Halden test site is located in the southeast of Norway, close to the Swedish boarder and approximately 120km south of Oslo seen in Figure 1.1. There has been performed several different in situ tests on this site (CPTU, SCPT, RCPTU, SDMT and other tests) [6]. Samples has also been collected using various samplers. In this thesis, the block samples HALB05 and HALB04 collected at 14.8-15.15m and 15.15-15.5m depth respectively will be investigated in the lab. Triaxial tests will be performed to investigate the effect of load applied at different rates. Further, the results from the laboratory will be compared to the tests conducted in the field (CPTU). The reason to carry out this thesis is that the silt is a genuinely difficult material to evaluate, especially for very low plasticity to non-plastic silt. In addition to this, there is no permanent framework to evaluate the sample quality. The samples of intermediate soils of high quality is often troublesome to obtain. Furthermore, there is quite little information regarding the topic of selecting the fitting engineering properties for practical use.

1.2 The Test Site

As of 2011, the test site in Halden has been used for different geotechnical purposes. The site contains layers of sand, clayey silt and clay. In this report, only the silt is to be investigated. The test site is located in the western part of the city Halden. As of now, the site is a public park owned by the municipality located close to a residential area. The total area of the site is about 6000 m² and the topography is mainly flat varying between +27 and +34 m.a.s.l from southwest to northeast [8]. As seen in Figure 1.1 there is adequate vegetation in the area. Right next to the site to the north and west, a ridge ascends up to about +55 meters. On the other side, to the east, another ridge rises up varying between +35 to +44 m.a.s.l [8]. This will lead the precipitation down towards the test site and influence the ground conditions to a certain amount.



Figure 1.1: Location of the Halden test site in Norway

1.3 Previous Study

A project was carried out in the fall semester of 2019 in the course TBA4510-Geotechnical engineering, specialization project. The goal with this project was to investigate the rate effect in the triaxial apparatus only, and a total of four tests were conducted. The rates 1.5%/hour and 15%/hour were used in the tests. The undrained shear strength ended up being in the expected range for the material, when comparing

the results with [6]. However, not enough tests were conducted to conclude if there are rate effects in the material at the test site.

1.4 Problem Formulation

This thesis aims to investigate the effect of different loading rates on the silt material during CPTU testing and in the obtained block samples from Halden, Norway in triaxial tests. The rates used in the triaxial apparatus in this thesis is set to 0.15%, 1.5% and 15% [9]. The rate is found by choosing a percentage which according to [10] is within acceptable range, and dividing this percentage by 60 minutes. The results from using 0.15%, 1.5% and 15% is shown in Table 1.1 below. 15% is a rather extreme value, and will shear the sample in a short amount of time. The reason for choosing such a high value is to determine if a rate of this magnitude will influence the resulting undrained shear strength.

Rate	Velocity [mm/min]
0.15%	0.0025
1.5%	0.025
15%	0.25

Table 1.1: Different rates used in the laboratory

Four samples have been tested prior to this thesis in the course TBA4510-Geotechnical specialization project. This project was a feasibility study to investigate if this subject is worth studying further. The main focus here was to investigate the rate effect in the triaxial apparatus only, which is why some of the tests had to be performed earlier. Only two rates with two samples each were tested. The rates used in this project were the 1.5% and the 15%.

The samples is being tested with a CIUC-test, which is an Isotropic Consolidated undrained test. This means that the sample is consolidated with axial stress σ_1 equal to the radial stress σ_3 , which is a very reasonable test method for silts.

Further, interpretations of CPTU soundings is conducted. The goal here is to compare and identify if the results are in the same range with regards to S_u . Five different rates are observed in the depth interval 5.2–5.6 meters, and will be treated the same way as the interpretations from the triaxial tests. Recordings treated in Microsoft Excel obtained from NGI containing information about tip resistance (q_c), side friction (f_s) and pore pressure (u_2) with regards to depth is interpreted with the goal to find the parameters q_t (correction of tip resistance for pore pressure effects), B_q (pore pressure ratio) and S_u . Data from the

field and laboratory will be compared, and the goal is to figure out if the data coincides with one another and which ones that gives the closest result. The drainage conditions which occurs in the depths where CPTUs and triaxial tests were performed will be investigated.

1.5 Objectives

The main objectives of this thesis are

1. First and foremost learn how the laboratory equipment work and how to treat a block sample to be able to run tests with the given material.
2. Run triaxial tests on silt sampled from the test site in Halden with different rates during the shearing phase.
3. Investigate the effect of the different rates on the undrained shear strength in the silt material.
4. Review the results critically with comparison to the CPTU's and available published literature and earlier findings in similar cases.

1.6 Limitations

The amount of tested samples was originally planned to be limited to three samples at each rate due to the available time in the laboratory. A number of seven samples was tested in the laboratory before the university were closed due to the recent events. The two tests missing are one at 1.5% and one at 0.15% rate.

The original plan was to run all the samples from the same block collected at 15.15-15.5m. However, the bottom half was quite dry and impossible to get whole samples when cutting. The samples cracked, fell apart and collapsed when touching it with the steel wire. Luckily, there was another block sample which was not taken far from the first block available. The majority of the tests are from the first block, but a few of the is from the other block. This has to be kept in mind when performing tests and comparing results.

Further, the block samples were stored for quite some time. Two years is a long time for a sample to stay in a fridge, and the consequence of this could interfere with the test results.

Also, there was some issues with one of the testing machines. All originally planned tests were conducted,

but the machine did not register the data correctly due to wrong calibration, which lead to incorrect data. Also, the machine would not "lock" correctly. The sample has to be locked when initiating the shear phase. When this procedure was started, the machine did not register contact between the sample and the piston, which lead to compression of the sample. This ruined two of the tests in the early stages of this thesis.

1.7 Structure of the Report

The rest of the report is structured as follows:

Chapter 2 considers the conducted literature review for this thesis.

Chapter 3 gives a description of the tests performed in the laboratory. The approach and execution of the tests is described.

Chapter 4 give a description of the methods used to process the obtained data from the laboratory.

Chapter 5 presents the results from the tests in the laboratory with figures and tables.

Chapter 6 discusses the obtained results. Results from similar previous tests is compared and evaluated.

Chapter 7 gives a final conclusion of the rate effect on the Halden silt, in addition to discuss further work.

Chapter 2

Literature Review

This thesis is an extension to the results from the journal article published by AIMS Geosciences, named *The Halden research site: geotechnical characterization of a post glacial silt* [6]. This article explains the characterization of the test site, sampling methods and contains results from several testing methods from the site. The block samples tested in this thesis are retrieved from the same site, and will be compared to the results from [6].

2.1 Block Samples

The procedure of retrieving undisturbed samples are an important aspect of geotechnical engineering. The information which could be collected from high quality samples in the laboratory is crucial for accurate design values in a project. If the samples are poor, the calculations will be inaccurate. Block samples might be the best sampling method with regards to quality of the samples.

2.1.1 Sampling Methods

There are several methods for collecting samples from the soil. One of the most common methods in Norway is the 54mm tube sampler. In some cases, a 76mm or a 95mm have been applied. However, if the material is highly sensitive, the tube sampler might not work and damage the structure of the material. In these cases, a block sampler could be useful. The Sherbrooke 250mm block sampler have been applied in such cases.

The Sherbrooke block sampler was developed at Sherbrooke university in Quebec, in the period 1975-

1978 [1]. It was originally designed for clays, but have proven effective in silt as well. The sampler cuts out cylindrical-shaped blocks with a 250mm diameter and 350mm in height. The borehole must have a slightly bigger diameter, a minimum of 450mm and filled with water to account for stability issues. First, a flat bottom auger is used to smooth out the bottom of the borehole, before the sampler is lowered down. When the sampler is in position (body of soil inside the sampler), three knives is cutting the sample loose at the bottom of the sampler by slowly closing while rotating. The velocity of the rotation is about 5 a minute. The sampler with the knives in open position can be seen in Figure 2.1. The closing of the knives is provided by springs. This process is continued until the knives are fully closed and the sample are separated from the deposit.

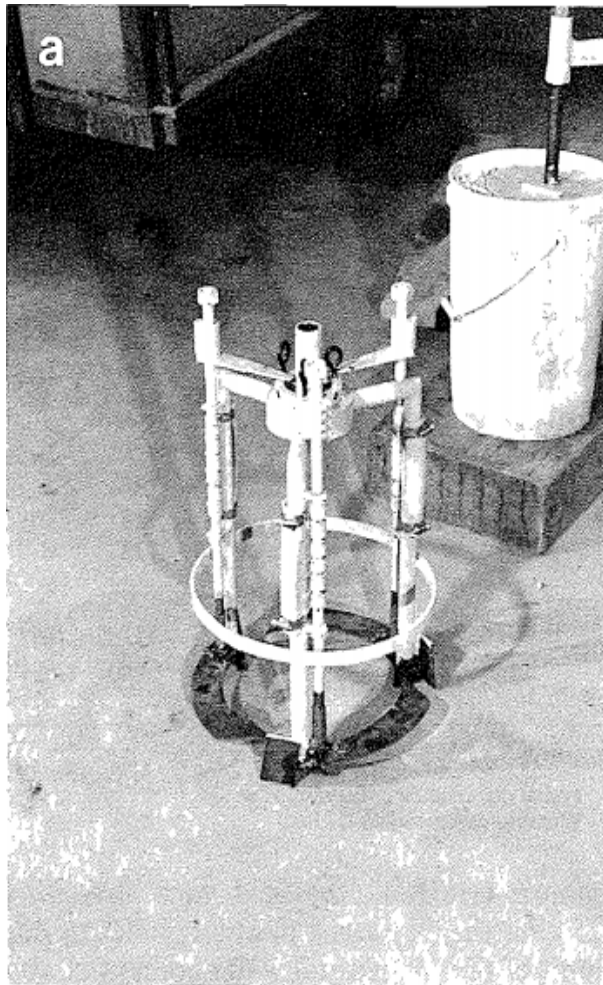


Figure 2.1: Sherbrooke block sampler. Borrowed from [1]

The block sample now rests at the knives while being pulled out of the borehole. Wrapping with plastic wrap and sometimes wax should be done quickly, when the block is placed safe at the surface, to maintain

the natural state of the water content and other characteristics. Further, the block is transported to the lab for storage in a fridge with around 6°C.

2.1.2 Water Content in Block Samples

Water content is a way of describing how much water there is in a material. The water content is an important parameter to investigate in the block, due to the long storage time. This will give a indication of the state of the blocks and if the samples will represent the in situ conditions. Previous measurements are performed in [6], which will be used for comparison.

The water content is found by weighing the material before and after drying. The material used in this thesis will be collected at different elevations within the block samples. The sample is immediately weighted in wet condition, then put into an oven at 105°C for 24 hours. The samples are then weighted after being taken out of the oven, and the water content can be calculated using the following formula from [11]:

$$w = \frac{m_w - m_s}{m_s} * 100\% \quad (2.1)$$

m_w = wet weight of the material minus the weight of the bowl [g]

m_s = dry weight of the material minus the weight of the bowl [g]

2.2 Sample Disturbance

The method for assessing sample quality for clays are based on the change in void ratio (Δe) relative to initial void ratio (e_0) on specimen recompressed to in situ pressure during oedometer or consolidated triaxial tests [12]. However, no framework to assess the sample quality for silt and other intermediate soils (clayey silt, silty clay etc.), as they can be sampled drained, partially drained and undrained depending on sampling rate, soil composition etc [8]. Volume change during sampling may or may not occur and alterations to the soil structure could be difficult to identify [8].

Preparing silt for triaxial testing without significant disturbance is difficult as described by [13];[14]. Disturbance of the sample will influence the measured shear strength and obscure the past consolidation pressure in consolidation tests [5]. Sample quality should always be evaluated when advanced tests is

conducted in the laboratory. If the tests are performed on poor quality samples, it could affect the engineering soil parameters which could lead to unsafe geotechnical design [6]. A visual inspection is performed on each sample. Cracks and dents in the sample is not favorable, and if the damages are to severe, the sample can not be used. However, disturbed samples can be used for something productive. The layering can be investigated, along with water content, grain size distribution and other parameters which does not represent mechanical characteristics.

2.3 Triaxial Testing

The triaxial test is a method which can be used to determine the shear strength on several types of materials, from soft soil to rock. Samples are either tested drained or undrained. Undrained tests are used to obtain the undrained shear strength. The usual setup for soils used in this thesis is a 54mm diameter and 100mm high sample. The sample has to be trimmed to the right dimensions ff the sample is collected as a block. Several samples could be trimmed out of one block, if proper care and planning is carried out.

The sample is subjected to an all-around liquid pressure ($\sigma_1 = \sigma_2 = \sigma_3$), and if applied correctly it will resemble the in situ conditions. Triaxial tests can be divided into two phases; consolidation- and shear phase. When the sample has been consolidated to the point were it was before extraction (same stress values as in the ground), the shear phase is initiated. This will test how far the sample can be loaded until failure occurs. This is done by selecting a rate in mm/min which the triaxial apparatus pushes the sample up into a piston. See Figure 2.2 for a detailed view of a normal setup. The test procedure is explained in more detail in Chapter 3.

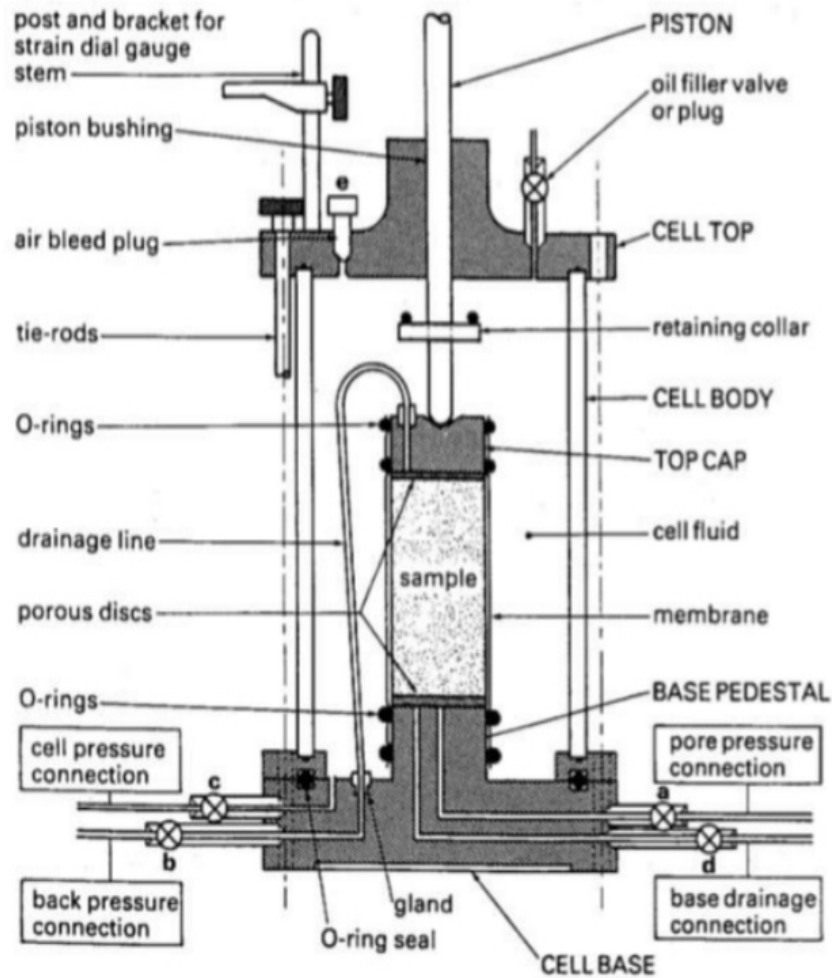


Figure 2.2: Conventional setup of a triaxial apparatus. Borrowed from [2]

2.3.1 Back Pressure

Pockets of air have a tendency to appear in materials like silt and sand. These air pockets do not usually disappear after consolidation of the sample, and can be difficult to get rid of. To control this, the saturation of the sample is controlled using a B-check. The B is one of Skempton's pore pressure parameters, and is explained in the equation from [10]:

$$B = \frac{\Delta U}{\Delta \sigma'_3} \quad (2.2)$$

Where:

ΔU = Change in pore pressure

$\Delta\sigma'_3$ = Change in confining pressure

The B-value should reach 0.95 or greater within one minute after initiation of the B-check before the consolidation could start [10]. Back pressure can be applied if this requirement is not met. The back pressure creates an artificial saturation in the sample. This can be achieved by a parallel or stepwise increase of both the internal pressure in the sample (pore pressure) and the cell pressure. This keeps the effective stresses unchanged.

2.3.2 Triaxial Test Parameters

The triaxial test register several important parameters. Principal stresses ($\sigma_1, \sigma_2, \sigma_3$), effective stresses ($\sigma'_1, \sigma'_2, \sigma'_3$), pore pressure (u) and strain (ϵ). The undrained shear strength can be determined with these parameters, in addition to the friction angle of the material and important plots for further interpretation. The plots relevant for this thesis will be further explained in Chapter 2.5.1.

2.3.3 Standards and Guidelines

The testing conducted in this thesis follows standards and guidelines commonly used for laboratory testing. The Norwegian standard NS-EN ISO 17892-9:2018 [10] is the main document securing the correct way to test the silt samples in the triaxial apparatus. Further, the article published by NGI [9], *Triaxial Testing at the Norwegian Geotechnical Institute* is used in addition to the standard to compliment the testing procedures. The tests in this project will be performed under these conditions, since the journal article published by AIMS Geosciences is based on the procedures from the NGI article in addition to the standard.

2.4 CPTU Field Testing

Undrained cone tests are a way of testing the soil material directly in the field. The method was developed in the Netherlands in the 1950's, and later modified in several countries. The CPTU measures the cone resistance by pushing steel rods with a cone-shaped electronic probe into the ground with a typical

velocity of 20 mm/s. Side friction and pore pressure are usually measured as well. The probe principle can be seen in Figure 2.3:

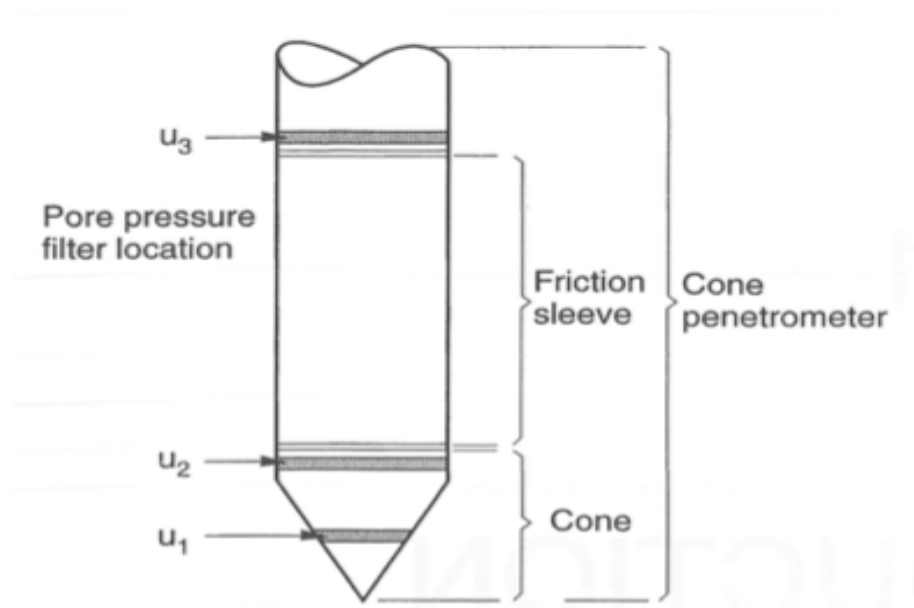


Figure 2.3: CPTU probe principle. Borrowed from [3].

2.4.1 CPTU Parameters

The cone resistance q_c , side friction f_s and pore pressure u_2 are continuously measured. Since there is pore pressure development in the probe while measuring q_c , the q_c has to be corrected [3]. The expression for the corrected cone resistance q_t is:

$$q_t = q_c + (1 - a) * u_2 \quad (2.3)$$

Where:

q_c = cone resistance

a = cone factor

u_2 = measured pore pressure

The pore pressure ratio B_q is also of great importance. This is used for classification of the soil. The original classification chart was developed by Senneset and Janbu in 1985 [15]. However, the most widely used chart is presented by [16]. The chart is based of B_q or friction ratio against q_t . B_q is calculated the

following way:

$$B_q = \frac{u_2 - u_0}{q_t - \sigma_{v0}} \quad (2.4)$$

Where:

u_0 = in situ pore water pressure

q_t = corrected cone resistance

σ_{v0} = in situ vertical overburden pressure

The chart was later modified by [4], and the normalized Q_t and F_r were introduced in order to be able to overcome issues with CPTU soundings in greater depths [17]. The modified equations is listed below:

$$Q_t = \frac{q_t - \sigma_{v0}}{\sigma'_{v0}} \quad (2.5)$$

$$F_r = \frac{f_t}{q_t - \sigma_{v0}} \quad (2.6)$$

Where:

σ'_{v0} = Effective vertical overburden pressure

f_t = corrected sleeve friction

(2.7)

The classification charts can be seen in Figure 2.4:

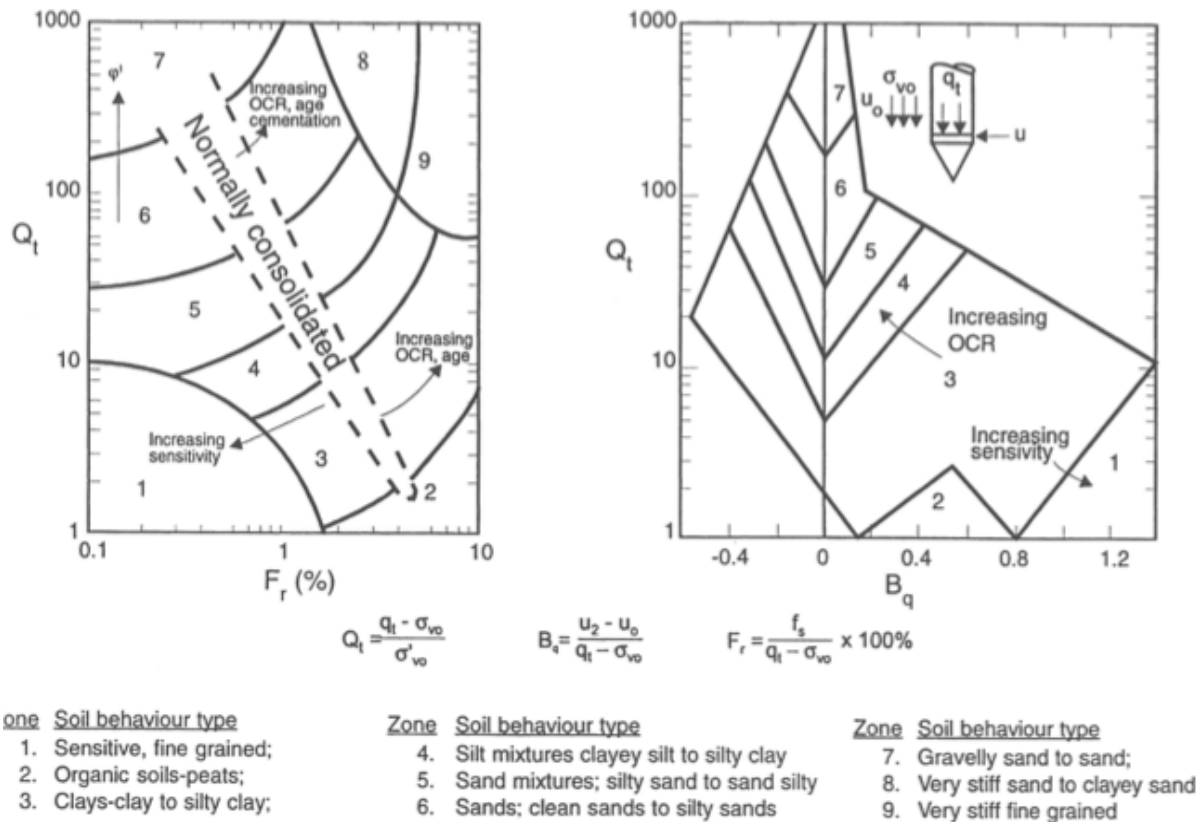


Figure 2.4: Soil classification charts. Borrowed from [4].

2.5 Undrained Shear Strength

The undrained shear strength (S_u) is defined as the maximum shear stress the soil can take, before collapsing. It is very important to estimate the S_u correctly for a project to be successful and sustainable. Since the S_u is rather difficult to determine in a silt material, there has to be applied some care into the process. No standard or guideline exists for interpreting silty materials, but the existing ones on clay can be applied and combined with some care. There are several methods to estimate and calculate the S_u , both in the laboratory and in the field, and the ones relevant for this thesis will be explained in this chapter.

2.5.1 Undrained Shear Strength in Triaxial Testing

Three different methods used in [6] for interpreting the S_u can be found in [5]. The paper explains how to calculate the S_u with six different methods in total, but all of them are not applied in this case. The methods used in [6] are U_{max} (most conservative), Limited strain method (user adjusted) and $\bar{A} = 0$ (close

to failure point). The different methods can be seen in Figure 2.5 which explains where on the stress curve the S_u is interpreted. The Limited strain method is not shown in to the figure, since this is a value which is chosen at a reasonable percentage and will vary. As seen in the figure, the U_{max} method is very conservative, as the effective stresses has not reached the effective stress strength line at the point on the stress path where the pore pressure reaches maximum value [5].

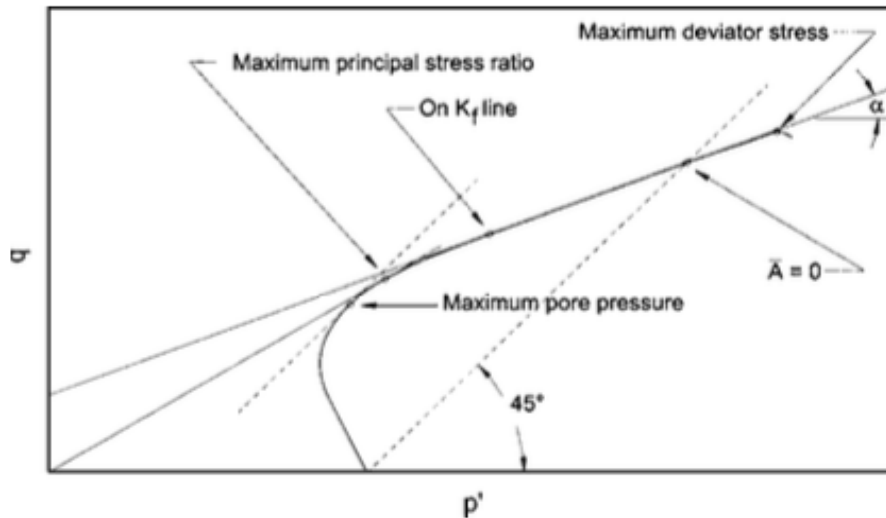


Figure 2.5: Different ways of interpreting S_u . Borrowed from [5].

The first method is to read the S_u where the peak pore pressure (U_{max}) is found. This is done by making a $\epsilon, \Delta u$ -plot where ϵ is the measured axial strain and u is the corresponding pore pressure. In this plot, the maximal pore pressure can be found at a certain strain, which then is applied in an ϵ, q -plot. Then, by reading the q with the strain found from where the u_{max} was located, the S_u can be obtained by dividing the q value by 2.

The next method is the Limited strain method. A 5 – 15% range have often been applied as a failure limit [18];[19]. The journal article from AIMS Geosciences uses a limiting strain of 5% [6], which will be applied in the results from the performed tests if possible. The S_u should be interpreted from the ϵ, q -plot directly at the chosen strain.

The last method is the $\bar{A} = 0$, also called $\Delta u = 0$ method as a failure criterion. The \bar{A} is one of Skempton's pore pressure coefficients and was first introduced in 1954 [20]. For dilative soils like the low plasticity silt from Halden, pore pressure increase before decreasing during shear. "When the pore pressure drops during shear below the value used to back pressure saturate the sample, air dissolved in the pore water

starts coming back out of solution. This would correspond to a condition of zero net change in pore pressure during shear" [5]. Meaning, at this point on the stress path, the $\bar{A} = 0$. \bar{A} is calculated the following way:

$$\bar{A} = \frac{\Delta u}{\Delta \sigma_1 - \Delta \sigma_3} \quad (2.8)$$

This method leads to quite high results for the S_u , and can lead to a wide scatter in the results according to [5];[6].

After a triaxial test is completed, the data can be plotted into several plots. The most relevant plots are in this case the ones listed below:

- $\varepsilon, \Delta u$ -plot
- ε, q -plot
- p', q -plot
- S, t -plot

The ε, u -plot consists of the parameters axial strain (ε) [%] and the change in pore pressure (Δu) [kPa]. The axial strain is measured directly in the apparatus, and the change in pore pressure is calculated with the following formula:

$$\Delta u = u_x - u_1 \quad (2.9)$$

Where u_x is a random point on the curve, and u_1 is the first recorded pore pressure reading after the start of the test. This plot is used to interpret the highest pore pressure u_{max} at the corresponding strain.

The next plot is the p', q -plot. This plot displays the stress path of the material using the mean effective stress p' , and the deviatoric stress q . The parameters have the following equations:

$$p' = \frac{1}{3} * (\sigma'_1 + \sigma'_2 + \sigma'_3) \quad (2.10)$$

$$q = \sigma_1 - \sigma_3 \quad (2.11)$$

The mean effective stress consists of the effective axial stress (σ'_1) and the effective radial stresses (σ'_2, σ'_3).

The deviatoric stress consists of the principal axial- and radial stresses (σ_1) and (σ_3). The S_u can be interpreted directly in this plot by dividing the highest q achieved in the test before collapse by 2. This is an exaggerated way to interpret the S_u , as it is calculated from the maximum value.

Further, Mohr Coulomb is introduced as a failure criteria. To be able to do this, the parameters b and M is introduced. The b parameter defines the size of the intermediate principle stress in relation to the minor and the major principal stresses. The M parameter defines the inclination of the Mohr Coulomb line. The definition of the parameters b and M can be seen in the equations below:

$$b = \frac{\sigma'_2 - \sigma'_3}{\sigma'_1 - \sigma'_3} \quad (2.12)$$

$$M = \frac{3 * (N - 1)}{3 + (1 + b)(N - 1)} \quad (2.13)$$

Where N is:

$$N = \frac{\sigma'_1 + a}{\sigma'_3 + a} \quad (2.14)$$

The a is the attraction in the material. The triaxial tests in this thesis is isotropical compression tests. This means that the radial stresses are equal ($\sigma'_2 = \sigma'_3$), which leads to $b = 0$. Then, equation 2.13 can be rewritten and the inclination in the plots is calculated as:

$$M = \frac{6 \sin \rho}{3 - \sin \rho} \quad (2.15)$$

Where:

$$\rho = \tan \phi \text{ (where } \phi \text{ is the inclination of the failure line)} \quad (2.16)$$

Equation 2.15 can now be used to find the friction angle. The expected value for friction angles in Norwegian silts is 32-36 degrees [21]. However, the friction angle varies from 34-39 degrees from the laboratory tests in [6]. A p' , q -plot is shown in Figure 2.6 below. The gray line indicates the stress path, and the black line represent the failure line.

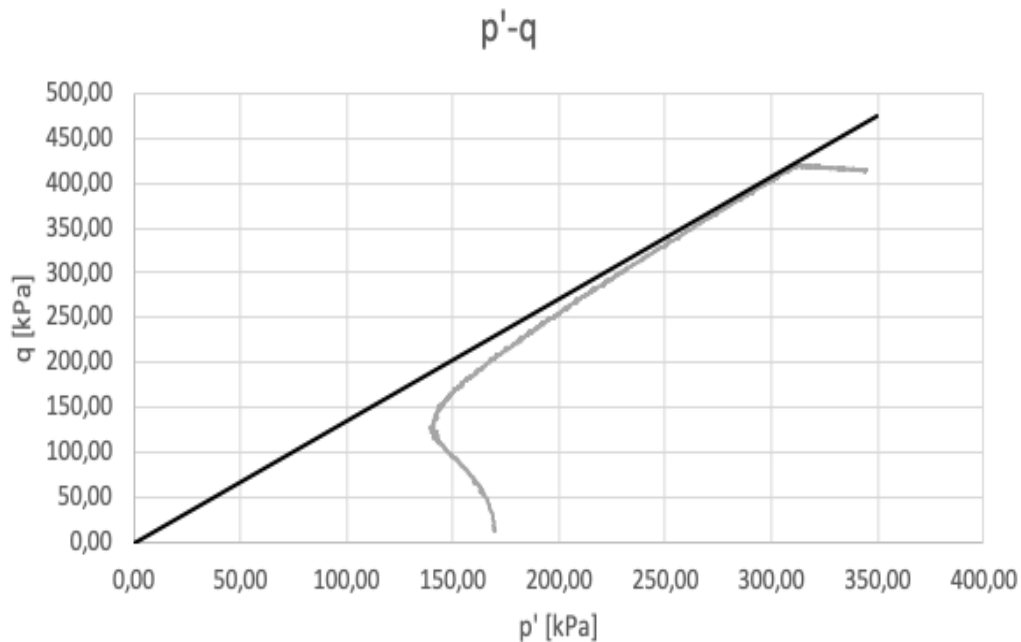


Figure 2.6: p',q -plot example, from test sample S1B

However, there are more than one way to interpret the S_u value from the p',q -plot as Figure 2.5 indicates. Three different methods are chosen, and can either be used alone, or combined. This thesis use the same methods as [6], to be able to compare the results.

The ϵ,q -plot can be used to interpret the S_u at any given strain. This plot is used next to the $\epsilon,\Delta u$ -plot to find the S_u . The strain value where the peak pore pressure is found can be put into this plot and the S_u is interpreted. Also, the limiting strain method, where the S_u is interpreted at a chosen strain can be used in this plot.

The S,t -plot is an alternative Mohr Coulomb presentation. The plot is also called NGI or MIT plot. The plot consists of the parameters S and t , and the equations is described below:

$$S = \frac{\sigma_1 + \sigma_3}{2} \quad (2.17)$$

$$t = \frac{\sigma_1 - \sigma_3}{2} \quad (2.18)$$

The inclination of the failure line is defined as $\sin \rho$. An example of a S,t -plot is shown in Figure 2.7. The gray line indicates the stress path, the black line indicates the failure line and the blue line indicates the line from the start of the test, to the point on the stress path where S_u is interpreted using the $\bar{A} = 0$

method.

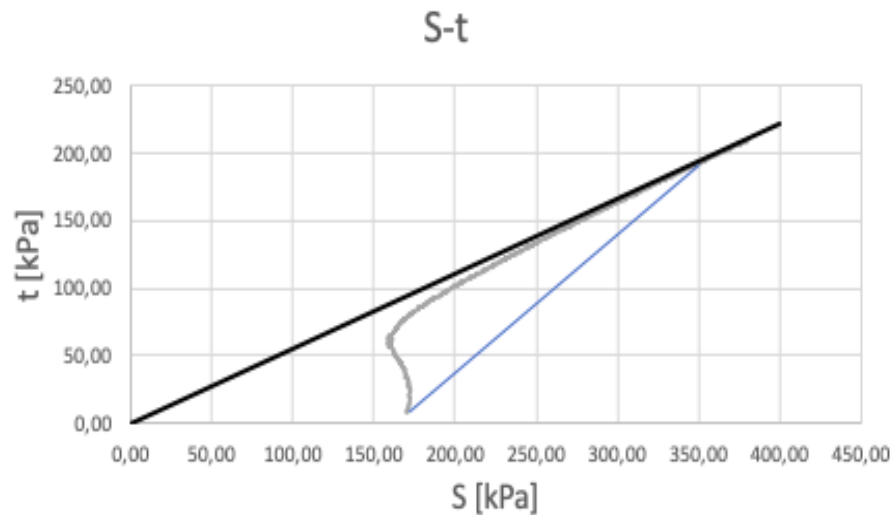


Figure 2.7: S,t-plot example, from test sample S1B

2.5.2 Undrained Shear Strength in CPTU Sounding

The S_u can be interpreted after the data from the CPTU is logged. In order to do so, a few parameters must have been calculated. As mentioned earlier, the q_t and σ_{v0} must be established. Further, the equation for calculating the S_u :

$$S_u = \frac{q_t - \sigma_{v0}}{N_{kt}} \quad (2.19)$$

The N_{kt} is the cone factor. The common N_{kt} values for clays and fine silts, are 15 ± 5 [11]. The tests performed in [6] used a N_{kt} factor of 15 and 18, and the same values will be applied in this thesis for comparison. "The N_{kt} for assessment of shear strength from undrained triaxial tests in compression (S_{uC} interpreted at the maximum excess pore pressure, u_{max}), is about 15" [6]. The correlation between the interpretation of S_u between CPTU and triaxial testing can be described with the following equation:

$$N_{kt} = \frac{q_t - \sigma_{v0}}{S_{uC}} = \frac{q_{net}}{S_{uC}} \quad (2.20)$$

Further, two focus intervals with regards to depth will be considered. Since the blocks in this thesis are collected between 14.5 and 15.5 meters, this will be one the main focus areas for undrained shear strength calculations. Five CPTU soundings in the interval 5.2-5.6 meters were conducted with different rates.

This interval will be used to investigate if Halden silt is subjected to rate effects from CPTU testing.

2.6 Rate Effects in CPTU Soundings

The rate effect from the CPTU on the undrained shear strength is a interesting field to investigate. Focus on silts and other mixed soil types have only occurred in the most recent years. There is relatively poor understanding in this particular field [7]. CPTU testing in saturated intermediate soils typically occur under partial drainage at a standard penetration rate of 20 mm/s [22].

In some stratigraphic conditions, such as silts, or transitional soils such as silty sands, clayey sands with silt, clayey sands etc., partial drainage is likely to occur [7]. "This is confirmed by the simple interpretation procedure proposed by Schnaid et al., based on plotting the normalized cone resistance Q_t vs. the pore pressure ratio B_q , in combination with the undrained strength ratio S_u/σ'_{v0} " [7]. This method assumes that partial drainage occur when $B_q < 0.3$. When this is the case, the resultant interpreted undrained shear strength ratio indicates higher values than what is acceptable for normal consolidated or slightly over consolidated soils [7]. This plot will indicate what type of drainage the CPTU soundings are experiencing, and will be used to classify the soil.

The next plot which explains the rate effects in the CPTU soundings is the rate (v) vs. the corrected cone resistance (q_t). Several researchers have observed the trend where the q_t increases with decreasing penetration rate [23]. This is explained in [24] as "partial consolidation effects occurring in front of the advancing cone during a slower penetration rate and allowing the pore pressure to dissipate and hence the cone resistance to increase". Typical drainage conditions during penetration change from drained (slow rate) to partially drained (medium rate) to undrained (slow rate) [23].

The average value of q_t within thin sublayers at a representative interval should be considered for this method. The method is used in [7] and was proven useful in silts. The paper from [7] also uses a v, u_2 -plot next to the v, q_t -plot to illustrate the corresponding pore pressure response at each rate. The last plot which is to be constructed is the v, S_u -plot. Here, the S_u is calculated in the same way as the plot above, where thin sublayers is considered for each rate. This plot is a more straightforward method of analyzing the rate effects, as the change in S_u can be directly observed with change in rate.

2.7 Carbon Dating of Shell Fragment

A well-conserved shell fragment were observed in the laboratory. Knowledge about the sedimentation rate in the test area can be obtained by investigating the age of the shell. The shell fragment were sent to another laboratory located in Poznań, Poland for carbon dating. Carbon dating is a method that provide objective age estimates for carbon-based materials and is designed to measure residual radioactivity. The method measures the unstable carbon 14 isotope of the element carbon which is unstable and weakly radioactive. The most modern carbon dating method is the Accelerator Mass Spectrometry (AMS). This method directly measures the carbon 14 content relative to the present carbon 12 and carbon 13, which is stable isotopes. The present carbon atoms in the sample and the proportion of isotopes is counted.

Chapter 3

Laboratory Testing

This chapter describes the tested material by using visual observation, previously conducted tests and the methods used in the laboratory during testing. The test procedure is explained in detail, in addition to a test plan. The purpose with the tests was to determine how the loading rate effects the resulting undrained shear strength in the material. This chapter consists of two parts. The first part details the material itself, and the second part is dedicated to the practical tasks of the tests.

3.1 The Test Material

The soil at the Halden test site is a natural fjord marine deposit with a low plasticity silt [8]. The water table is approximately 2.3 meters below ground level. The silt layer is relatively uniform, starting at 4.5 meters depth to about 15 meters below ground. The material varies from silt, sandy clayey around 5 meters, to a clayey silt from 6.5 meters [8]. The grain size distribution ranges from a medium sand to clay for the layer where the block samples were retrieved from. By looking at Figure 3.1 it is observed that Units II and III which is the silt layers have approximately 80% silt material and 8% clay. The material is classified as a silty clay with sand to lean clay with sand [6]. The grain sizes were determined using the hydrometer method described in [25]. The soil can be classified as a silt mixed with clay by observing Figure 3.2 at around 15 meters depth. The average unit weight of the material is found to be 19.9 kN/m^3 in the layer of interest. This value is estimated from a Multi Core sensor Logger (MSCL) in [6].

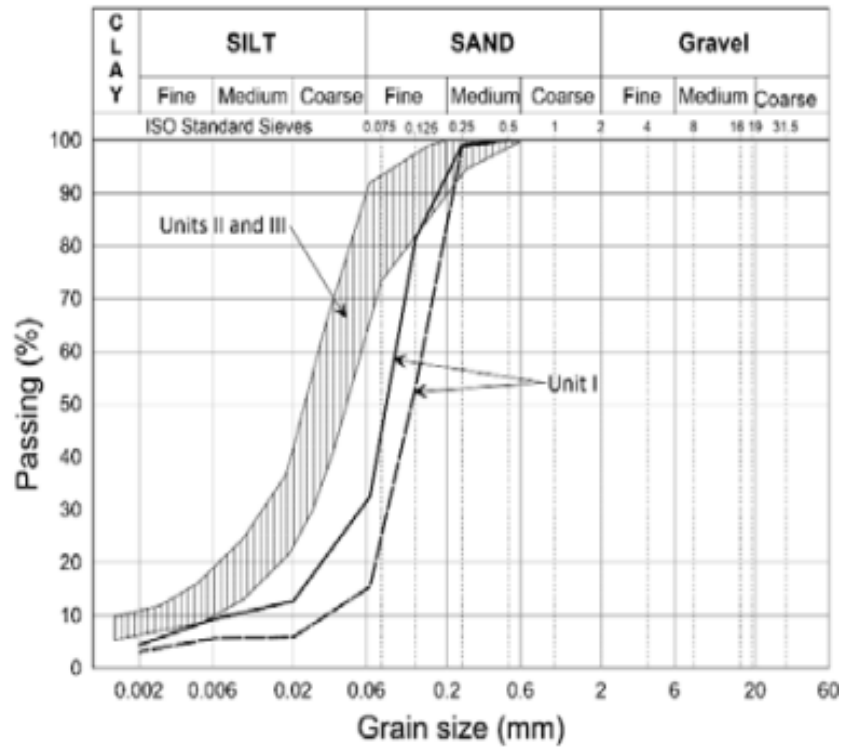


Figure 3.1: Grain size distribution. Borrowed from [6]

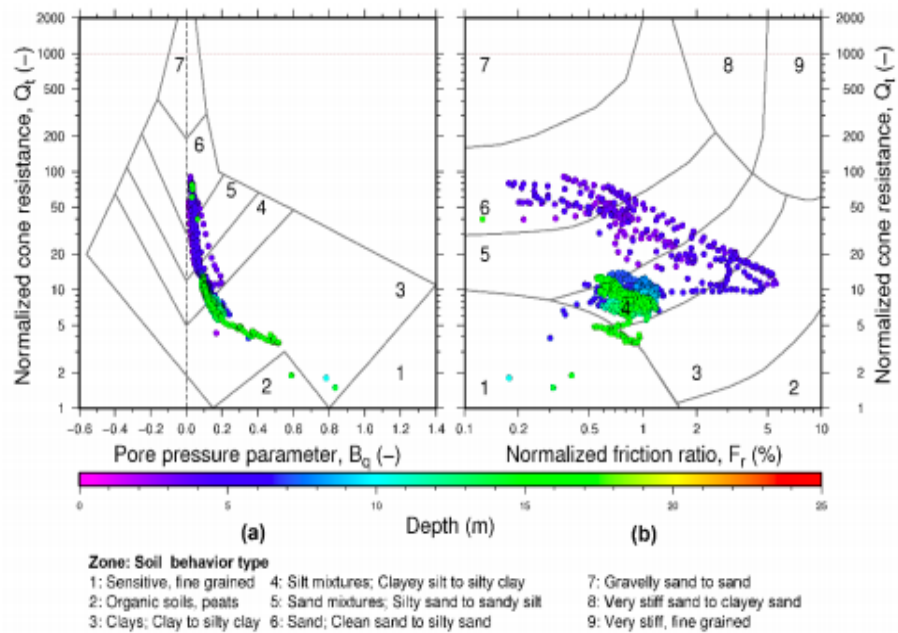


Figure 3.2: Soil classification after [4]. Borrowed from [6]

3.2 The Block Sample

The block samples used for this thesis was collected using a Sherbrooke block sampler with Ø250 mm. The blocks was taken from 14.8-15.15 (HALB05) and 15.15-15.5 (HALB04) meter below the surface and has been stored in plastic containers wrapped in plastic wrap and aluminium foil in a fridge after transportation to Trondheim, Norway. The block sample has been stored in the fridge for about two years, which is quite some time.

Block HALB05 were opened on 10th of October 2019. Preparations for the first tests were carried out immediately. Material were collected for water content measurements, and two samples were trimmed out of the block. Two triaxial tests were conducted on the same day, and sheared the day after. Five of the tests were conducted on this block. Block HALB04 were opened on 27th of February 2020. Two triaxial tests were immediately initiated, in addition to water content measurements.

The block has to be cut in different parts to be able to run tests. Since the triaxial apparatus used in this project requires a final sample height of 10 cm, the block is split in half. By cutting the block in half, ten samples can be cut out of the block for testing.

3.2.1 Inspection of the Block Sample

First the sample was taken out of the container, and the plastic wrap was removed. The first observation is that the outside of the block seemed quite dry. The material was easy to fracture simply by touching it. The state of the block sample can be observed in Figure 3.3. The crust at the top and the sides were completely dry. Shell fragments could be seen when the top of the block were examined further.

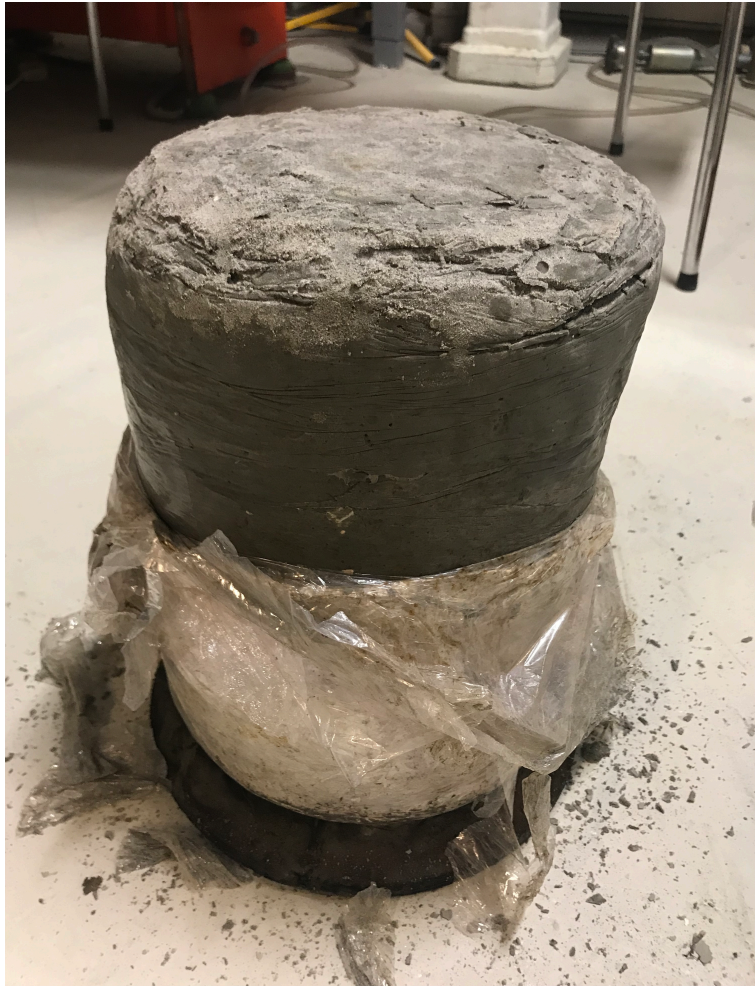


Figure 3.3: The block sample used in the tests

3.2.2 Cutting the Block Sample

A device is used in order to be able to cut the block sample. It is made of wooden plates and is designed for $\text{Ø}250$ mm samples. A steel wire saw is dragged along the surface of the device to cut it. By placing the sample in the device after the height is adjusted correctly by placing ~ 1 cm thick plates under the sample, the sample can be cut at the desired height. Since the sample was a bit dry in the edges, it was quite the struggle to cut through the sample, and assistance was required from the geotechnical staff to be able to perform this without ruining or disturbing the sample.

First, the block were cut by 3 cm at the top. A circle of about 2 cm around the edges was rather dry as seen in Figure 3.4 by the lighter shades. The block was in good condition apart from the dry edge. Furthermore, there was observed a small black circle with some organic material. There was also detected that the block

contained a substantially amount of shells. One of the shells in the top was quite big compared to most of the other inspected shells. When the block was trimmed the shells got stuck in the steel wire, which made the process somewhat difficult. The larger shell made quite the hole in the block and disturbed the sample a bit.

From Figure 3.4 it is possible to witness the V-shaped mark were the shell was placed in the upper center of the block. The dark organic material can also be seen to the left of the center.

Further, the block sample was split in half for a total height of 12 cm. The bottom half of the block were put back in the fridge for further storage. The other half was first cut in half circles. One piece were cut out from the half circle and put in the soil sample trimming device. The other parts were concealed with plastic wrapping and then placed back in the fridge. During the testing period, samples were taken out of the fridge only when needed. This was done to secure that the samples was not dried out between test preparations.



Figure 3.4: The block sample after trimming at the top

3.2.3 Trimming the Block Sample

The triaxial apparatus requires a certain geometry of the samples. The samples are required to have a height of 10 cm and a diameter of 54 mm. The main goal is to trim the sample as circular as possible. To be able to accomplish this, the samples were put in a soil sample trimming device. The device was adjusted to a diameter of 54 mm which is one of the preferred sample diameters for several different institutions in Norway [26]. The sample piece is first roughly trimmed at the edges to get rid of most of the unnecessary parts. Some of the parts which is trimmed was put in an oven to measure water content at different elevations in the sample. Then the sample is placed on to the trimming apparatus and secured by lowering the top plate down on to the top of the sample. The top plate is screwed tight so the sample can not move in any directions when the cutting is performed.

For trimming of the sample, the same steel wire is used. The steel wire is dragged along the adjusted steel plates in the apparatus which is there to make sure the sample is trimmed equal each time. When the sample is trimmed in one direction, the sample is turned simply by spinning it as both the top- and bottom plate can be rotated. The process continues until the sample have achieved satisfactory shape. The results from cutting and trimming of the sample can be seen in Figure 3.5 and Figure 3.6. It is important to dry of the steel wire between each trimming, as some material tended to stick to the wire. The sample could be damaged if the wire were not cleaned properly.

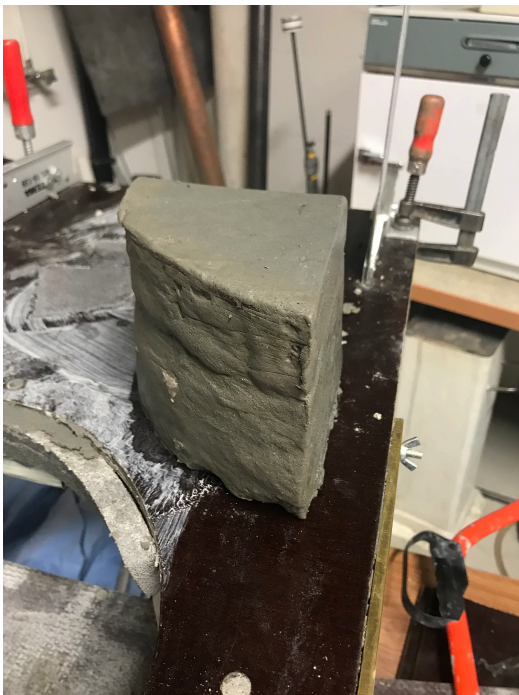


Figure 3.5: Piece cut out from the block



Figure 3.6: Sample after trimming on the sides

Further, the sample is placed in a steel casing which is 10 cm long. The top and the bottom of the sample is trimmed simply by dragging the steel wire carefully along the edges of the steel casing. The in situ direction of the sample is always kept track of. The sample is then built in to the triaxial apparatus in the same direction as it had in-situ. After the trimming of the sample is completed, a visual inspection of the sample was conducted. This is done to make sure that the sample is not disturbed in any way.

3.3 The Triaxial Apparatus

The triaxial apparatus used in the laboratory is a device from GDS-instruments. A 50 kN loading-frame which applies the axial load on the sample, in addition to a triaxial cell and two advanced pressure volume controllers. Pore pressure- and linear strain transducers are also mounted on the system. This equipment measures pore pressure and linear strain/displacement in addition to other important parameters in the sample during testing.

3.3.1 Preparing the Triaxial Apparatus

Before the sample is placed into the triaxial apparatus, some preparations were made. First, the pedestal and all the related components are cleaned with water. It is also important to make sure that the O-ring in the pedestal is clean, to prevent any leakage. Then the advanced pressure volume systems which regulate the cell- and back pressures is filled with de-aired water. The "fast empty" function on the pressure systems is used to clean out the drainage tubes in the top cap and the bottom pedestal, in case there is some residue from previous tests. Furthermore, the porous discs are cleaned and saturated in a container with de-aired water. Filter paper is cut out in 54 mm circular shapes and saturated, and the "drainage paper" used around the side of the sample is saturated as well. Prior to each test, all the testing equipment was given a visual inspection to make sure there was no damages to the system and preparation equipment.

3.3.2 Building the Sample into the Triaxial Apparatus

The sample is trimmed down to the required size and shape as described in Chapter 3.2.2 and 3.2.3. The next step is to build in the sample into the triaxial apparatus. This is executed as described in NS-EN ISO 17892-9:2018 [10] with elements from [9], to make sure that the procedure is done equally each time. The steps relevant to this thesis regarding sample mounting is listed below:

1. Applied grease to the top cap and the pedestal to make sure the rubber membrane is simple to remove after the test is completed.

2. The rubber membrane was fitted onto the membrane stretcher with the four O-rings, before the membrane stretcher was connected to an air compressor.
3. Saturated filter paper was placed on the top and bottom of the sample, in addition to the filter paper on the sides.
4. The pedestal was filled with a water film using the pressure device, meaning water was covering the pedestal, before the porous disc was slid onto the pedestal to keep air out of the system.
5. The sample is placed on the pedestal in the in-situ direction.
6. The air compressor is turned on, and the membrane stretcher are slid over the sample using a steel rod which is screwed into the pedestal. When the membrane stretcher is covering the sample and locked in position, the membrane is pulled down onto the pedestal, followed by the O-rings.
7. The porous disc is then placed on top of the sample, followed by the top cap. The membrane is pulled onto the top cap followed by the last two O-rings.
8. The membrane stretcher is then dismantled and the sample is ready to be covered by the triaxial cell.

The result from the building into the apparatus can be observed in Figure 3.7.



Figure 3.7: The sample prepared for testing

This process is carried out with care to make sure the sample is not disturbed during installment. A new rubber membrane was used in every test to make sure each sample were tested in the same conditions.

3.3.3 Final Preparations of the Triaxial Apparatus

After the triaxial cell is mounted and fastened properly, and the piston is lowered to a point where it does not have contact with the top cap, the filling of water into the cell is initiated. When the water level reaches the midpoint on the sample, the pressure is set to zero on the pressure devices to make sure this is the reference point. The pore pressure is set to zero as well. When the pressure is zero, the filling of the cell is continued. When the water reaches the top, the air valves are tightened one by one until all the air is out of the cell.

The next step is to get rid of all the air in the system (tubes). First the cell pressure is increased to 10 kPa. The back pressure is still 0 kPa. Then the valves for the top cap and the pedestal are opened separately, and water flows through the tubes using gravity. This process is completed when the air bubbles are no longer

observed leaving the system. Now the sample is ready to get saturated.

3.4 Start of Test

The software is initiated when the sample is placed in the cell and ready for testing. Available information about the sample is filled in to the software. Then the pressures are given an offset of 0 kPa for reference, and the saturation of the sample is started using the option "Saturation ramp". The valves for the cell- and back pressures is in open position on the backside of the pedestal, in addition to the valve for the pore pressure transducer. The pore pressure and the back pressure should at this point read off about the same value in kPa.

3.4.1 Saturation of the Sample

Effective stress triaxial tests (CU) requires that the sample is saturated for testing [27]. This is done to get reliable pore pressure measurements due to no air in the specimen. The saturation ramp option is there to make sure that the sample get completely saturated. When adding the saturation ramp to the test plan in the software, a preferable value for the pressures is chosen. The cell pressure is at all times 10 kPa higher than the back pressure during this stage. The interval used in this thesis is an increase of 50 kPa for each saturation ramp, for both the cell- and back pressures. If the sample struggle to reach full saturation,

3.4.2 B-value Check

The saturation ramp is checked with a following B-check. The valves at the back of the pedestal for the back pressure is closed When initiating the B-check. The cell pressure in this stage is increased additionally by another 10 kPa, while the back pressure remains at the same value. The saturation ramps usually required a few tries to be able to reach the appropriate B-value of 0.95. If the sample struggle to reach full saturation, back pressure can be applied.

3.5 Consolidation of Sample

After the required B-value is obtained, the consolidation phase is initiated. To be able to run consolidation, the mean effective in-situ stress must be determined. This was already determined in the NGTS project, but also controlled by using equation 3.1 below retrieved from [11]:

$$\sigma'_m = \frac{\sigma'_v}{3} * (1 + 2 * K'_0) \quad (3.1)$$

Where:

σ'_m = Effective mean in-situ stress

σ'_v = Effective vertical stress, ($\sigma'_{v0} = \gamma * z$)

K'_0 = At rest stress ratio

The mean effective stress was read out from Figure 6 in [6] to be ~ 170 kPa. This value is then the difference between the back pressure and the cell pressure in the consolidation phase. The duration of the consolidation phase was a minimum of 24 hours to ensure that the samples was given enough time to return to its natural state. Furthermore, the tests was performed isotropically meaning the stresses inn all directions are the same ($\sigma_1 = \sigma_3$).

Since this test is carried out as an effective stress test the sample will be consolidated to an effective pressure. In this test, the pore pressure will be replaced by the back pressure to be able to define the effective stresses. Once the mean effective in-situ stress is applied, excess pore pressure will develop in the sample. During the consolidation phase, the excess pore pressure will dissipate out of the sample and decrease its volume. This process is complete when the change in volume is less than 0.1% of the sample volume per hour and 95% of the excess pore pressure have dissipated [10]. At this point the pore pressure is similar or equal to the back pressure, and is used to calculate the effective stress conditions in the sample [27].

3.6 Shearing of Sample

When the requirements for the consolidation phase were met, the shear phase was initiated. In the shear phase the axial stress σ_1 is gradually increased while the confining pressure σ_3 remains constant. The increase in axial stress is achieved by moving the piston into the triaxial cell with a constant rate. This process continues until failure occur. When the sample reaches failure, the maximum shear stress the sample can take is determined. The test will proceed until 15% strain is reached according to [10]. Figure 3.8 below illustrates a successful shear test. The failure line is clearly visible through the rubber mem-

brane.

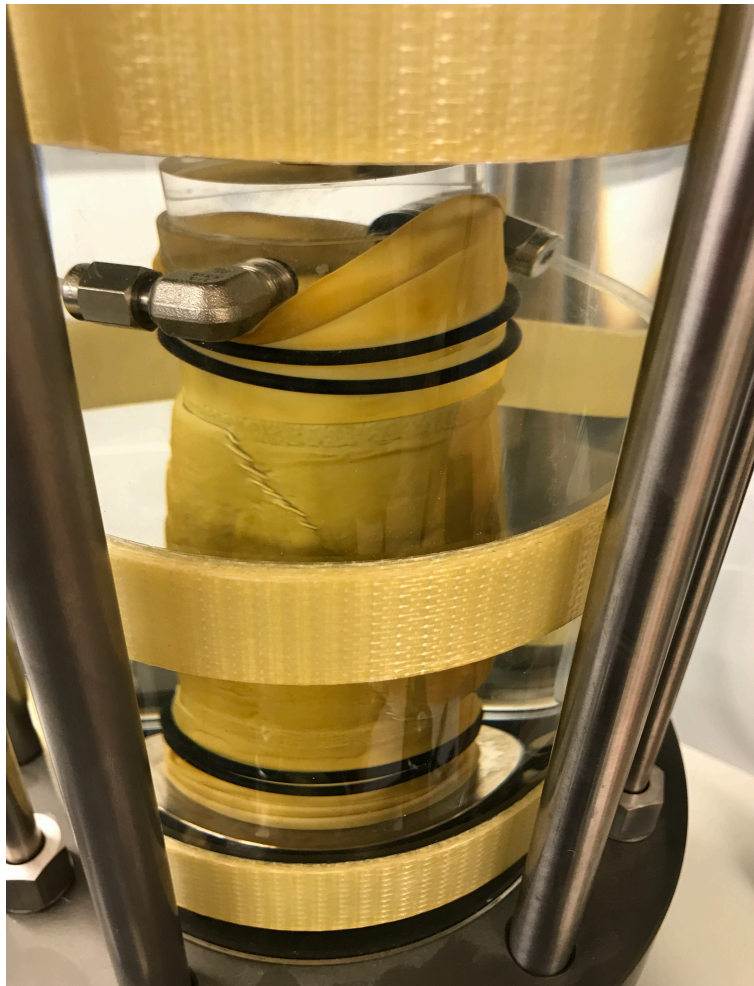


Figure 3.8: The sample after complete shearing

The loading rate is determined before the initiation of the shear test. The chosen velocities used in this project is described in Table 1.1 in Chapter 1.4. The shear test was performed undrained, meaning no water is allowed to drain out of the sample. The volume of the sample will remain constant during testing. However, the geometry of the sample will change.

From the shear test, the parameters ϕ (friction angle), c' (cohesion) and S_u (undrained shear strength) can be established. These parameters are important regarding geotechnical engineering, hence it is crucial to estimate as accurate as possible.

3.7 Test Plan

The goal of this thesis was to run nine tests in total. Four of the tests were conducted in the fall semester in 2019, in a project as mentioned earlier. This was a great learning experience, with regards to procedures and to get familiar with assessment of time-use in the laboratory. Table 3.1 below shows the test plan.

The start date represents the start up phase of the test. Two tests were started at the same date, one at the time. Here, the following tasks were executed:

1. Cleaning of the equipment if necessary
2. Cutting and trimming of the sample
3. Building the sample into the apparatus
4. Start the test, i.e. the saturation ramp and B-check
5. Initiate consolidation

The consolidation phase was running for approximately 24 hours, but often a couple more hours. The shear phase was planned to be initiated the day after the starting date. The end date represent the procedure of saving data, dismantle the apparatus, clean the work space and prepare for the next tests.

Three tests per rate are necessary to get satisfactory comparing grounds. By running three tests, it is possible to observe if one of the tests stands out in any way, or if something went wrong. Three practice samples consisting of clay were tested before the real test could start to get some experience and perfecting the procedures.

Sample	Rate [%/hour]	Test Type	Start date	End date
S1A	1.5	CIUc	10.10.2019	11.10.2019
S1B	1.5	CIUc	4.11.2019	5.11.2019
S1C	1.5	CIUc	22.1.2020	27.1.2020
S2A	15	CIUc	10.10.2019	11.10.2019
S2B	15	CIUc	4.11.2019	5.11.2019
S2C	15	CIUc	22.1.2020	23.1.2020
S3A	0.15	CIUc	27.2.2020	3.3.2020
S3B	0.15	CIUc	3.3.2020	7.3.2020
S3C	0.15	CIUc	27.2.2020	3.3.2020

Table 3.1: Test plan for triaxial testing

The dates is scattered due to additional users of the laboratory. A system was established for reservation of the laboratory. The reason for this is that the main laboratory is currently being redesigned, and only two triaxial apparatuses are available at the time.

Chapter 4

Processing the Test Data

The processing of the collected raw data from the laboratory and the field are explained in this chapter. Microsoft Excel have been used for all the calculations and plots in this thesis.

4.1 Triaxial Test Data Processing

The triaxial apparatus was operated through a program called GDSLlab. Essential data from the triaxial test includes:

- Principal and effective stresses in all directions ($\sigma_a, \sigma_r, \sigma'_a, \sigma'_r$) [kPa]
- Pore pressure (u) [kPa]
- Axial- and radial strain ($\varepsilon_a, \varepsilon_r$) [%]

All these parameters are logged with respect to time (in seconds), at 10 second intervals. The program also calculate some important parameters, such as the deviator stress (q) and the effective Cambridge (p'). All data are measured in seconds, % or kPa, which leads to the ability of immediately calculate the necessary parameters without conversion of the measurements.

The data is saved as a .txt document, which is opened in Microsoft Excel. The first step of processing the data was to clean the spreadsheet and to make sure every cell had the correct format. The next step was to calculate the necessary parameters (q, p', S, t and Δu). These parameters were then used to create the plots needed for interpretation of the S_u with the different methods explained in Chapter 2.5.1. The S_u

and the friction angle was then interpreted using the different plots for the triaxial tests. This procedure was repeated for all seven successfully completed tests.

The spreadsheets were in some cases very large, especially the tests conducted at 0.15%. The program logged data every 10 seconds from the start of the first saturation ramp. Usually, it took about 6 saturation ramps, which lead to 6 B-checks before the consolidation could start. After 24 hours of consolidation, the shear phase was initiated and lasted for about 3 days. The program logged the test steps, which made it simple to locate the data of interest and separate it from the rest. The shear phases were extracted and put in separate sheets to be able to keep better track of all the data.

4.2 Data from the Field

The CPTU data was delivered by NGI. The data can also be obtained by creating an user at the following website: www.geocalcs.com/datamap. This website gives access to the different test sites and the report from the field tests. Spreadsheets can also be downloaded and interpreted. The spreadsheets comes as .xls files, which is opened directly in Microsoft Excel. The files contain the following parameters:

- Depth [m]
- Tip resistance q_t [mPa]
- Sleeve friction f_s [mPa]
- Pore pressure at u_2 [mPa]
- Rate [mm/s], tilt angle [degree] and cone factor α

The parameters are given in mPa, which is converted to kPa before processing of the data.

4.2.1 Establishing Necessary Parameters

Before the data can be interpreted, two parameters must be established. The vertical stress (σ_{v0}) with regards to depth in kPa, and the in situ pore pressure (u_0) with regards to depth. The vertical stress was established with the following formula:

$$\sigma_{v0} = \gamma_s * z \quad (4.1)$$

where γ_s [kN/m^3] is the soil unit weight, equal to $19.9 \text{ kN}/\text{m}^3$, and the z is depth in meters. The in situ pore pressure were established by observing piezometer measurements from NGI and Appendix E in [8]. Points of interest where the pore pressure changed in depth were extracted from the appendix, and plotted into a graph. a total of 4 equations were needed for completing the in situ pore pressure profile. Further, the equation on the form $y=Ax+B$ between each line were extracted. Here, y represents the depth, z , and x represents the in situ pore pressure, u_0 . The equation is rewritten to be able to be applied as:

$$u_0 = \frac{z - B}{A} \quad (4.2)$$

The starting point for the in situ pore pressure is at 2.3 meters below surface level, and the interval for the pore pressure change is at every 5 meters.

The parameters can be observed in Figure 4.1.

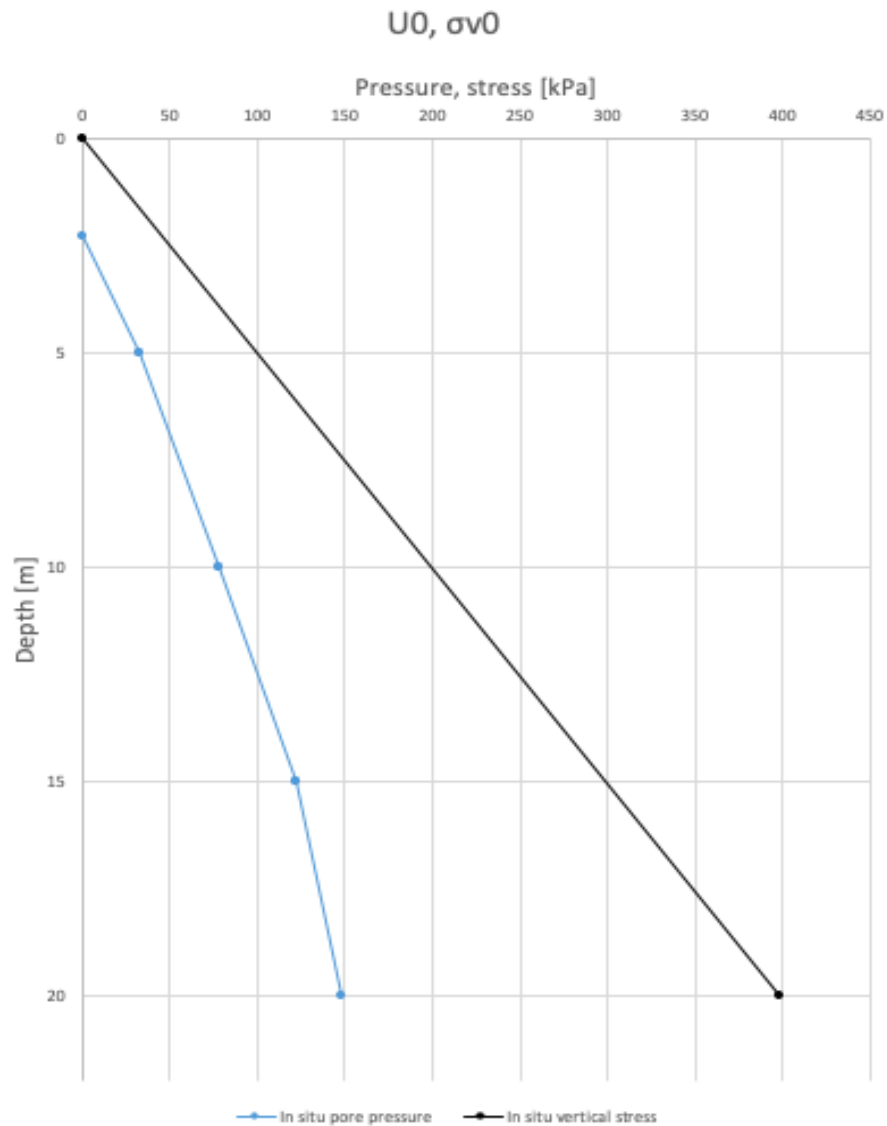


Figure 4.1: In situ stress conditions (u_0, σ_{v0}).

4.2.2 Processing Data from CPTU Tests

After all the necessary parameters have been established, the equations from Chapter 2.4.1. The q_t , B_q and the S_u with $N_{kt} = 15$ and 18. The S_u is plotted with depth. This figure then displays the strength profile down to the end of the sounding. An example of this type of plot is shown in Figure 4.2. The results from the triaxial tests can be put directly into this plot, which can be seen in Chapter 5.

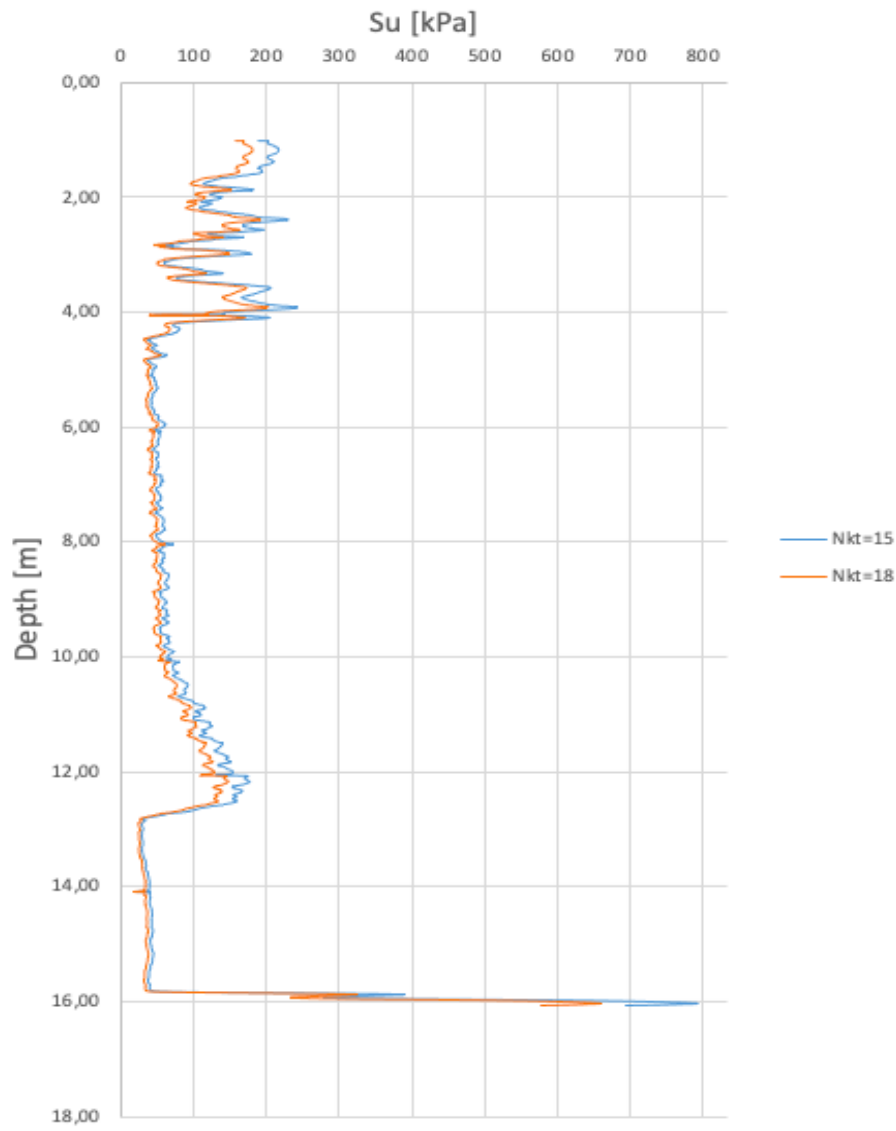


Figure 4.2: CPTU interpretation, from test HALC01

The next plot which is to be made is the $B_q, (S_u/\sigma'_{v0}, Q_t)$ -plot inspired by [7]. B_q is plotted with S_u/σ'_{v0} and Q_t on separate y-axes. Limits for B_q at 0.3 and 0.5 are added to the plot, which explains the limits for the drainage conditions. Partial drainage occurs at $B_q < 0.3$, mainly undrained at $0.3 - 0.5$ and undrained at $B_q > 0.5$. Figure 4.3 illustrates the plot from HALC13. This plot is made for both intervals of 5.2 – 5.6 and 14.5 – 15 – 5 meters.

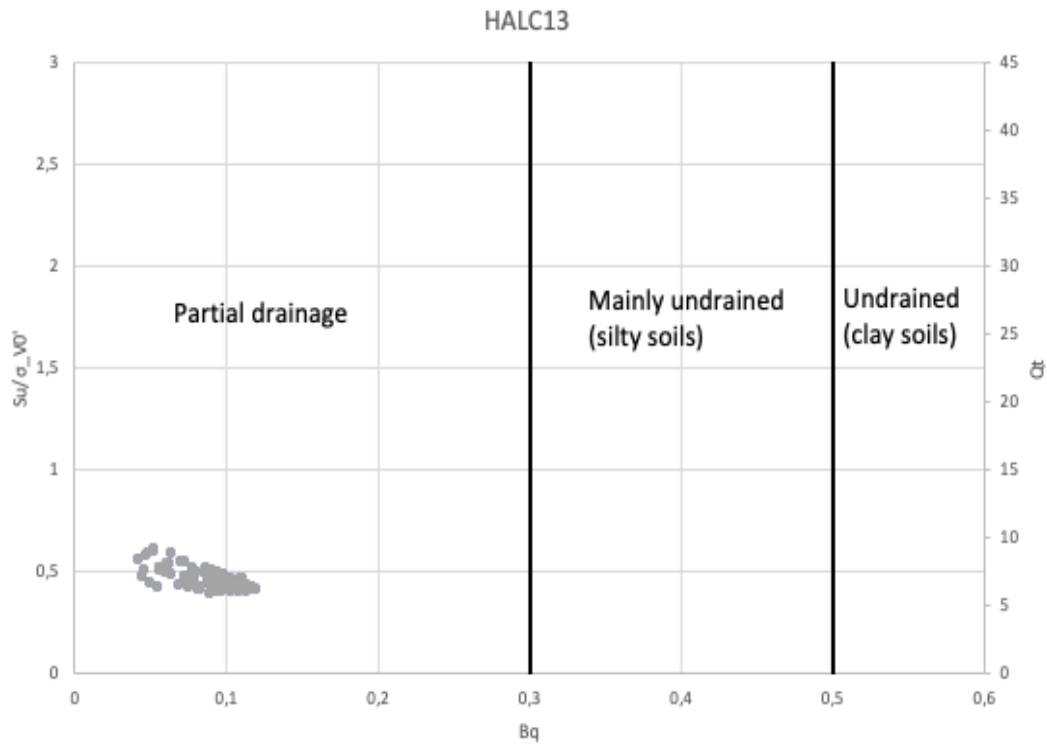


Figure 4.3: Drainage conditions in HALC13 at 14.5-15.5 meters.

The last plots made to investigate the rate effects in CPTU is the v, q_t -plot, v, u_2 -plot, and v, S_u -plot. The rate (v) is plotted with the average q_t , u_2 and S_u within thin sublayers of 0.1 meters. Then by observing the plot, it is possible to see the rate effects from the CPTU soundings.

Chapter 5

Results

This chapter presents the results from the different tests and calculations performed in this thesis. Some selected plots, tables and figures illustrates the findings both in the laboratory and in the field. However, all the results and plots can be found in Appendix B and C.

5.1 Triaxial Tests

The test results are shown in Table 5.1. For a total overview of all the test results, see Appendix B.

Sample	Rate [%/hour]	Friction Angle	$S_u - U_{max}$ [kPa]	$S_u - 4\%$ strain [kPa]	$S_u - \bar{A} = 0$ [kPa]
S1A	1.5	27.3	94.5	114	130
S1B	1.5	33.6	80	156	208
S2A	15	37.9	126	234	225
S2B	15	36.5	96	211.5	210
S2C	15	36.9	75	98	225
S3A	0.15	32.5	73.4	105.1	176.7
S3B	0.15	40	71.5	96.8	225.4

Table 5.1: Results from triaxial testing

The different plots can be observed in Figure 5.1 below. The figure is chosen randomly, as all the different tests have a similar look. Failure lines and points of interests have been added for interpretation. In the upper two plots, the black horizontal line represent the point were S_u is interpreted at u_{max} . The point is found in the ε, u -plot, and then inserted into the ε, q -plot for further interpretation.

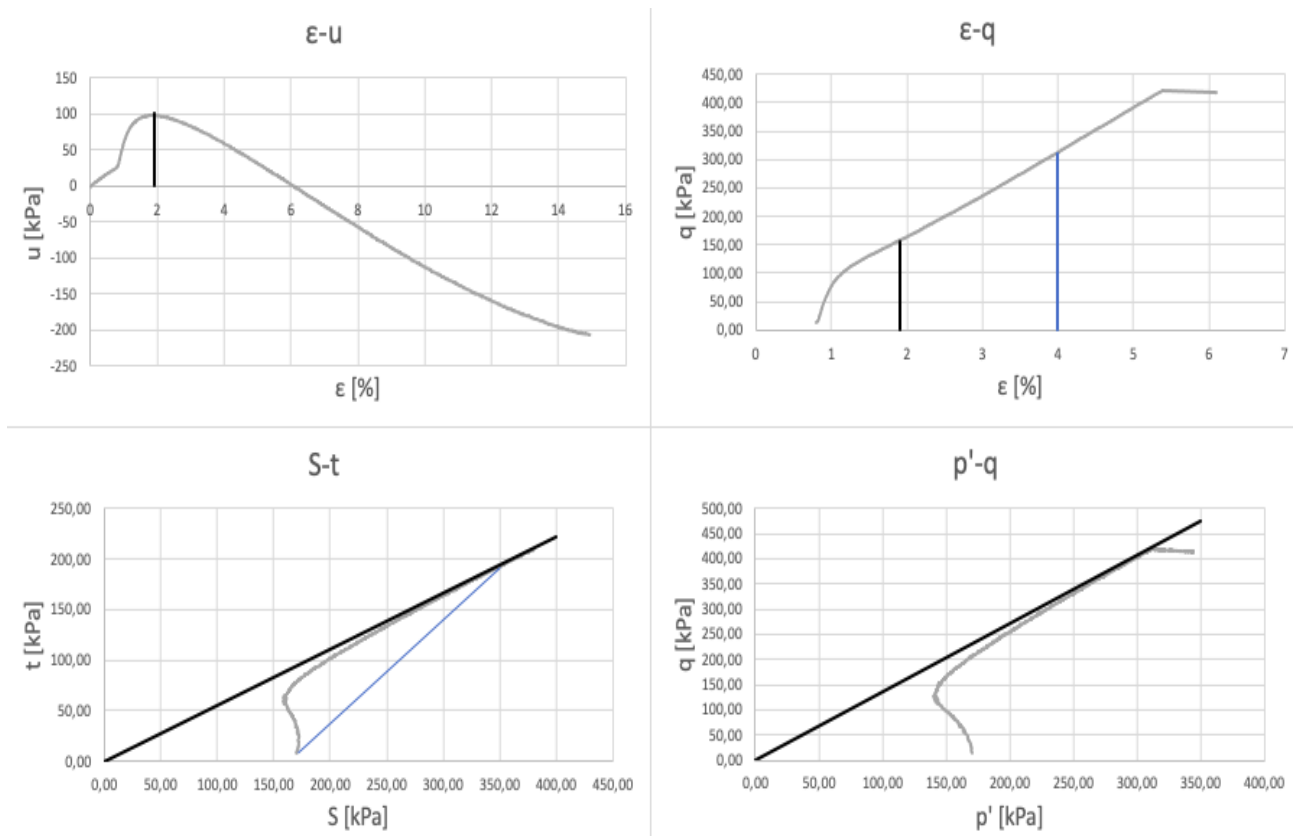


Figure 5.1: The different plots, here from S1B.

The friction angle and the S_u are interpreted from the two lower plots. By inserting the failure line into both plots, it is possible to see if the calculations are correct. It is correct when the friction angles are equal.

The material show a strong dilative behavior, which makes it more difficult to interpret the S_u , as there is no characteristic peak in the lower plots that usually occurs during tests on clayey materials. The material reaches failure in an abrupt way. This is the general trend among the tests.

The obtained results is borrowed from Figure 26 in [6], and can be seen in Table 5.2.

Depth [m]	$S_u - u_{max}$ [kPa]	$S_u - 5\% \text{ strain}$ [kPa]	$S_u - \bar{A} = 0$ [kPa]
5	35	54	58
8.4	45	62	70
11.5	48	71	82
12.5	59	98	94
13.6	63	131	103
14.5	72	177	111

Table 5.2: Results from triaxial testing in [6]

Further, all the tests could not be interpreted with 5% strain. Some of the samples did not reach the limit before collapsing, which is why the new strain limit of 4% were applied. The last method where the S_u is read at $\bar{A} = 0$ gives significantly higher values than the other methods in general. The two methods have a wider spread in the results as well.

However, two of the test were not successful. Sample 1C [1.5%] were crushed by the apparatus, as it did not register impact between the piston and the sample. The apparatus was supposed to slow down the rate automatically when a change in axial strain was registered. For sample 3C [0.15%], the measurements were not correct. The apparatus was suddenly not calibrated correctly, which meant that the recordings were not registered properly. Also, it failed to register any pore pressure readings.

5.2 CPTU Soundings

First, the CPTU soundings which were conducted deep enough to the chosen interval of 14.5-15.5 meters were selected. This resulted in a total of 15 soundings at the test site. The location of each tests can be seen in Figure 5.2. The S_u was then interpreted for these boreholes with N_{kt} values of 15 and 18. The triaxial results were then added to these plots for comparison of the results. The result of this from borehole HALC12 can be seen in Figure 5.3. In this plot, the triaxial results interpreted with the U_{max} method shows a good fit with the S_u -values from the CPTU.



Figure 5.2: Location of CPTU soundings with the interval 14.5-15.5 meters.

However, when the S_u interpreted with the chosen strain method and the $\bar{A} = 0$, the values did not fit that well. A wider scatter in the triaxial results can be seen in Figure 5.4. The undrained shear strength does not correspond as well with the CPTU measurements. Most of the tests have the same features with regards to undrained shear strengths from triaxial testing and CPTU measurements, i.e. a good fit with S_u at u_{max} , and a wider spread with 4% strain and $\bar{A} = 0$.

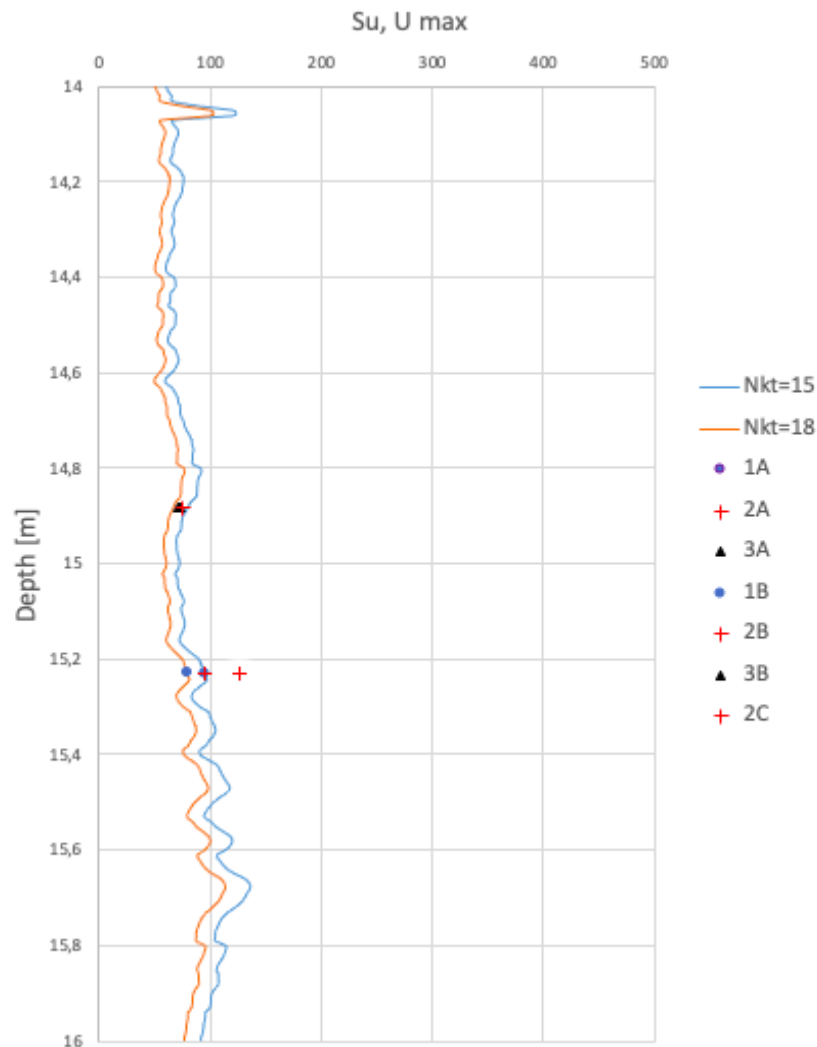


Figure 5.3: S_u plotted with depth, and the triaxial results at U_{max} is added.

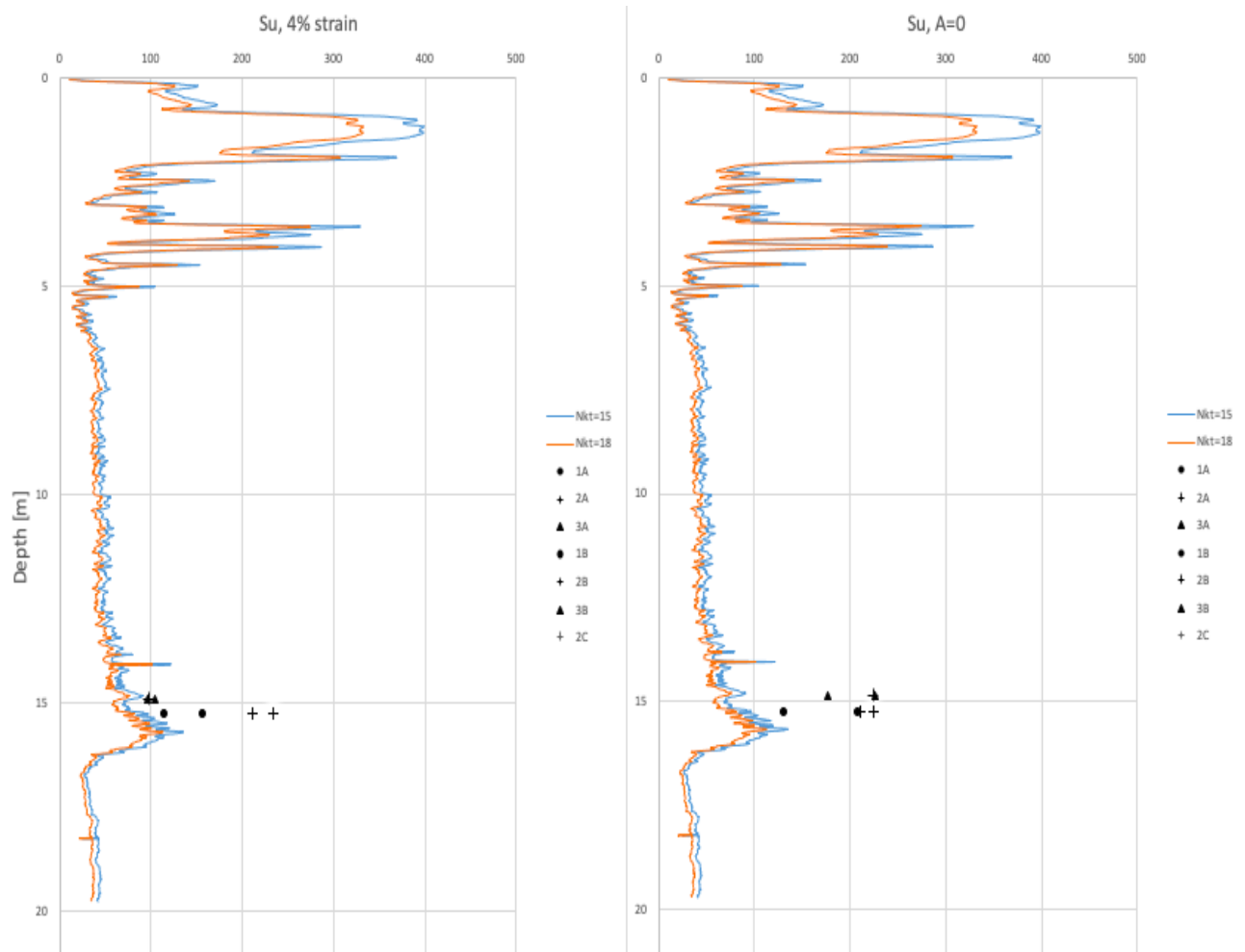


Figure 5.4: S_u plotted with depth, and the triaxial results at 4% strain (left) and $\bar{A} = 0$ (right) is added.

Further, when looking at the interval at 14.5-15.5m were the blocks used for triaxial testing, partial drainage are occurring during most of the CPTU soundings. Several of the conducted CPTUs experience this type of behavior in the chosen interval. However, a few of the tests shows results scattered over all the drainage zones. All the plots can be observed in Appendix E.

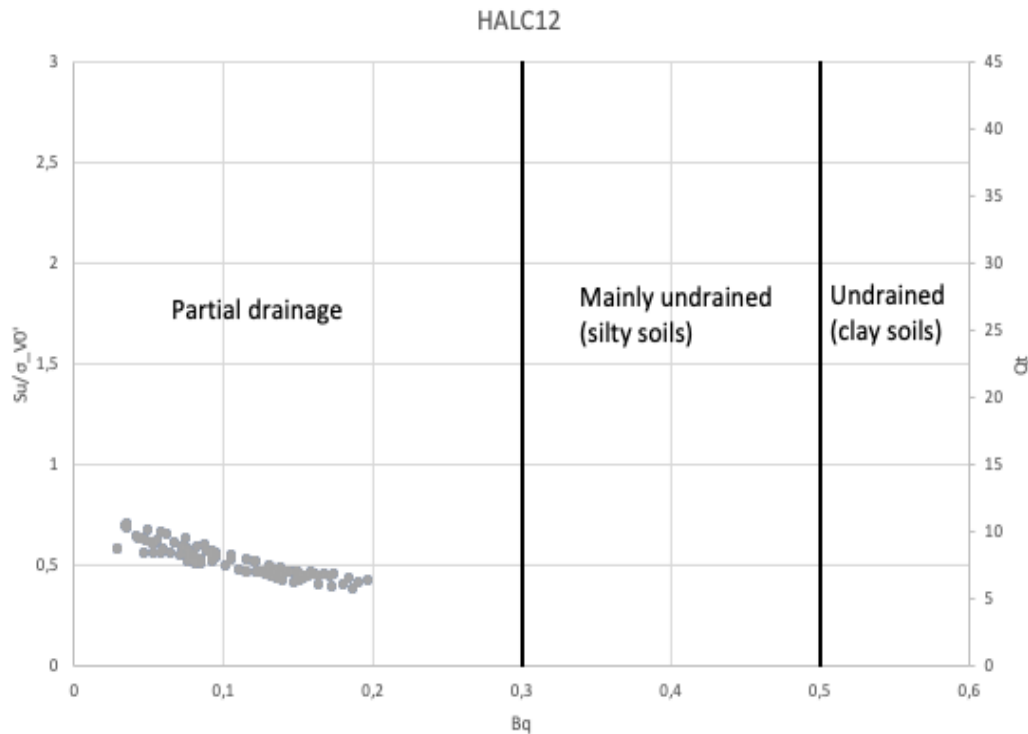


Figure 5.5: Drainage conditions in the focus interval at 14.5-15.5m. Figure after [7].

5.2.1 Rate Effects in CPTU Soundings

Five different rates were observed in the CPTU soundings at the depth interval 5.2-5.6 meters. The points were made with intervals between sublayers of 0.1 meters. The average results can be seen in Table 5.3 and the overall results are plotted in Figure 5.6 and 5.7. The average values were also used to construct a trend line for each of the plots. These trend lines can be seen in Figure 5.8 and 5.9. Further, Figure 5.10 illustrates the occurring drainage conditions at the respective depth interval. All the rates experience partial drainage. The remaining plots can be seen in Appendix D. The final plot is the v, S_u -plot, which can be seen in Figure

CPTU	Rate [mm/s]	Average q_t [kPa]	Average u_2 [kPa]	Average S_u [kPa]
HALC07	2.2	712	115	41
HALC12	20	459	65	29
HALC17	40	609	104	37
HALC23	240	704	56	46
HALC08	322	726	135	40

Table 5.3: Results from interpretation of rate effects from CPTU soundings at depth interval 5.2-5.6 meter.

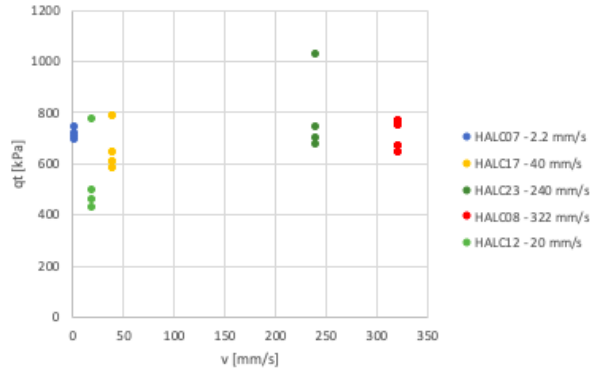


Figure 5.6: Rate vs. corrected tip resistance.

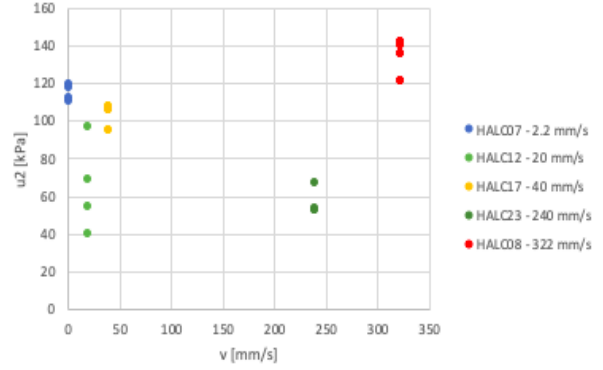


Figure 5.7: Corresponding pore pressure.

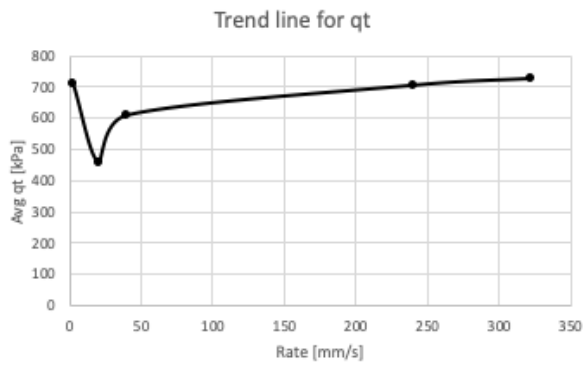


Figure 5.8: Trend line for rate vs. corrected tip resistance.



Figure 5.9: Corresponding trend line for the pore pressure.

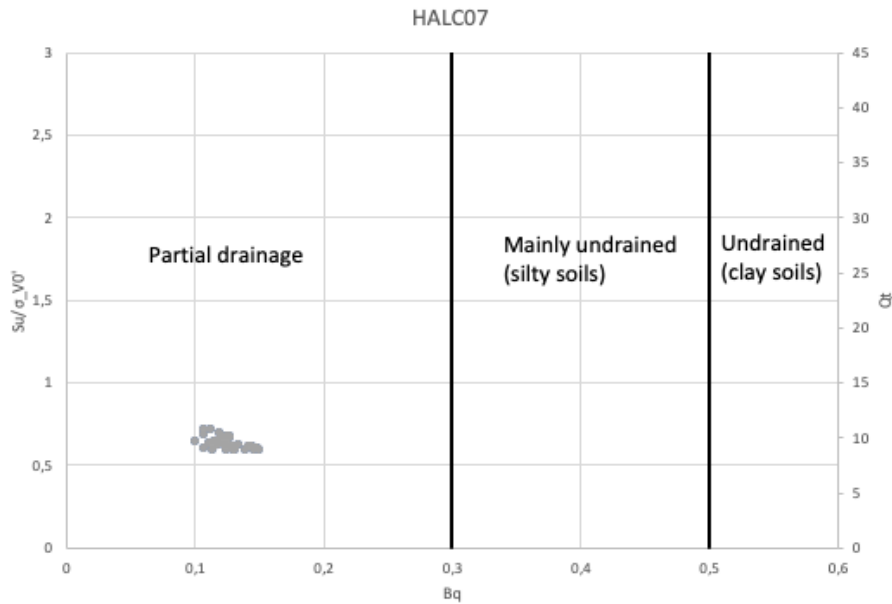


Figure 5.10: Drainage conditions in the focus interval at 5.2-5.6m for HALC07 with 2.2 mm/s rate. Figure after [7].

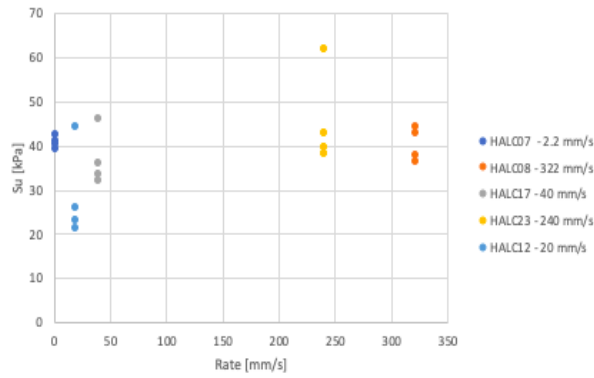


Figure 5.11: Average S_u plotted for each rate.

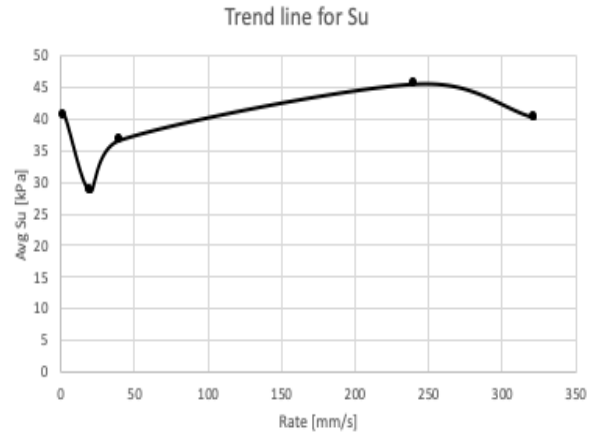


Figure 5.12: Corresponding trend line for the S_u .

5.3 Results from Water Content Measurements

The results from water content measurements can be found in Table 5.4. Previous findings in [6] is presented in Table 5.5. Block HALB04 is within the expected range, where as HALB05 shows a slightly lower water content than what is expected. This might indicate that the sealing of the sample might not have stayed intact over the last two years.

Block	Depth [m]	Water Content [%]
HALB05	15.12	16.8
HALB05	15.09	16.1
HALB05	15.06	14.4
HALB05	15.03	13.8
HALB04	15.47	22.3
HALB04	15.43	21
HALB04	15.38	20.1

Table 5.4: Results from water content measurements

Depth [m]	Water Content [%]
2-4	30-35
4-8	27-32
8-12	24-32
12-15	19-28
Obtained results	13.8-22.3

Table 5.5: Results from water content measurements in [6].

5.4 Result from Carbon Dating of Shell Fragment

Previous carbon dating tests at the site are performed at two different depths. A marine shell fragment from the clayey silt at 6.4 meters depth (22 m.a.s.l.) and a fragment in the clay at about 16.3 meters (12 m.a.s.l.). The first fragment indicates 6455 ± 25 years before present (BP), and the second fragment indicates $11,820 \pm 25$ years BP [6]. The result from the carbon dating test performed on the shell fragment is found to be 8290 ± 40 BP. This corresponds well with earlier findings in [6]. The complete report can be seen in Appendix A.

Chapter 6

Discussion

This chapter presents a discussion of the results obtained in the laboratory and from the calculations performed on the field tests.

6.1 Sample Quality

The block samples was in a good condition with regards to disturbance. There were no visible signs of disturbance on the outside. However, the outsides of the blocks was rather dry. This could indicate that some water have dissipated from the blocks over the last two years. The reason for using two blocks is that the first block (HALB04) was too dry in the bottom half, which made the trimming of the samples impossible without them breaking. However, the top half was in a very good shape. The second block (HALB05) were in equally good condition in the top half as the first block. This was first and foremost evaluated by a visual inspection of the blocks and trimmed samples.

6.2 Water Content

Block HALB05 from 14.8-15-15 meters showed a lower obtained water content than what was expected. With an average value of 15.3% which is ~ 19% lower. The slight decrease in water content could influence the undrained shear strength. Block HALB04 from 15.15-15.5 meters showed a much better fit. The average value is 21.1%, which is in the middle of the expected range from [6]. The water content is still in rather good shape, even though the blocks have been stored in the fridge for quite some time.

6.3 Triaxial Tests

6.3.1 Methods of Interpreting the Undrained Shear Strength

The u_{max} -method for interpreting the S_u obtained the most reasonable results. The scatter is not very wide between the rates, but there is a small difference. The expected value at around 15 meters is ~ 75 kPa. A substantial increase in S_u occurs at 15 meters can be seen in Figure 26 in [6]. Table 5.1 shows that the samples tested with 1.5% rate are close to the expected range at around 15 meters depth. The results are a little higher than expected when the 15% were used. S2C sheared at 15% from HALB05 which had lower water content, resulted in a S_u of 75 kPa. This is a good match, but the results from the other two tests were a bit higher. The samples sheared at 0.15% had the closest values. The results are almost equal, and very close to the results from [6].

The limited strain method had to be changed during the calculations of the tests. The limit of 5% was too high for a few of the samples, as two of the samples went to failure before this point. A new limit of 4% was used to determine the S_u , which will lead to slightly lower values than [6] interpreted. The results using this method is very scattered, both between the rates and within tests at each rate. The expected value at around 15 meters is ~ 200 kPa at 5% strain. However, since the results in this thesis is interpreted at 4% strain, a new expected value is necessary. By looking at Figure 25 (a) in [6], there is observed that the S_u at 4% strain is ~ 100 kPa. The samples sheared at 1.5% and 15% have a higher value. The exception here is sample S2C again, which obtained a resulting S_u of 98 kPa. The other two samples sheared at 15% reached S_u values > 200 . The two samples sheared with 0.15% rate achieved a S_u of 100 ± 5 kPa. This is tolerably close to the estimated value. However, the results have a wide spread which makes it difficult to use this specific method alone to determine the S_u .

The $\bar{A} = 0$ -method resulted in a wide scatter between and among the rates. The expected value at around 15 meters is 140 kPa. Sample S1A sheared at 1.5% rate is the only test which is close to the expected value. All the other tests reached a much higher S_u . The tests sheared at 15% have the least spread between the results. However, the results are much higher than the expected value, which again was expected. Sample S1B and S3B reached unexpected high values with this method. This could indicate that something went wrong during these tests. Further, this method would be too radical to use alone for estimates of the S_u , as the results are interpreted fairly close to the point where failure occurs.

6.3.2 Friction Angle

The results from the friction angle calculations can be seen in Table 5.1. The results have a good fit with the expected values presented in [6], [21]. The only test that stands out is S1A, which were performed first. Sample S1A achieved a friction angle of 27.3 degrees. This could indicate that the sample contain some fine sand as well, or something went wrong during the test.

6.3.3 Rate Effects in Triaxial Tests

The different rates had a neglectable impact on the tests. The difference can be seen by looking at the average S_u for each rate. The 0.15% interpreted with the u_{max} -method have an average value of 72.5 kPa. The 1.5% rate have an average S_u of 87 kPa and the 15% rate 99 kPa. However, the two missing samples would have contributed to a more accurate result.

6.4 CPTU Soundings

6.4.1 CPTU with Triaxial Results

The plots from the CPTU soundings were constructed using N_{kt} -values of 15 and 18, which have been proven effective in silts. The triaxial results were added in these plots, to investigate which of the methods is proven most effective for interpreting the S_u with regards to triaxial results and CPTU soundings. The u_{max} -method for interpreting the S_u shows the best fit with what is to be expected at around 15.15 meters below ground, if compared to the CPTU soundings with a N_{kt} -value of 15. First, the samples sheared with 0.15% and 1.5% fits very well with the S_u from the CPTU soundings, which is expected. The samples sheared at 15% rate have a wide spread, but with the average S_u of 99 kPa is not far from a good fit.

Further, the other two methods does not fit that well. The S_u interpreted with 4% strain and 0.15% rate have a decent match, not to far from the CPTU results. However, all the other tests resulted in a significant higher S_u , and should be used with care. A good way to interpret the final S_u might be to combine the results from the U_{max} -method and the 4% strain method. Then the S_u would increase higher up on the stress path, but not too far.

6.4.2 Rate Effects in CPTU Soundings

There was observed five different CPTU soundings with different rates at the same depth interval of 5.2-5.6 meters. However, none of the soundings had the same rate for the entire test. The soundings were

usually carried out at a standard rate to a certain depth, before the rate was changed. In some cases, the rates changed during the sounding, and went from a rate of interest (322 or 2.2 mm/s) to a lower or higher rate. This might lead to some inconsistency in the tests. Each test should possibly have the same rate from start to finish.

However, the rate effects were investigated with the available data. The rate effects can be seen in the plotted trend lines. A high q_t is reached at the slowest rate of 2.2 mm/s, but also for the high rates of 240 and 322 mm/s. However, the standard rate of 20 mm/s experience a sudden drop in q_t . The usual case is a high q_t for the lower rates, and a decreasing q_t with increasing rate. The calculations in this thesis is carried out with inspiration from the paper from [7]. The CPTU soundings in this paper ranges from low rates starting at 1 mm/s to a high rates ending at 62 mm/s. The lowest rate achieves the highest q_t , but the lowest q_t occurs at 40 mm/s before the q_t starts to increase again, resulting in a saddle-shaped trend. This behavior is not occurring in the Halden silt.

Also, undrained drainage conditions usually occurs at high rates, partial drainage at medium rates and drained conditions at slow rates. This is not valid in the tests from Halden. Here, partial drainage occurs in all the tested rates in the focus interval of 5.2-5.6 meters. Even for the fast rates, which is not to be expected.

Chapter 7

Conclusion and Further Work

7.1 Conclusions

The main focus of this thesis was to investigate the rate effects on Halden silt in a triaxial apparatus. The conducted triaxial tests indicates that there is no significant rate effects in the Halden silt. The average S_u for each rate using the u_{max} method shows some scatter. The lowest rate almost reached the expected value, if compared with the CPTU results using $N_{kt} = 15$ and the results from [6]. Then, by increasing the rates, the estimated S_u increases slightly. A total of 16 CPTU soundings were compared with the u_{max} -method, and all the soundings had an acceptable fit with the triaxial results.

The other two methods for interpreting the S_u did not fit that well. The methods are less conservative, but leads to a more scattered result. With proper care, the methods could be combined with the u_{max} -method for a more fitting estimate.

Further, the drainage conditions in the interval 14.5-15.5 meters were investigated. A total of 15 out of the 16 CPTU soundings indicated partial drainage in this depth interval, by using the method described by [7]. Since the triaxial tests are performed undrained, the drainage conditions measured in the field will not impact the results in the laboratory.

CPTU soundings from the same test site as the block samples were investigated. Five CPTU soundings were observed within the same depth interval of 5.2 – 5.6 meters at different rates. The S_u was estimated for all rates, and the results shows no clear pattern that suggests there is rate effects. The reached values does not have a huge variation between the rates. The trend in both field and laboratory appear to be

similar, which is expected as the S_u in the CPTU is based on results from laboratory testing. The CPTU tested with standard rate experience a rather large drop in q_t when compared to the other tests. This is likely due to drainage conditions and the influence of a coarser layer at around 5 meters and up. The drainage conditions were investigated for the specific interval, and resulted in partial drainage for all the soundings. This leads to unreliable results for the estimation of the S_u .

To summarize:

- No clear sign of significant effects from the different rates used both in the field and in the laboratory.
- The drainage conditions in the area is within the partial drainage range, which makes the S_u results more complicated to establish correctly.

7.2 Recommendations for Further Work

The general recommendation is to conduct more tests, both in the field and in the laboratory. More rates could be added in the triaxial laboratory, and more tests should be conducted at each rate for a more accurate interpretation. The samples should also be as fresh as possible, as the storage time could interfere with the results.

As for the field, new tests should be conducted with the current knowledge. The conducted tests should have been performed further down, were a thicker layer of silt is observed and no other layer can influence the results. The silt layers can be observed in Figure 5.4 at around 6 meters down to about 16 meters. Each new test should use one rate only in the intervals of interest, and a larger velocity interval might be necessary to establish the drainage conditions more accurate. Additional rates could be added, which consider the points between the already known intervals. The general trend would then be more clear with regards to the S_u at each rate. Rate effects have been proven before in intermediate soils by other researchers, hence emphasizing the need for further research into the understanding of intermediate soils and the corresponding behavior during CPTU testing. The interpretation methods and procedures are a subject which needs more attention as well.

Bibliography

- [1] G. Lefebvre and C. Poulin, “A new method of sampling in sensitive clay,” *Canadian Geotechnical Journal*, vol. 16, no. 1, pp. 226–233, 1979. [Online]. Available: <https://doi.org/10.1139/t79-019>
- [2] K. Head, “Manual of soil laboratory testing,” *Civil Engineering*, vol. 64, no. 6, p. 90, 06 1994, copyright - Copyright American Society of Civil Engineers Jun 1994; Last updated - 2017-10-31; CODEN - CIEGAG. [Online]. Available: <https://search.proquest.com/docview/228471413?accountid=12870>
- [3] T. Lunne, P. K. Robertson, and J. J. M. Powell, “Cone-penetration testing in geotechnical practice,” *Soil Mechanics and Foundation Engineering*, vol. 46, no. 6, pp. 237–237, Nov. 2009. [Online]. Available: <https://doi.org/10.1007/s11204-010-9072-x>
- [4] P. K. Robertson, “Soil classification using the cone penetration test,” *Canadian Geotechnical Journal*, vol. 27, no. 1, pp. 151–158, 1990. [Online]. Available: <https://doi.org/10.1139/t90-014>
- [5] T. L. Brandon, A. T. Rose, and J. M. Duncan, “Drained and undrained strength interpretation for low-plasticity silts,” *Journal of Geotechnical and Geoenvironmental Engineering*, vol. 132, no. 2, pp. 250–257, 2006. [Online]. Available: [https://doi.org/10.1061/\(ASCE\)1090-0241\(2006\)132:2\(250\)](https://doi.org/10.1061/(ASCE)1090-0241(2006)132:2(250))
- [6] Ø. Blaker, R. Carroll, P. Paniagua, D. J. DeGroot, and J.-S. L’Heureux, “Halden research site: geotechnical characterization of a post glacial silt,” in *AIMS Geosciences*, vol. 5, no. geosci-05-02-184, 2019, pp. 184–228.
- [7] M. Garcia Martinez, L. Tonni, and G. Gottardi, “On the interpretation of piezocone tests in natural silt and sand mixtures,” in *Cone Penetration Testing 2018*, 03 2016, pp. 63–68.
- [8] R. Carroll, P. Paniagua, and Ø. Blaker, “Norwegian GeoTest Sites (NGTS) FIELD AND LABORATORY TEST RESULTS HALDEN,” NGI, Tech. Rep. 20160154-04-R, Jun. 2018.
- [9] T. Berre, “Triaxial testing at the norwegian geotechnical institute,” *Geotechnical Testing Journal*,

- vol. 5, no. 1/2, pp. 3–17, 1982. [Online]. Available: https://compass.astm.org/DIGITAL_LIBRARY/JOURNALS/GEOTECH/PAGES/GTJ10794J.htm
- [10] ISO, “Geotechnical investigation and testing - laboratory testing of soil,” in *ISO 17892-9:2018*, ser. Part 9: Consolidated triaxial compression tests on water saturated soils. Geneva, Switzerland: CEN, 2018.
- [11] R. Sandven, K. Senneset, A. Emdal, S. Nordal, N. Janbu, L. Grande, and H. A. Amundsen, *Geotechnics - Field and laboratory investigations*. Trondheim: NTNU Geotechnical division, 2015.
- [12] T. Lunne, T. Berre, and S. Strandvik, “Sample Disturbance Effects in Deep Water Soil Investigations,” in *SUT-OSIFB-98-199*. London, UK: Society of Underwater Technology, Jan. 1998, p. 22, journal Abbreviation: SUT-OSIFB-98-199. [Online]. Available: <https://doi.org/>
- [13] L. N. Fleming and J. M. Duncan, “Stress-deformation characteristics of alaskan silt,” *Journal of Geotechnical Engineering*, vol. 116, no. 3, pp. 377–393, 1990. [Online]. Available: [https://doi.org/10.1061/\(ASCE\)0733-9410\(1990\)116:3\(377\)](https://doi.org/10.1061/(ASCE)0733-9410(1990)116:3(377))
- [14] K. Høeg, R. Dyvik, and G. Sandbækken, “Strength of undisturbed versus reconstituted silt and silty sand specimens,” *Journal of Geotechnical and Geoenvironmental Engineering*, vol. 126, no. 7, pp. 606–617, 2000. [Online]. Available: [https://doi.org/10.1061/\(ASCE\)1090-0241\(2000\)126:7\(606\)](https://doi.org/10.1061/(ASCE)1090-0241(2000)126:7(606))
- [15] R. C. Chaney, K. R. Demars, and A. C. D.-. on Soil and Rock, Eds., *Strength testing of marine sediments: laboratory and in-situ measurements: a symposium sponsored by ASTM Committee D-18 on Soil and Rock, San Diego, CA, 26-27 Jan. 1984*, ser. ASTM special technical publication. Philadelphia, PA: ASTM, 1985, no. 883.
- [16] P. K. Robertson, R. G. Campanella, D. Gillespie, and J. Grieg, “Use of piezometer cone data: Use of in situ tests in geotechnical engineering (papers to the conference, blacksburg, 23–25 june 1986)p1263–1280. publ new york: Asce, 1986 (asce geotechnical special publication no 6),” *International Journal of Rock Mechanics and Mining Sciences & Geomechanics Abstracts*, vol. 25, no. 6, p. 288, 1988. [Online]. Available: <http://www.sciencedirect.com/science/article/pii/0148906288912053>
- [17] A. Bihs, S. Nordal, M. Long, P. Paniagua, and A. Gylland, *Cone Penetration Testing 2018*. Leiden: CRC Press., 2018, oCLC: 1096835664.
- [18] L. Borgesson, “Shear strength of inorganic silty soils: Borgesson, I proc 10th international

- conference on soil mechanics and foundation engineering, stockholm, 15–19 june 1981, v1, p567–572. publ rotterdam: A. a. balkema, 1981,” *International Journal of Rock Mechanics and Mining Sciences & Geomechanics Abstracts*, vol. 20, no. 3, pp. A69 – A70, 1983. [Online]. Available: <http://www.sciencedirect.com/science/article/pii/0148906283913621>
- [19] L. Fleming and J. Duncan, “Stress-deformation characteristics of Alaskan silt.” *American Society of Civil Engineers. Journal of Geotechnical Engineering*, vol. 116, no. 3, pp. 377–393, 1990. [Online]. Available: <http://search.proquest.com/docview/25032362/>
- [20] A. W. Skempton, “The pore-pressure coefficients a and b,” *Géotechnique*, vol. 4, no. 4, pp. 143–147, 1954. [Online]. Available: <https://doi.org/10.1680/geot.1954.4.4.143>
- [21] M. Long, G. Gudjonsson, S. Donohue, and K. Hagberg, “Engineering characterisation of norwegian glaciomarine silt,” *Engineering Geology*, vol. 110, no. 3, 2010. [Online]. Available: <http://www.sciencedirect.com/science/article/pii/S0013795209002774>
- [22] R. Carroll and P. Paniagua, “Variable rate of penetration and dissipation test results in a natural silty soil,” in *Cone Penetration Testing 2018*, 1st ed. Routledge, 2018, pp. 205–212.
- [23] A. Bihs, S. Nordal, M. Long, P. Paniagua, and A. Gylland, “Effect of piezocone penetration rate on the classification of norwegian silt,” in *Cone Penetration Testing 2018*. Routledge, 2018, pp. 143–149.
- [24] K. Kim, M. Prezzi, R. Salgado, and W. Lee, “Effect of penetration rate on cone penetration resistance in saturated clayey soils,” *Journal of Geotechnical and Geoenvironmental Engineering*, vol. 134, no. 8, pp. 1142–1153, 2008.
- [25] ISO, “Geotechnical investigation and testing - laboratory testing of soil,” in *ISO 17892-4:2016*, ser. Part 4: Determination of particle size distribution. Geneva, Switzerland: CEN, 2016, Book.
- [26] Vegdirektoratet, *Håndbok R210 Laboratorieundersøkelser*. Vegdirektoratet, 2014.
- [27] P. Gawen. (2017) Triaxial testing - an introduction. <https://www.vjtech.co.uk/blog/triaxial-testing-an-introduction>[Accessed: 21 November 2019].

Appendix A

Report-Carbon Dating of Shell

Report

on C-14 dating in the **Poznań** Radiocarbon Laboratory

Customer: **Priscilla Paniagua**
Norwegian Geotechnical Institute
Postboks 5687 Torgarden
7485- Trondheim
Norway

Job no.: 15773/19

Sample name	Lab. no.	Age 14C	Remark
HALB04-15	Poz-122148	8290 ± 40 BP	

Comments:

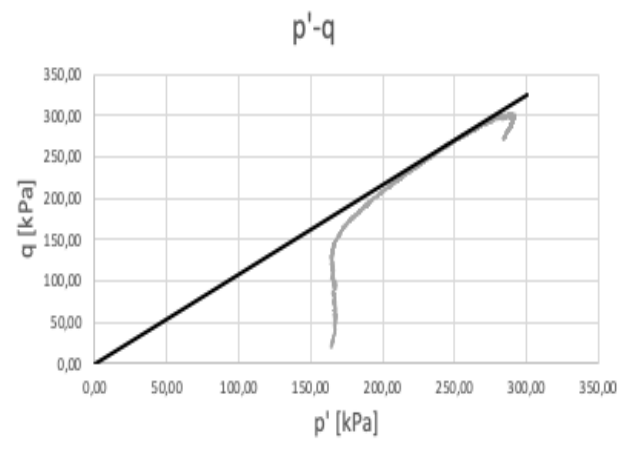
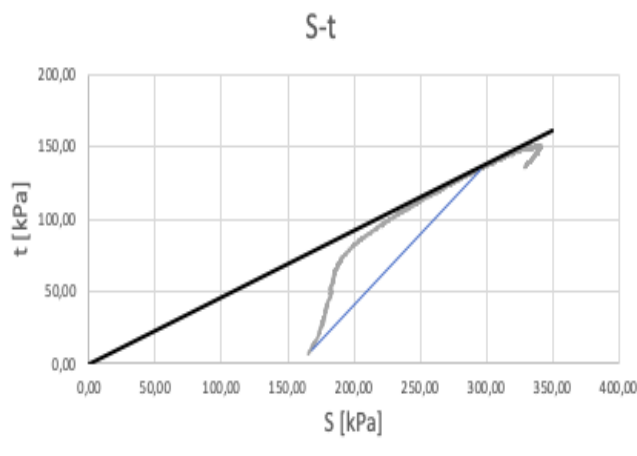
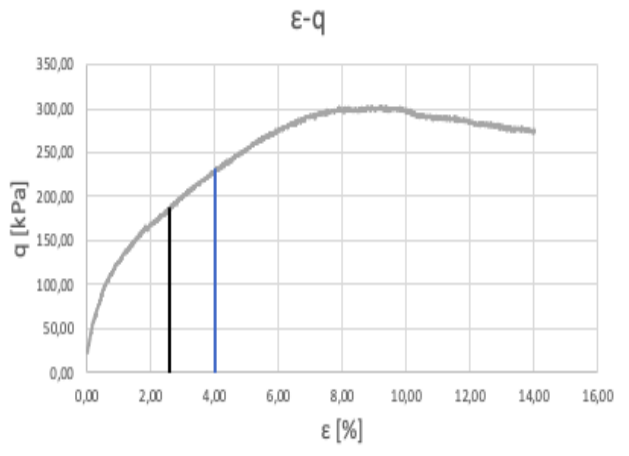
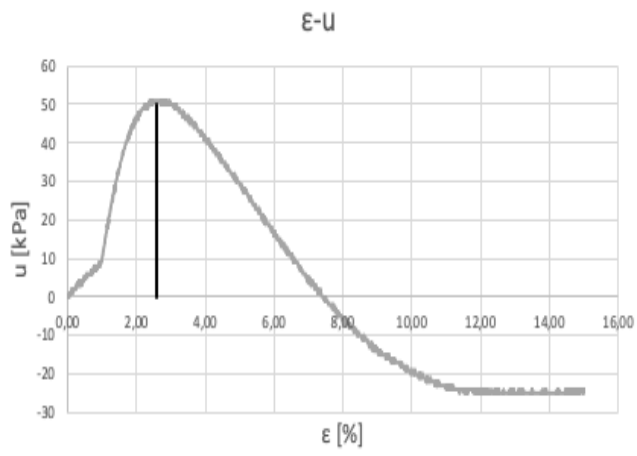
Head of the Laboratory

Prof. dr hab. Tomasz Goslar

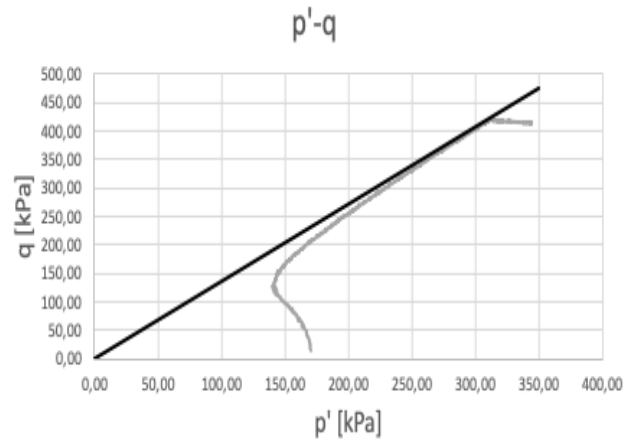
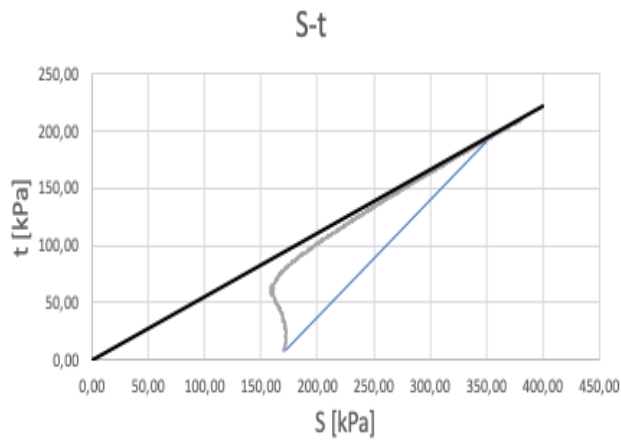
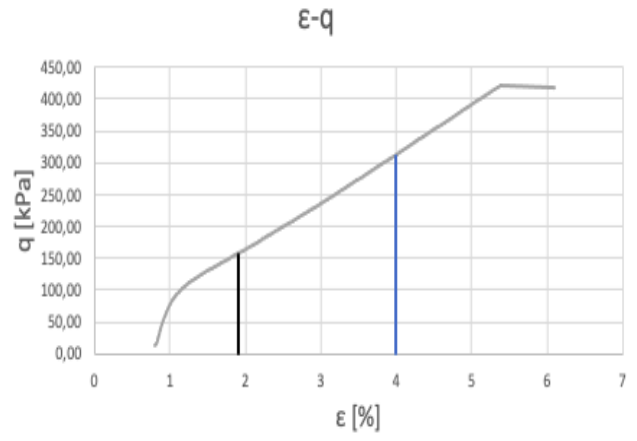
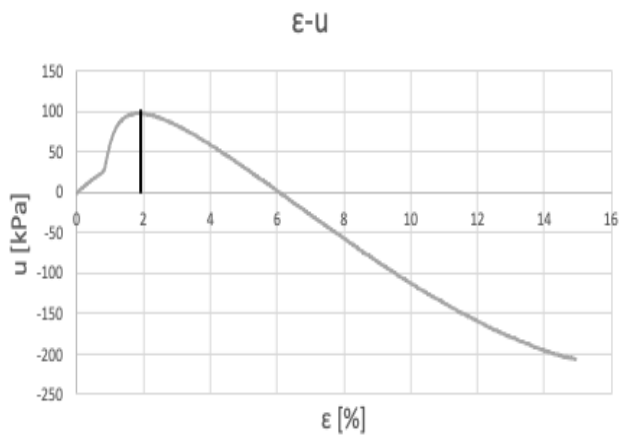
Appendix B

Triaxial Results

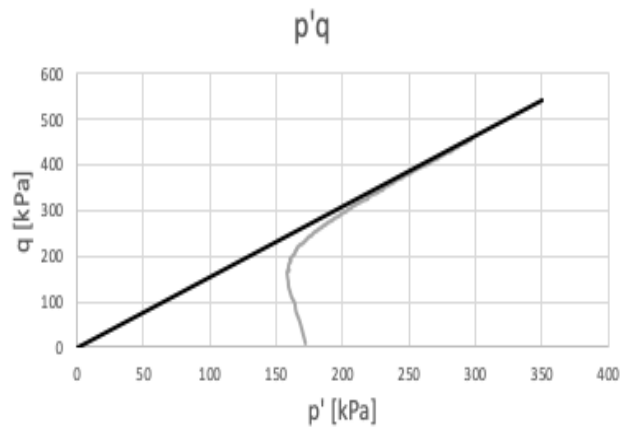
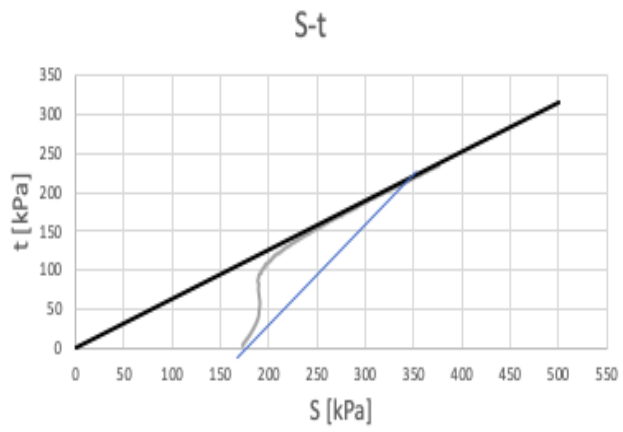
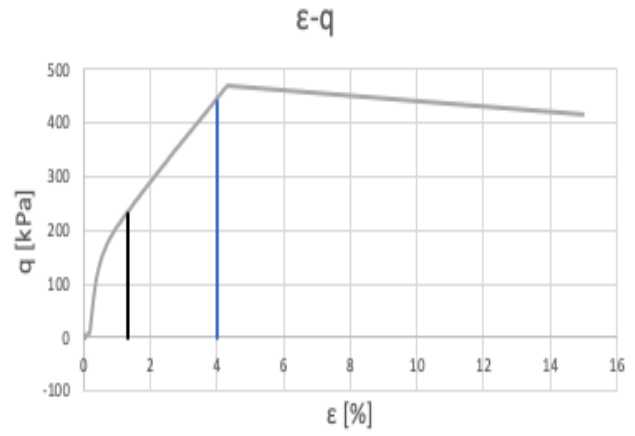
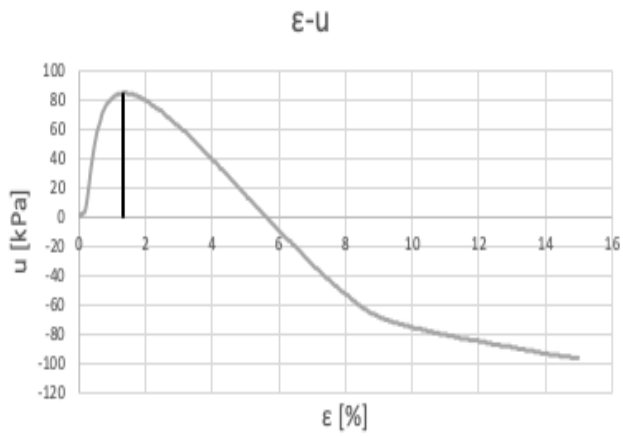
S1A



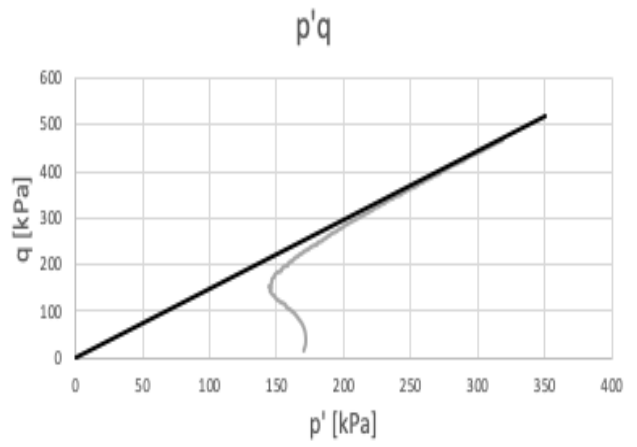
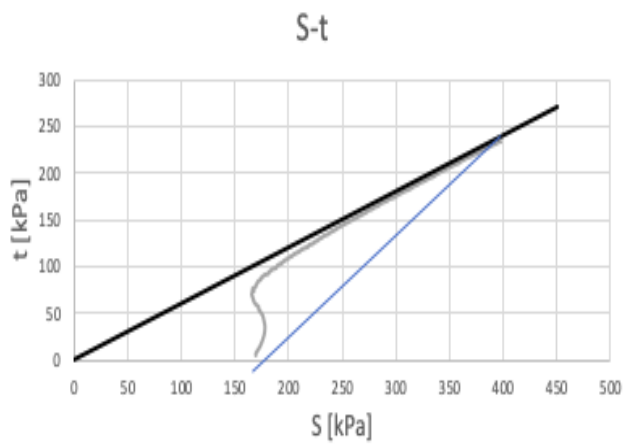
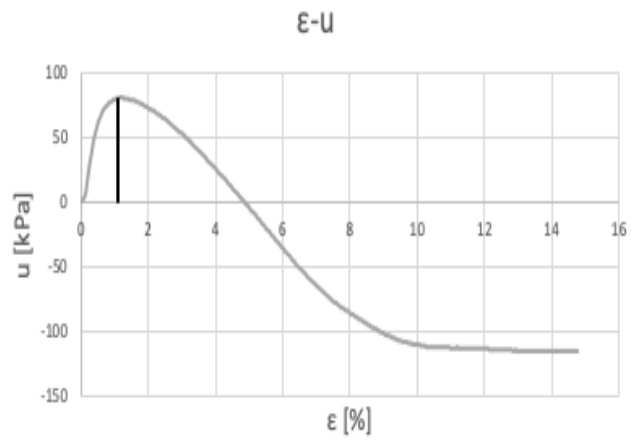
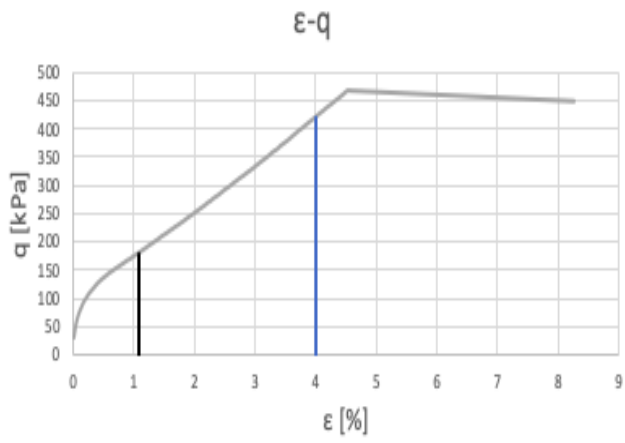
S1B



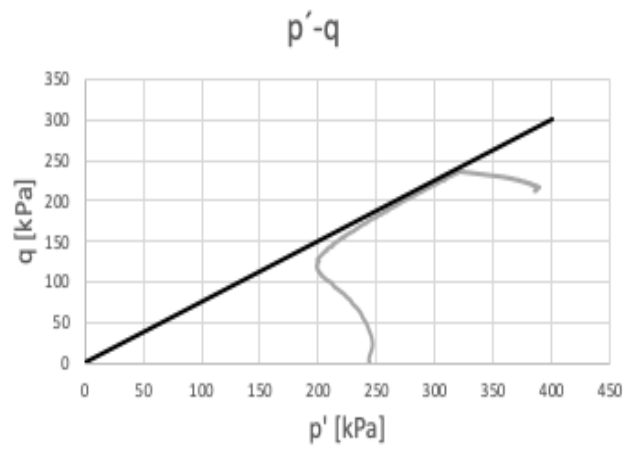
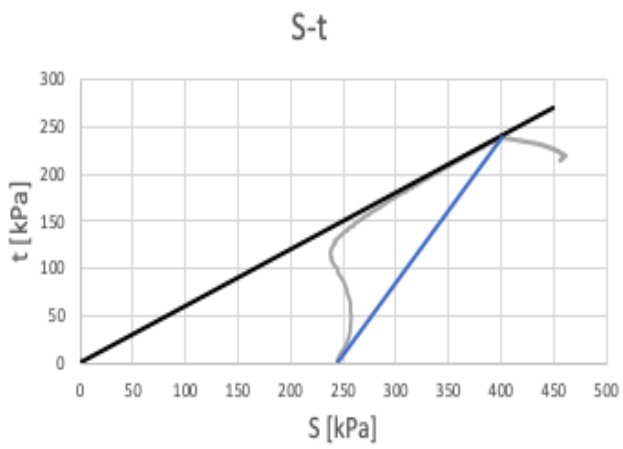
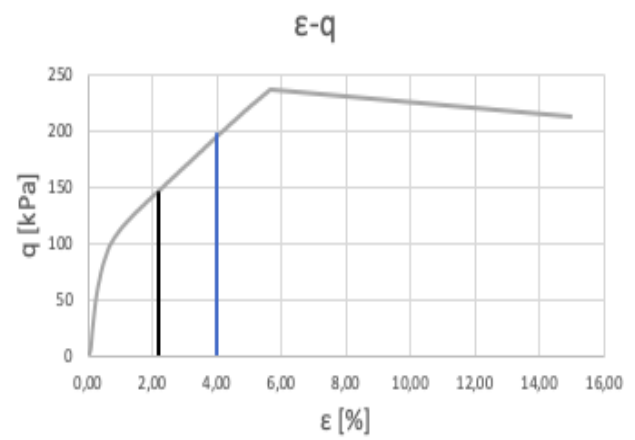
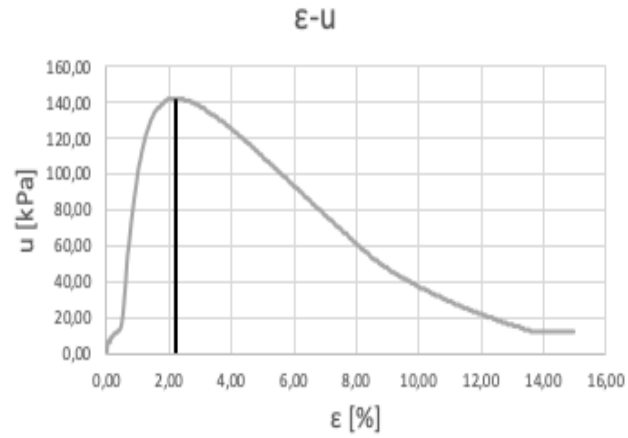
S2A



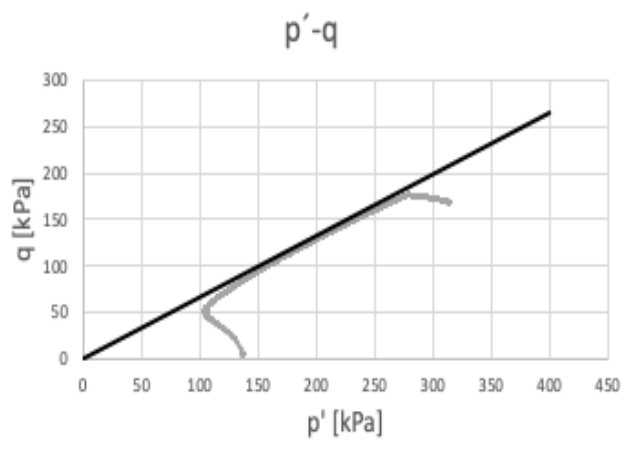
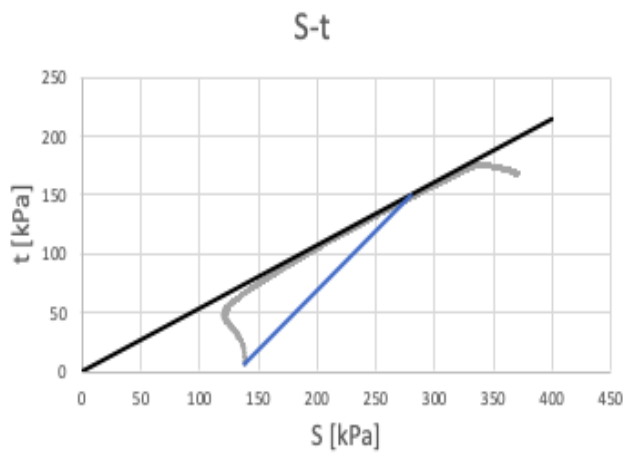
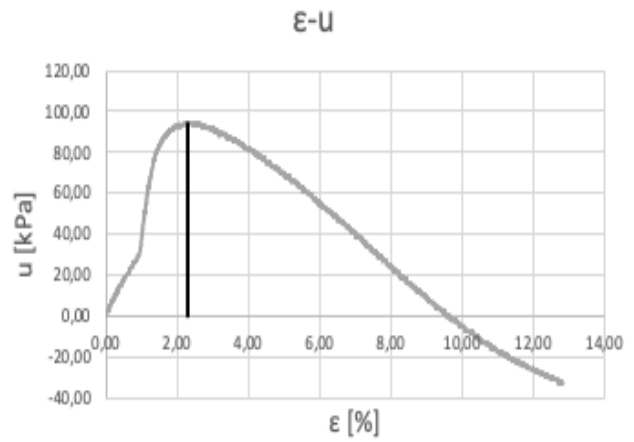
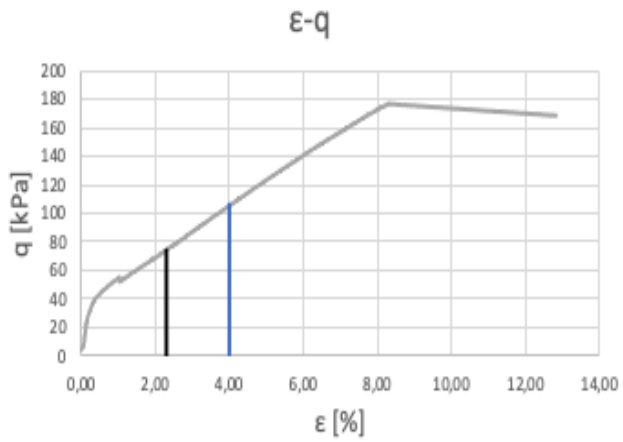
S2B



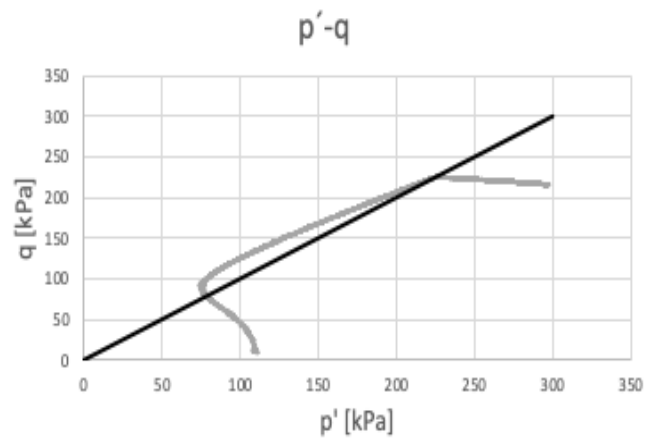
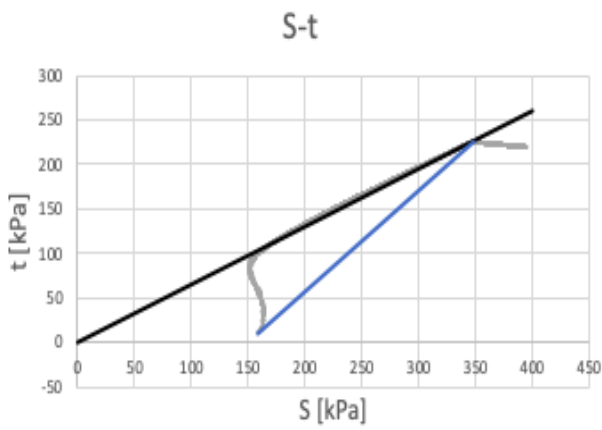
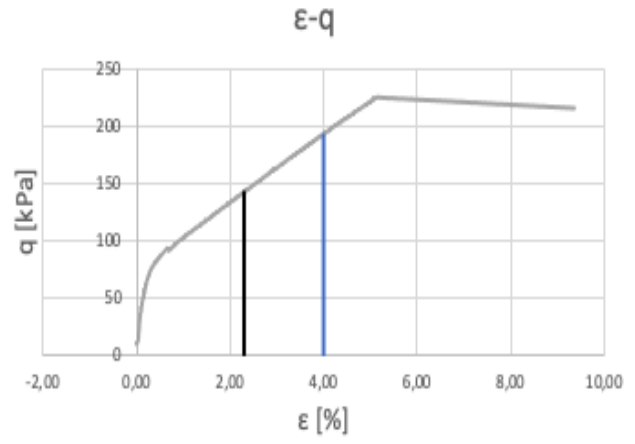
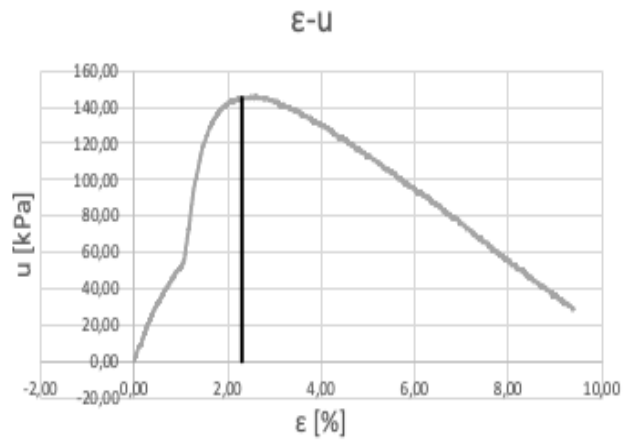
S2C



S3A



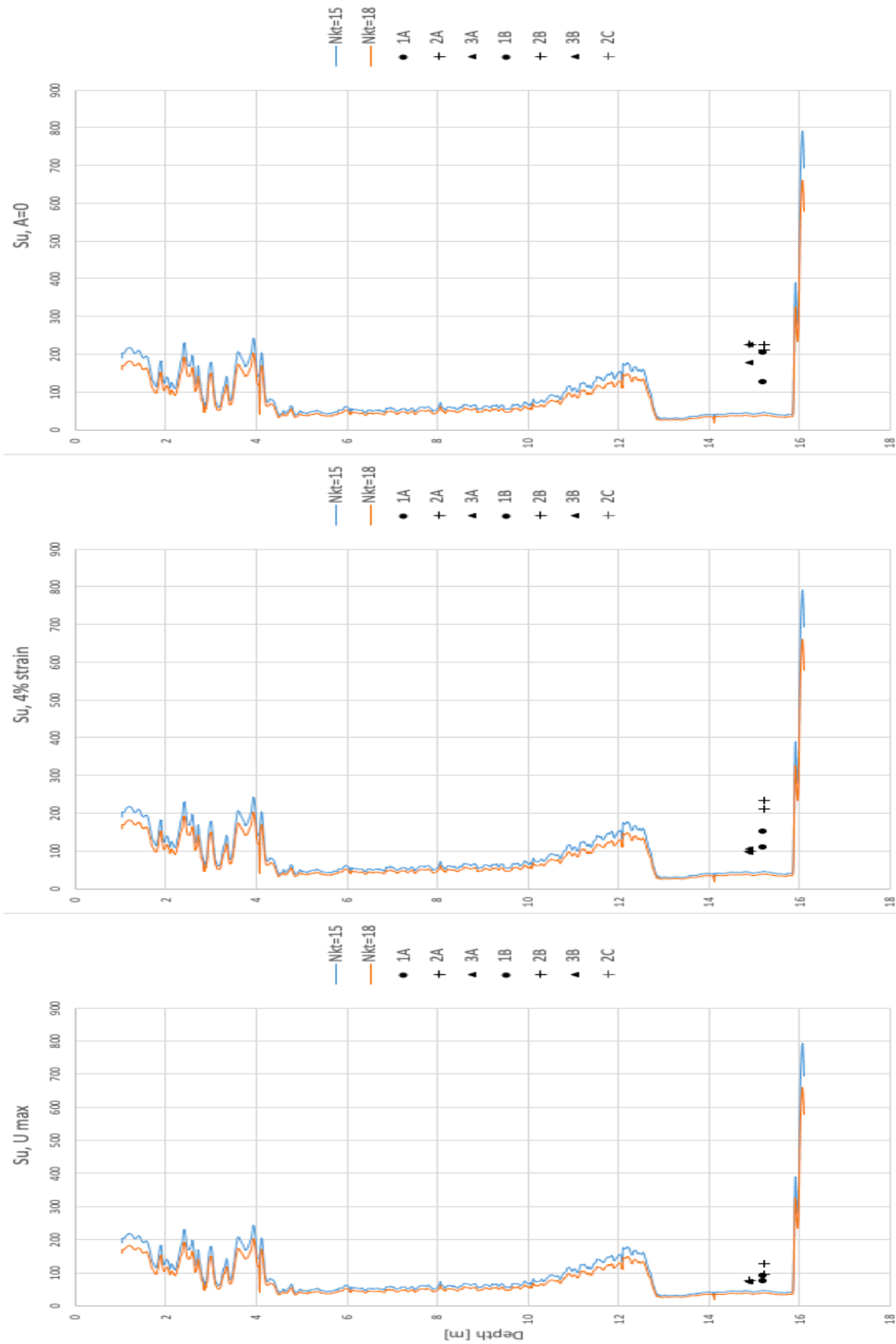
S3B



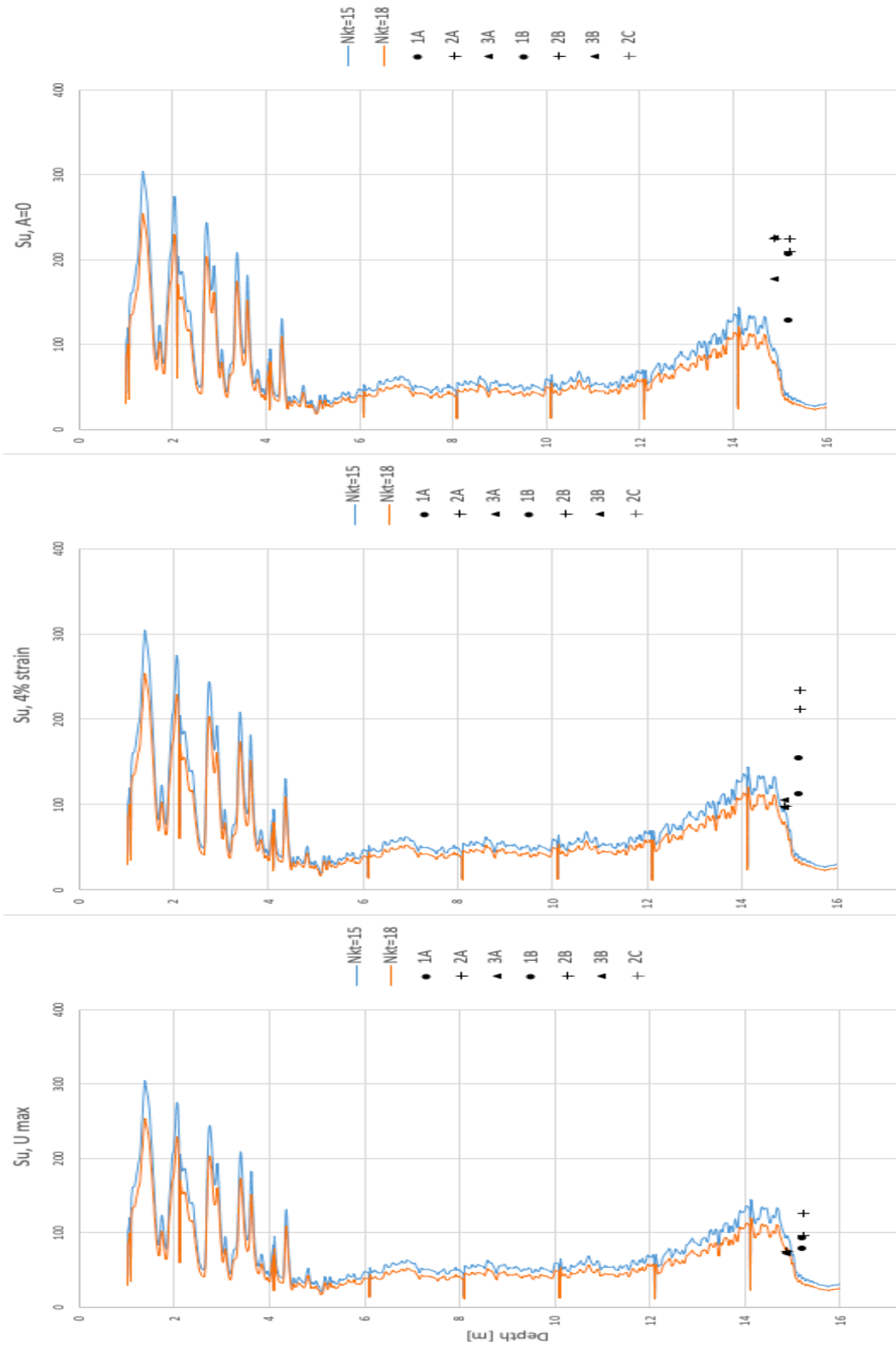
Appendix C

CPTU Soundings with Triaxial Results Included

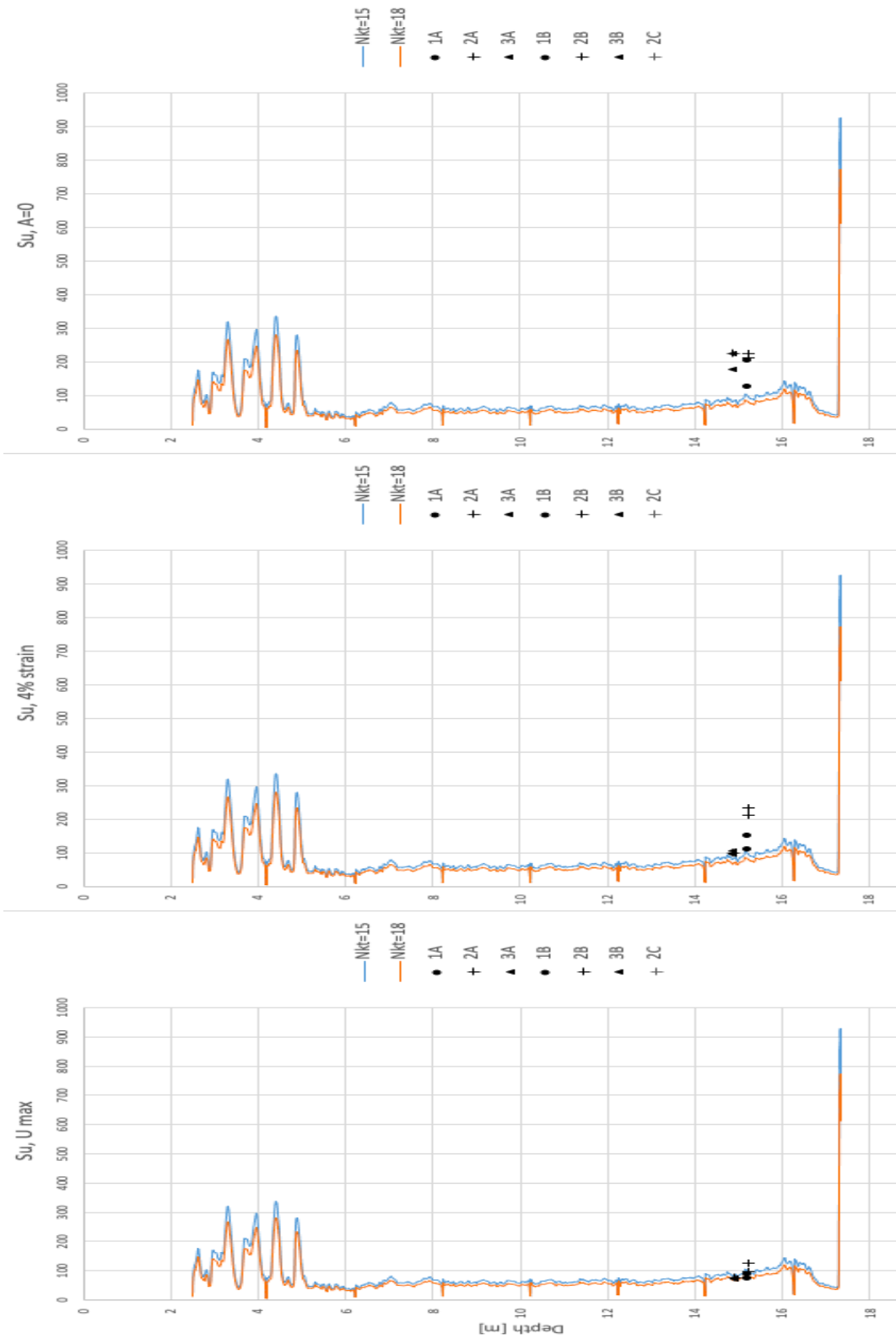
HALC01



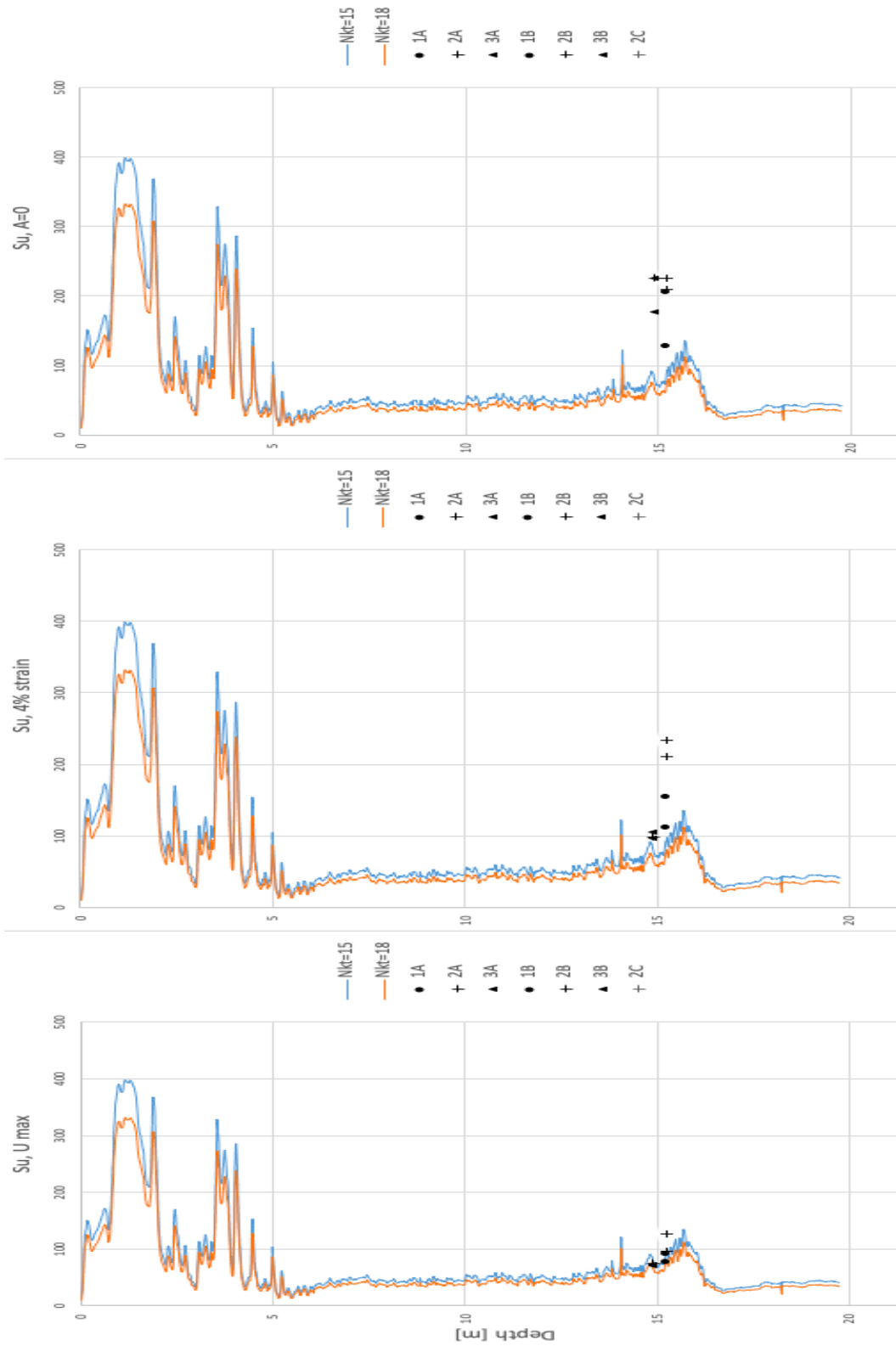
HALC05



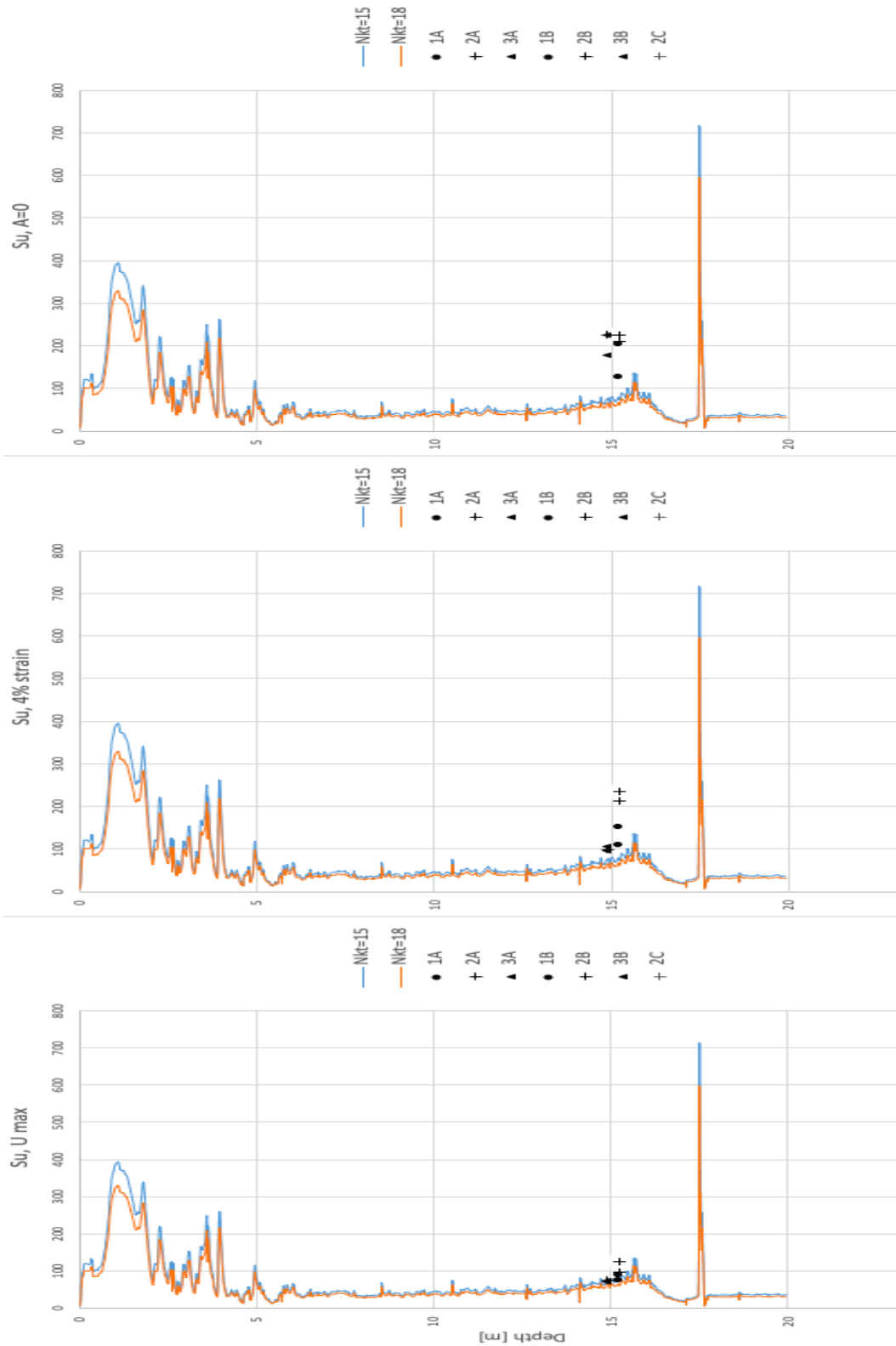
HALC11



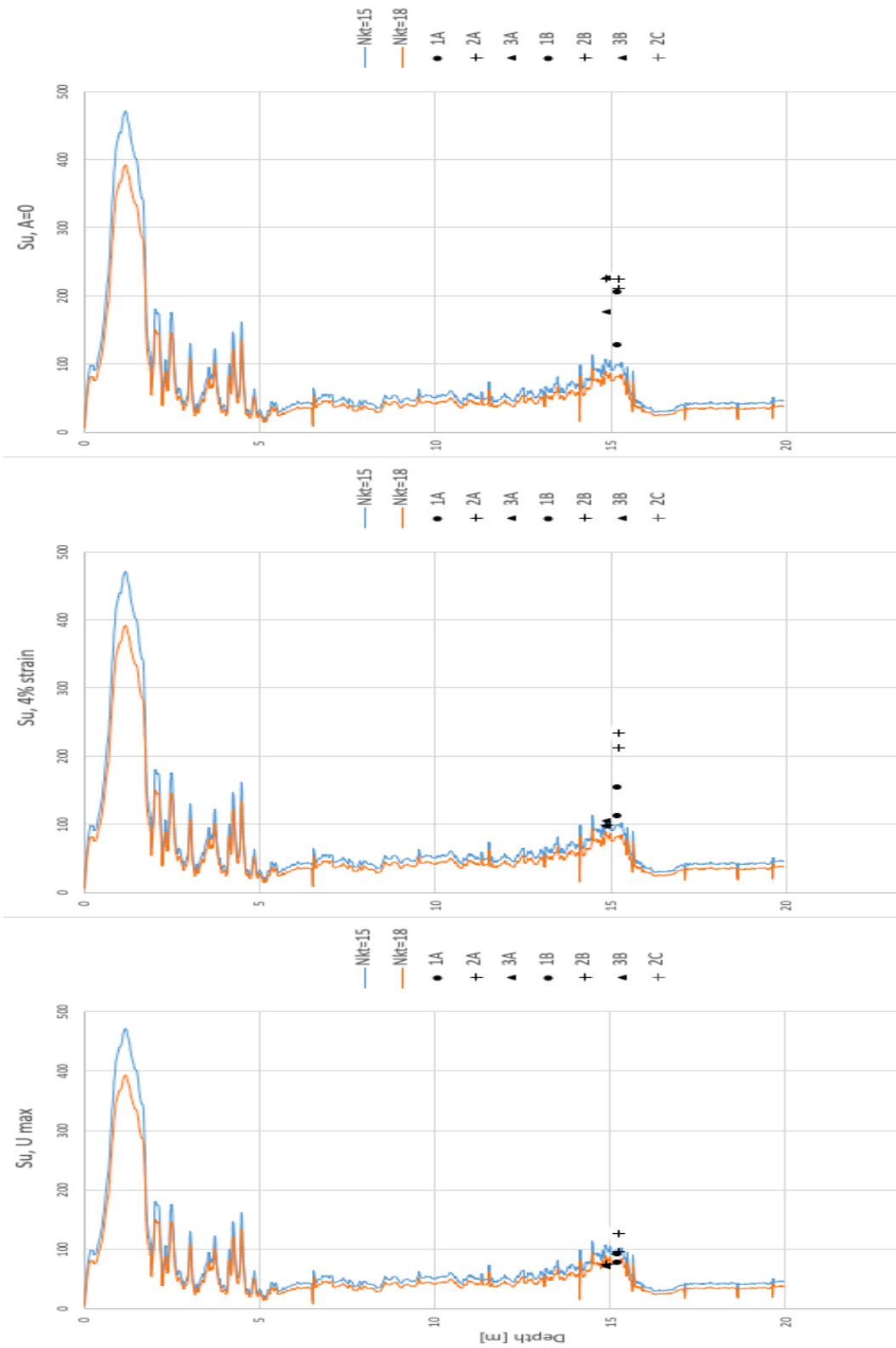
HALC12



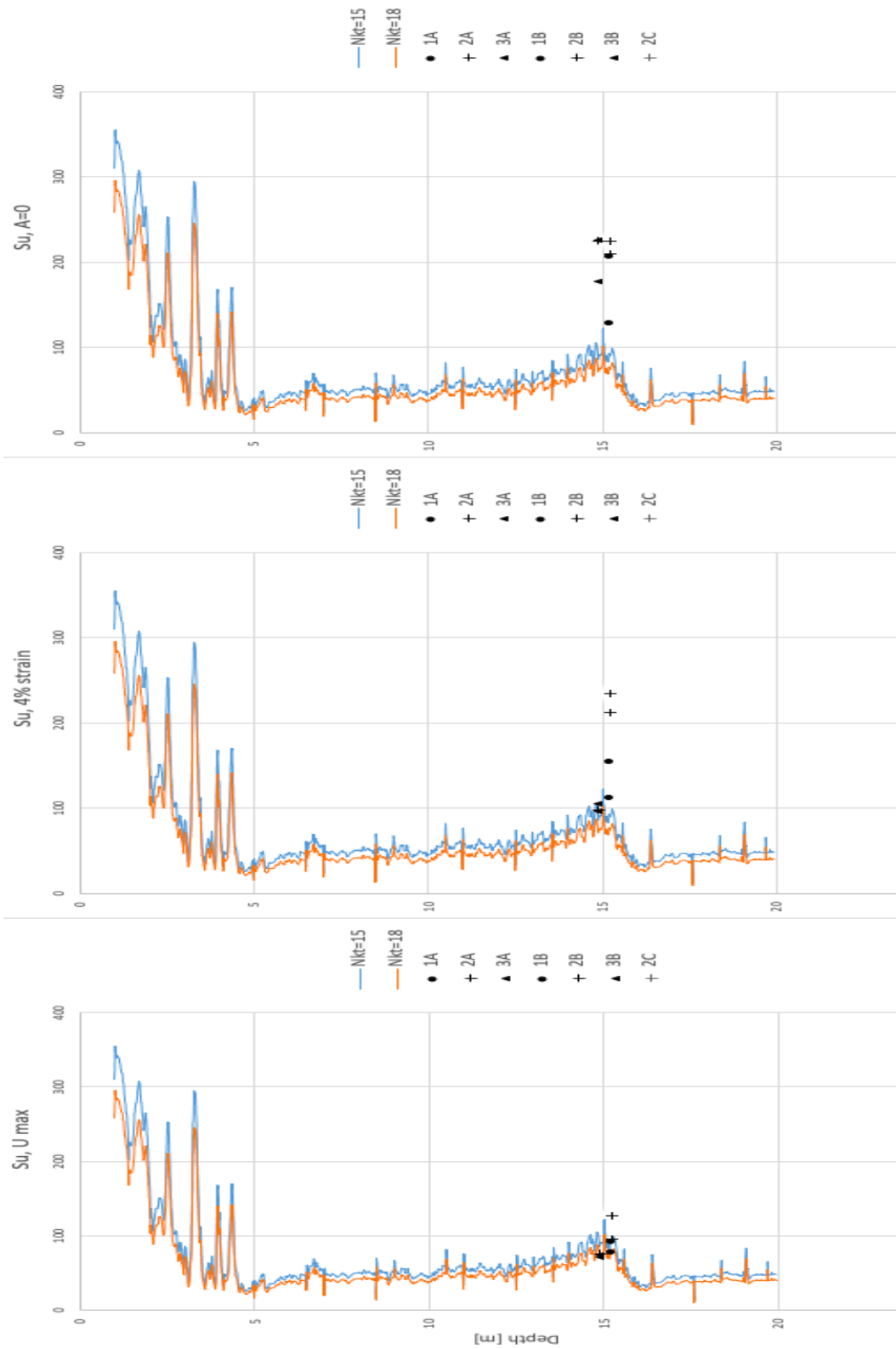
HALC13



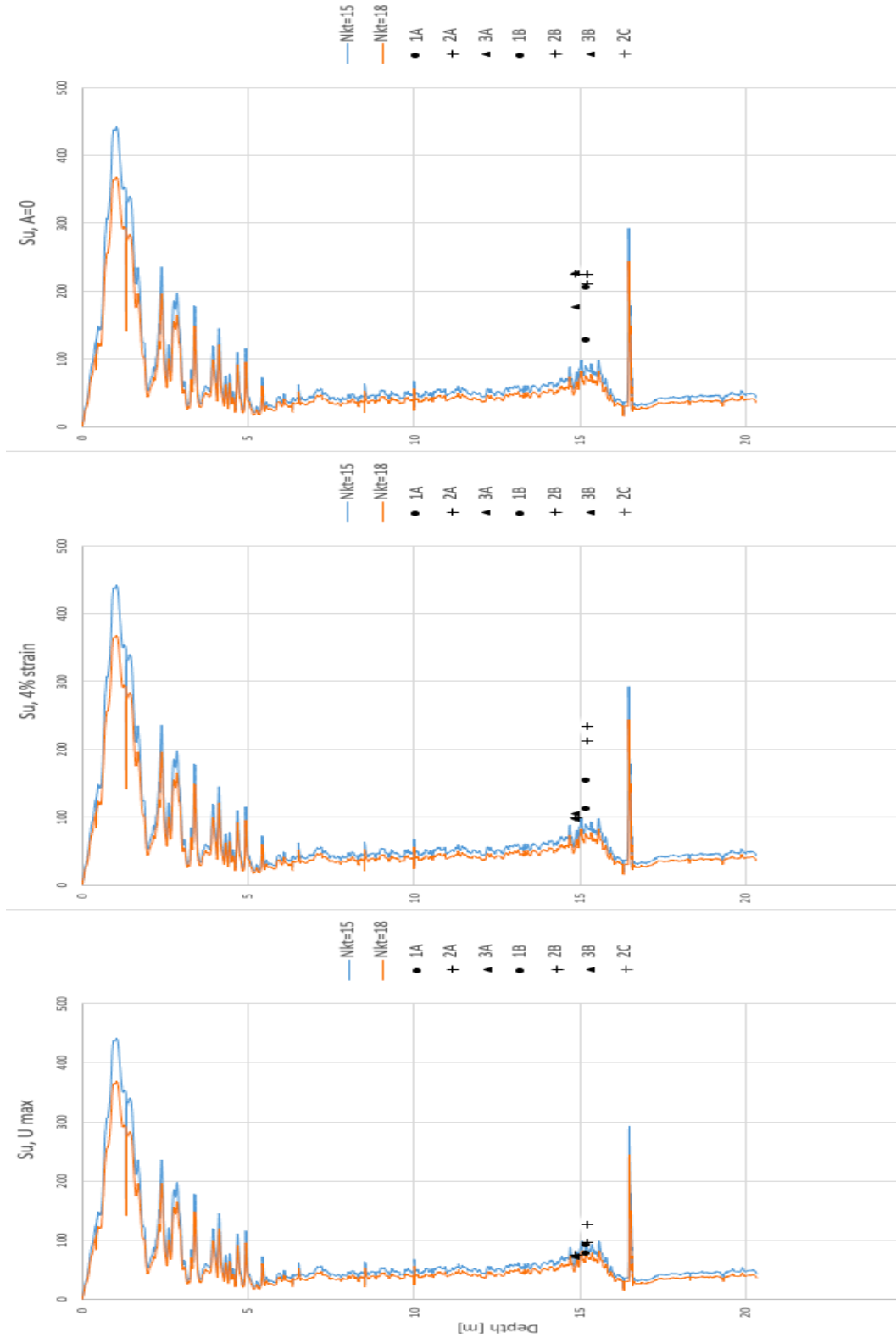
HALC14



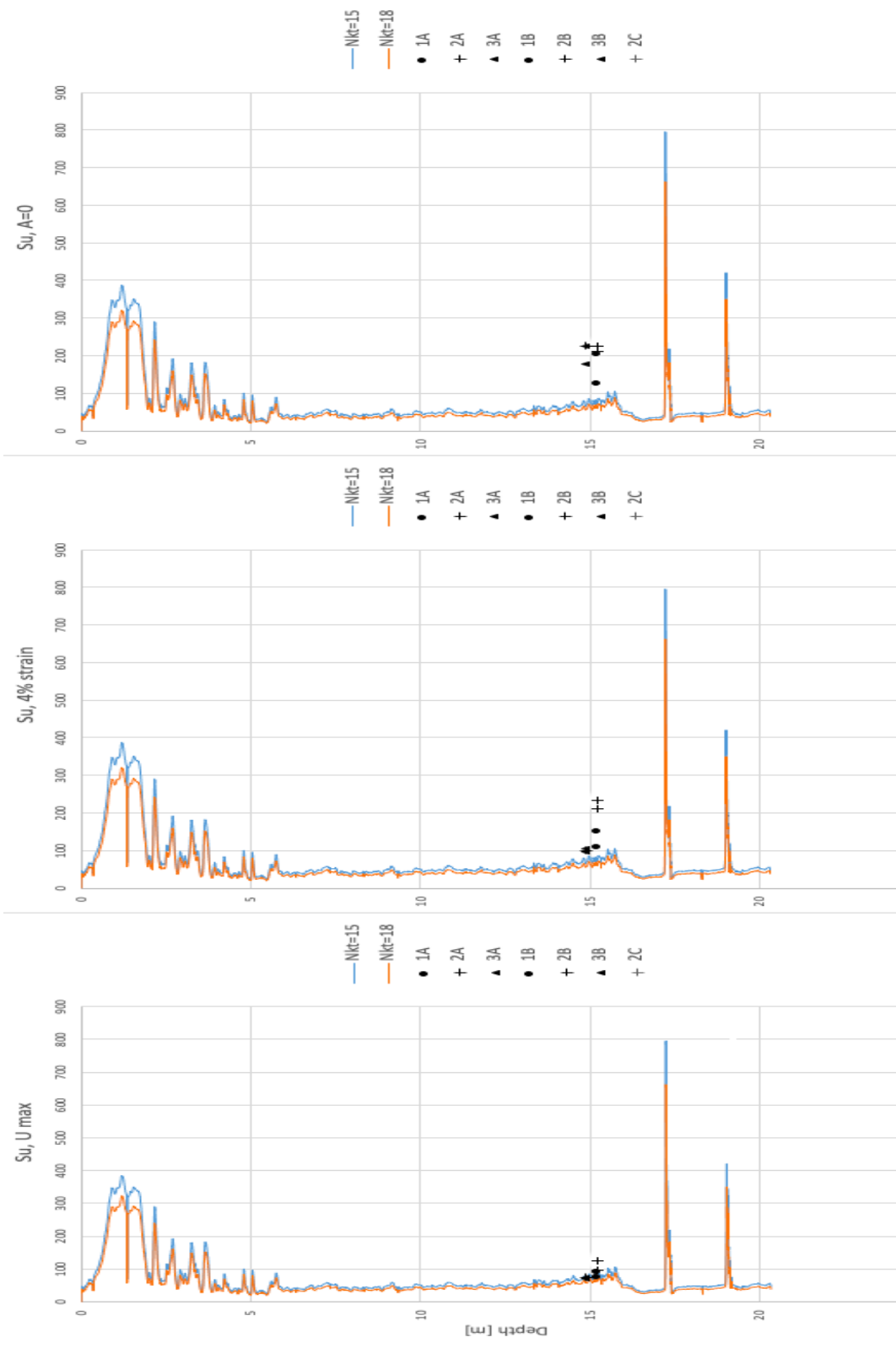
HALC17



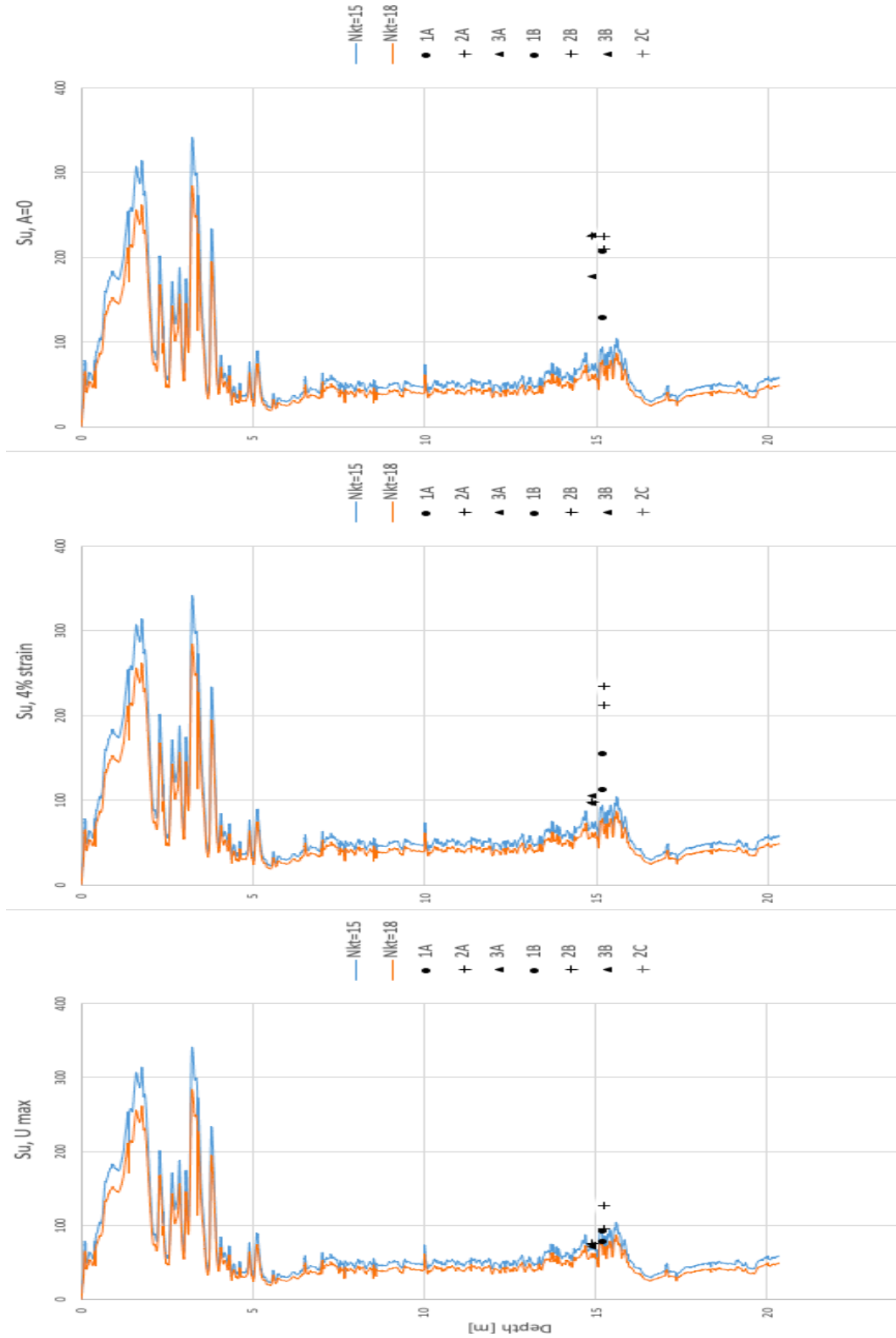
HALC18



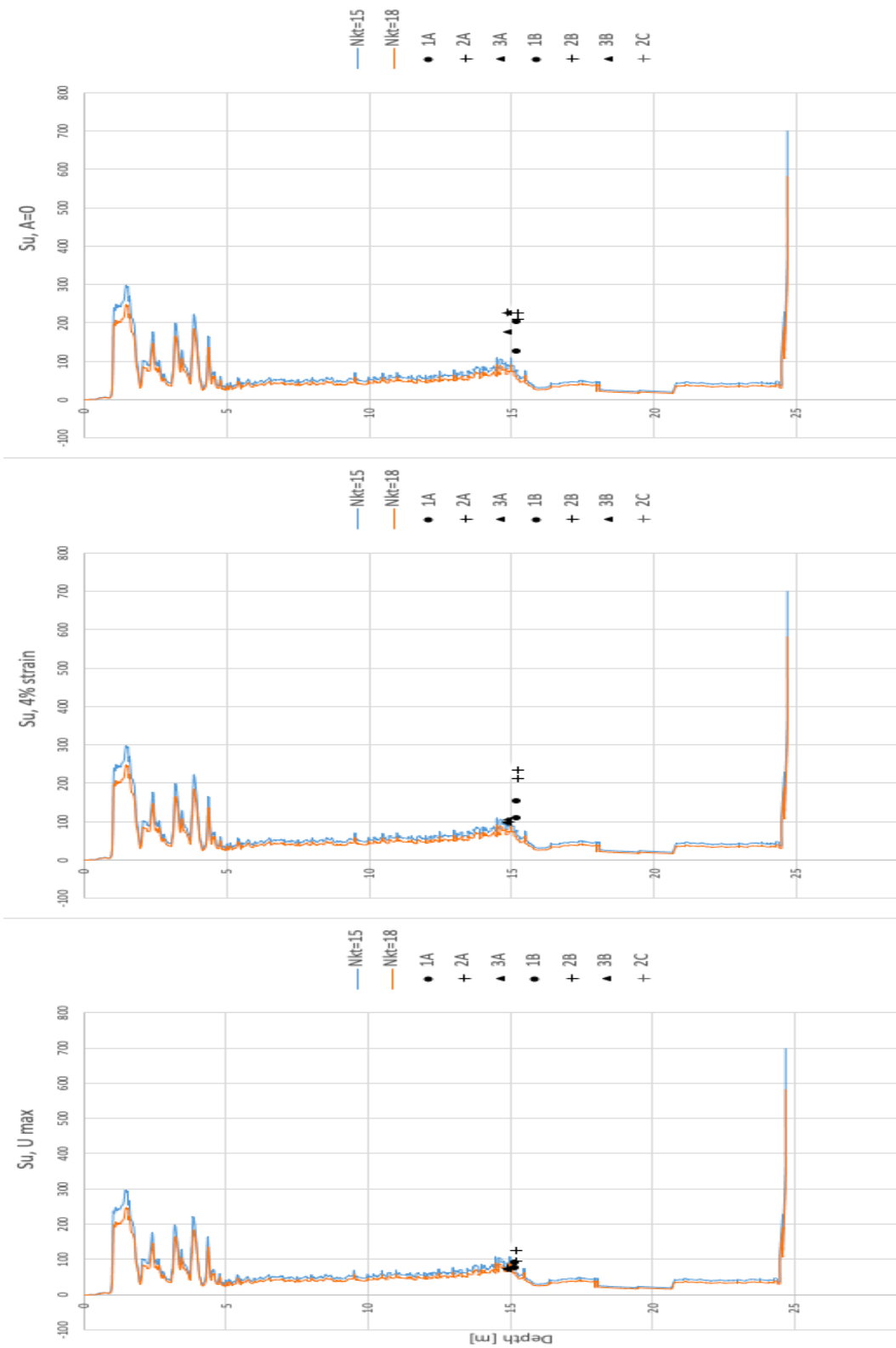
HALC19



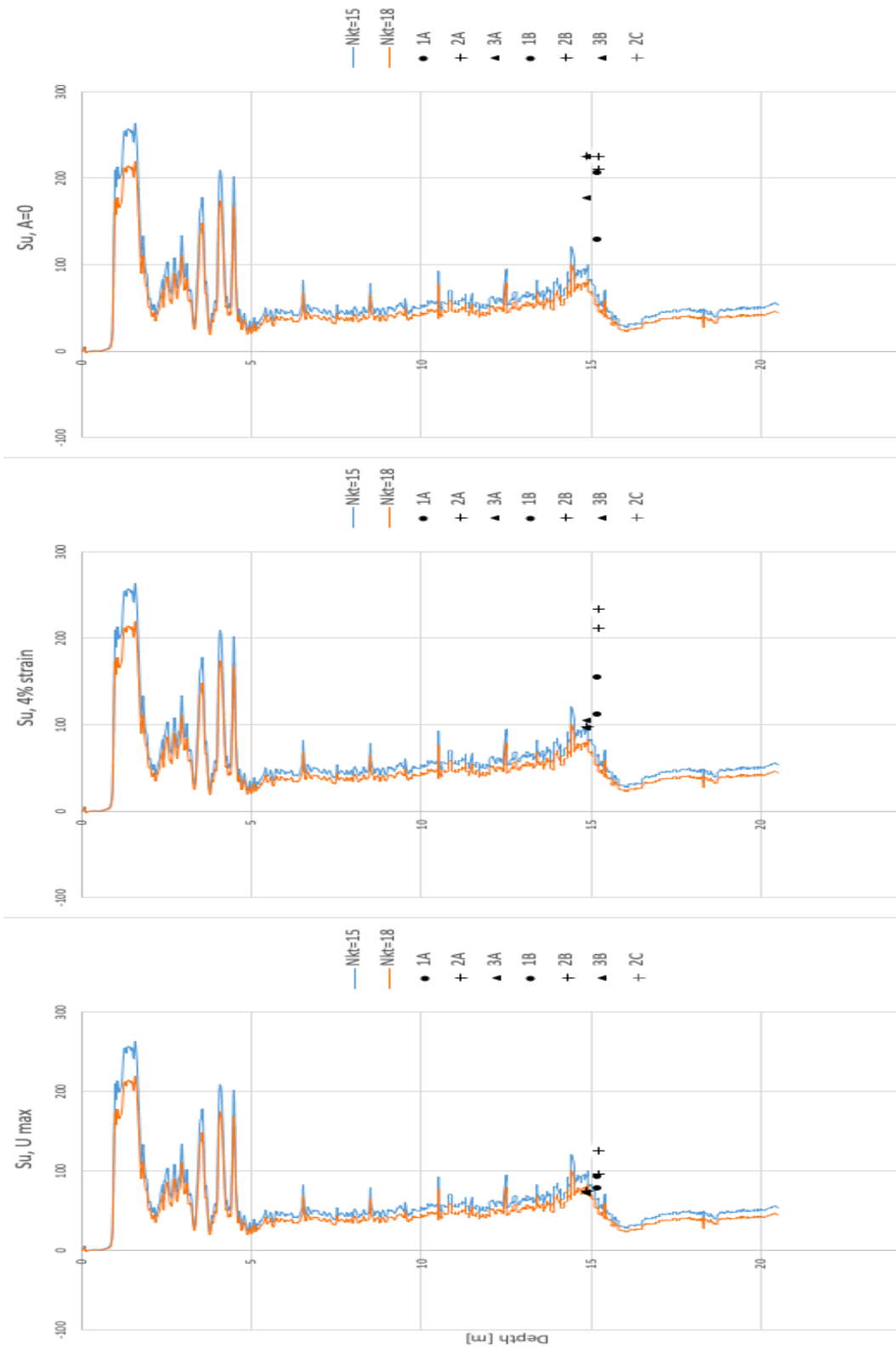
HALC20



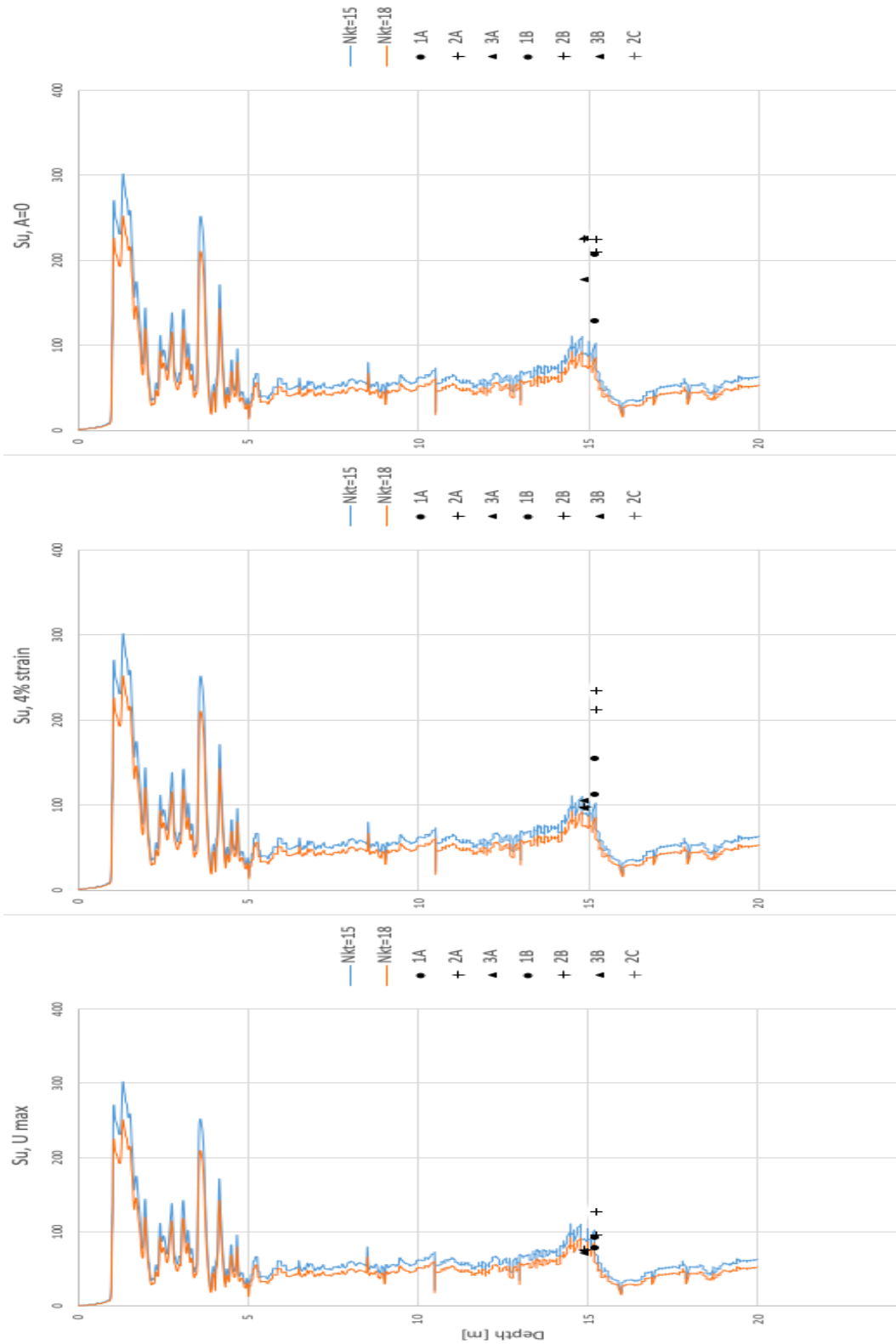
HALC21



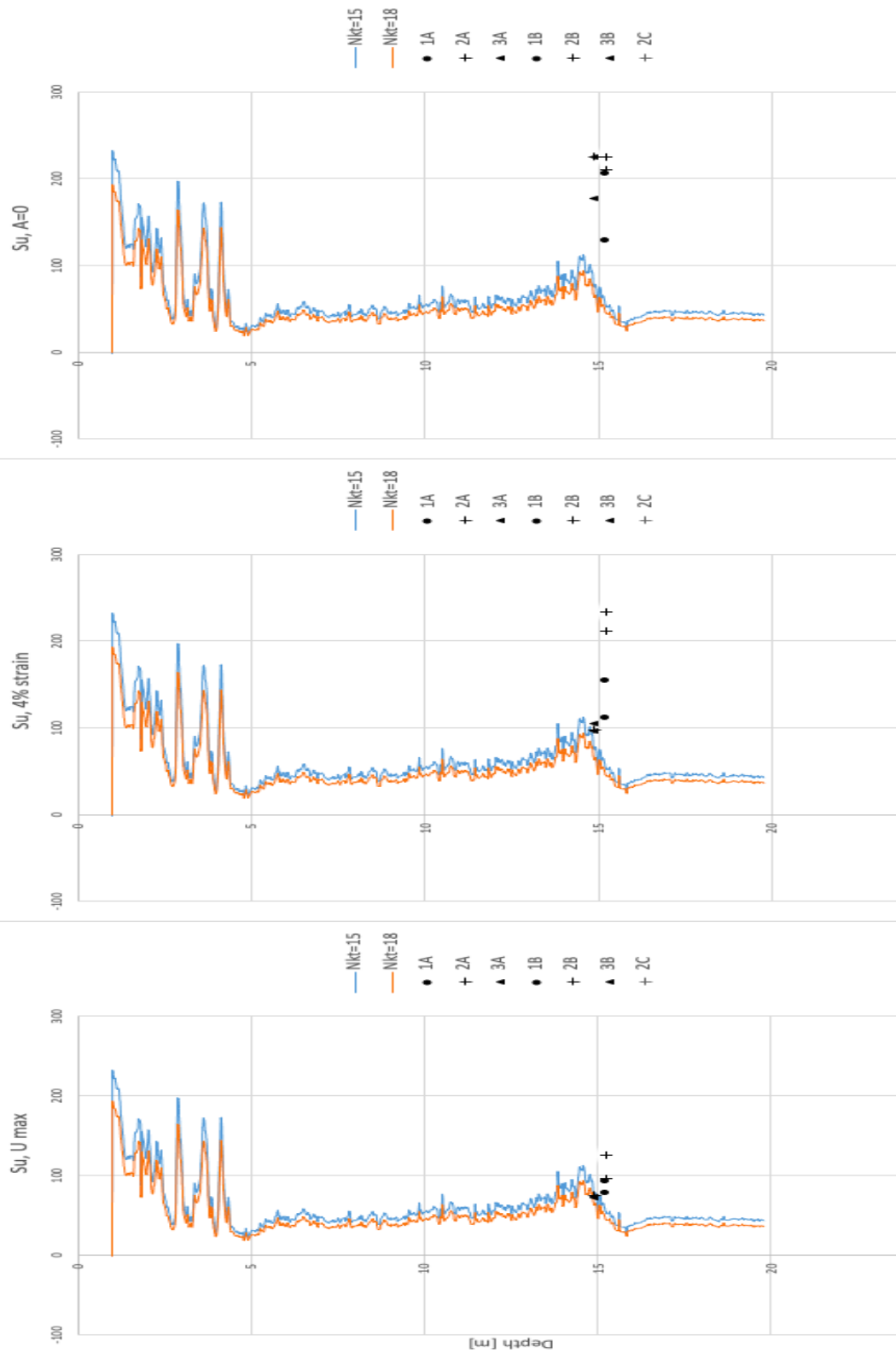
HALC22



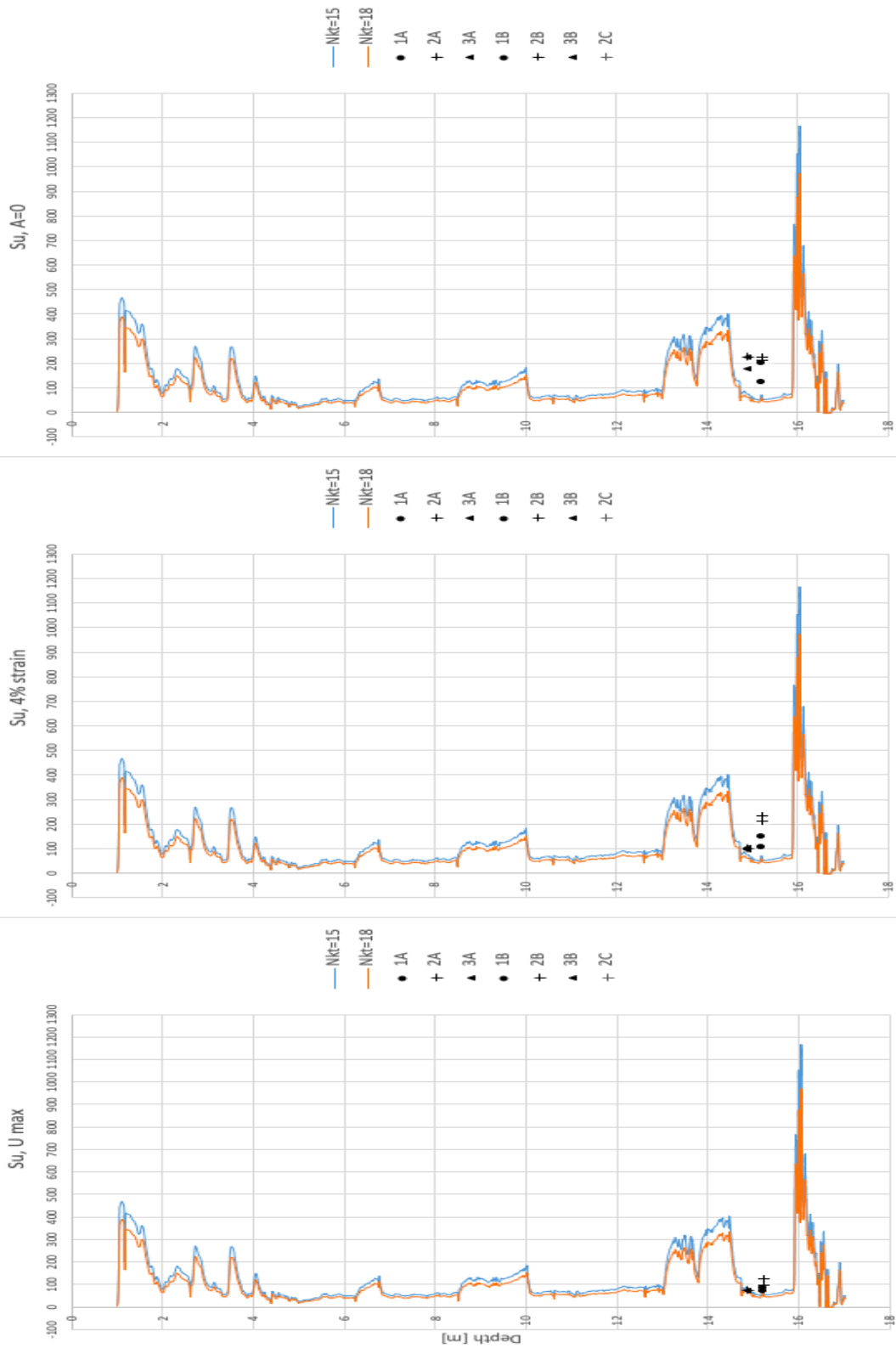
HALC23



HALC24



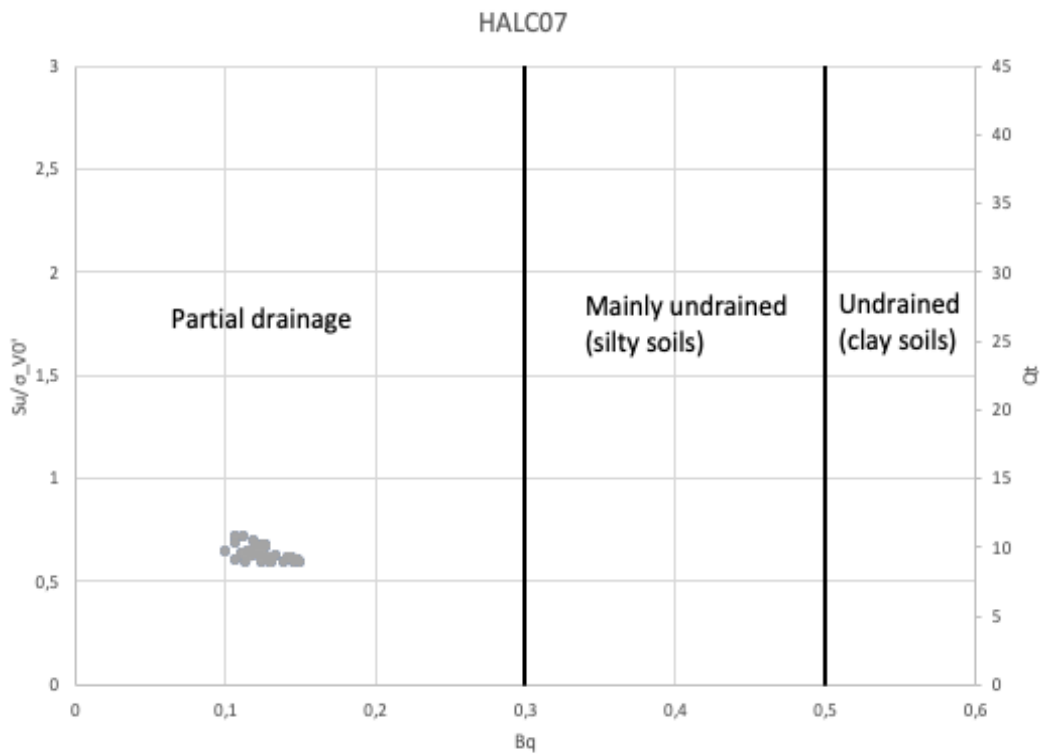
HALC25



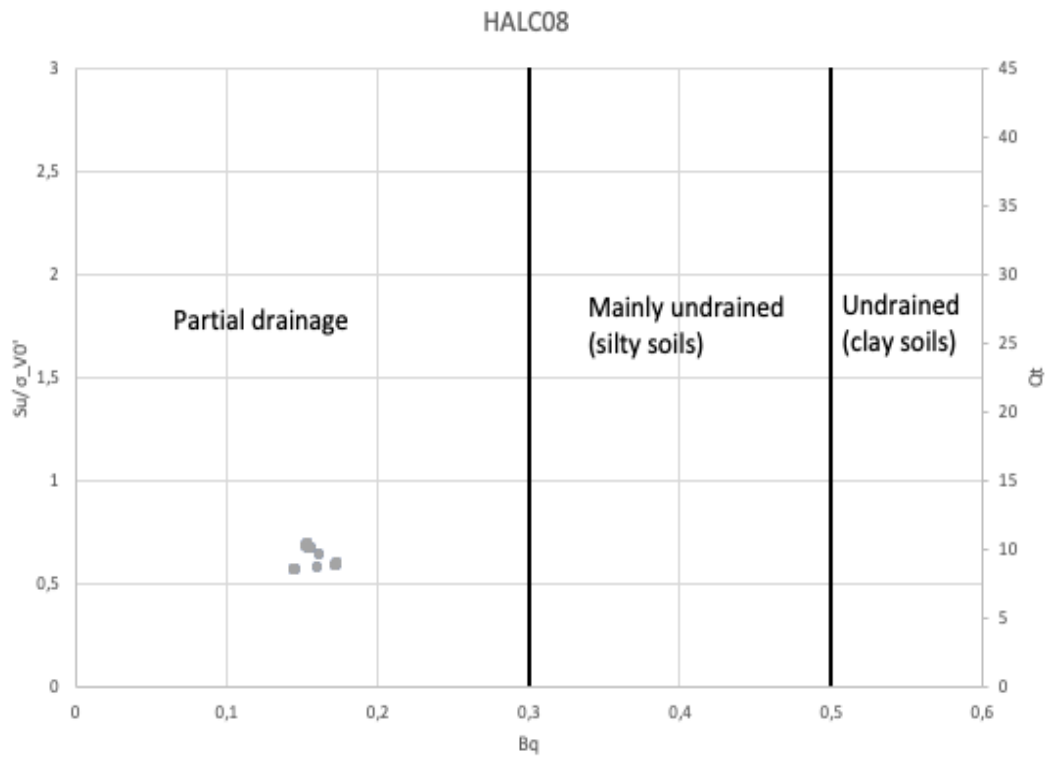
Appendix D

Drainage Conditions at Depth Interval 5.2-5.6 meters

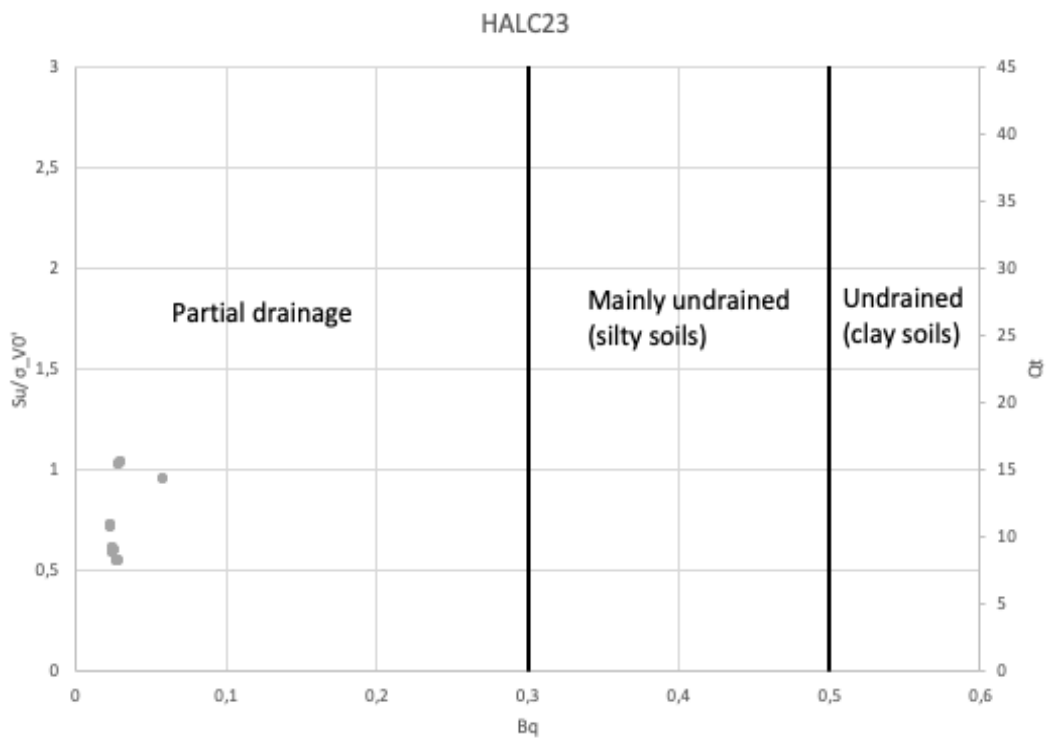
HALC07



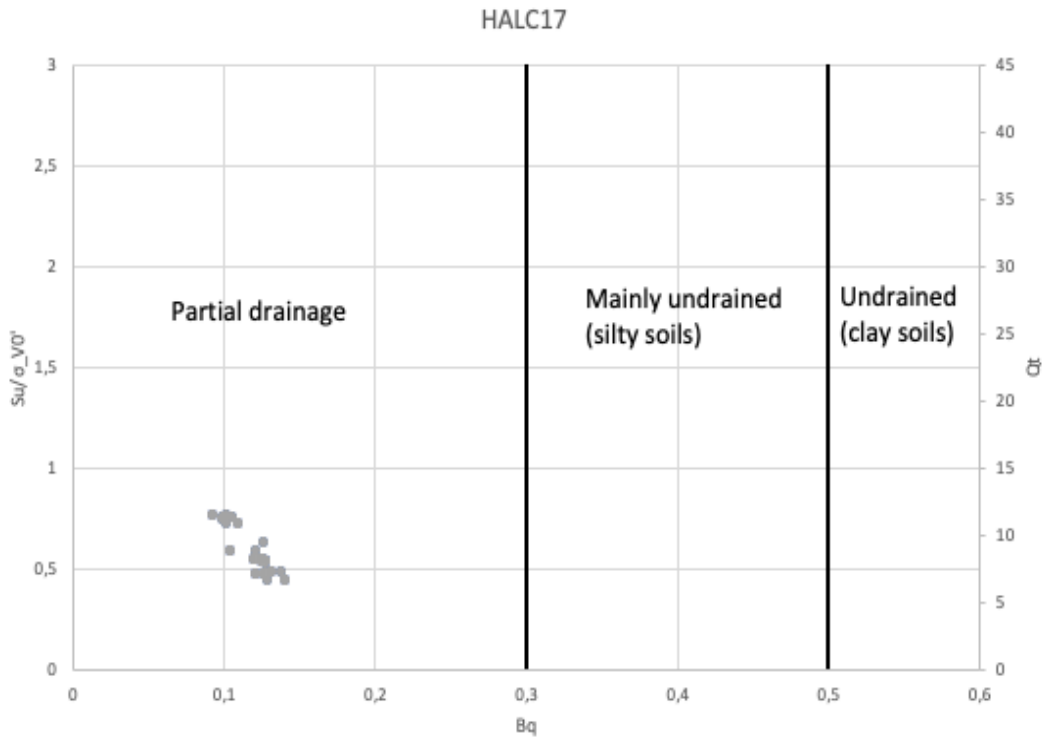
HALC08



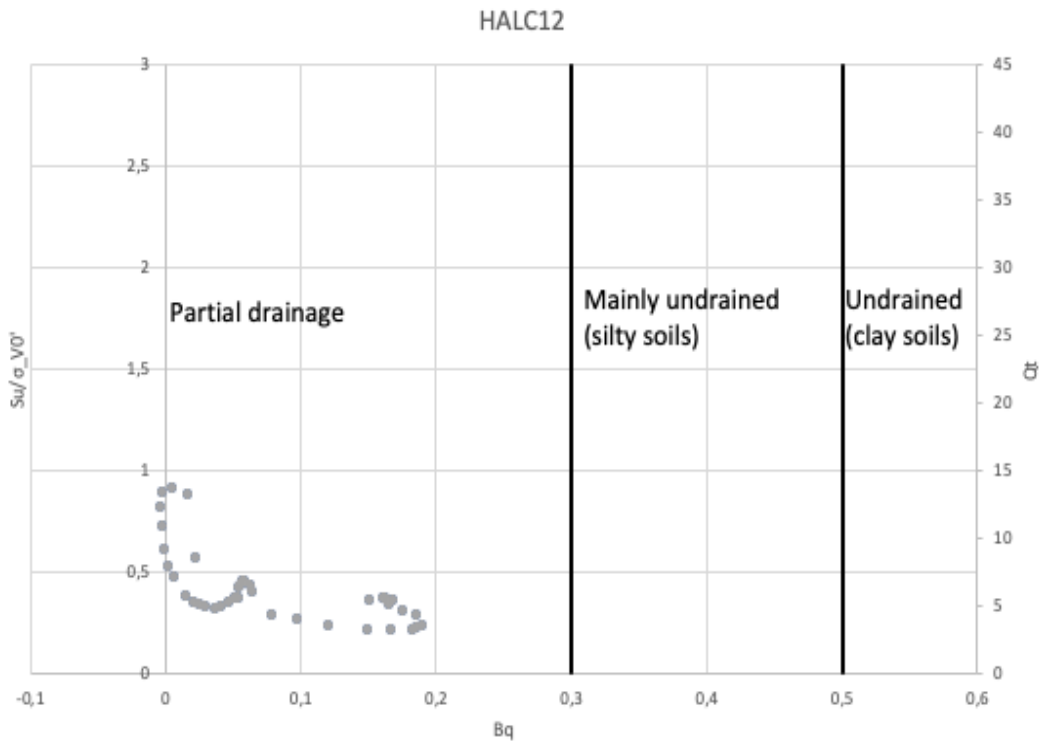
HALC23



HALC17



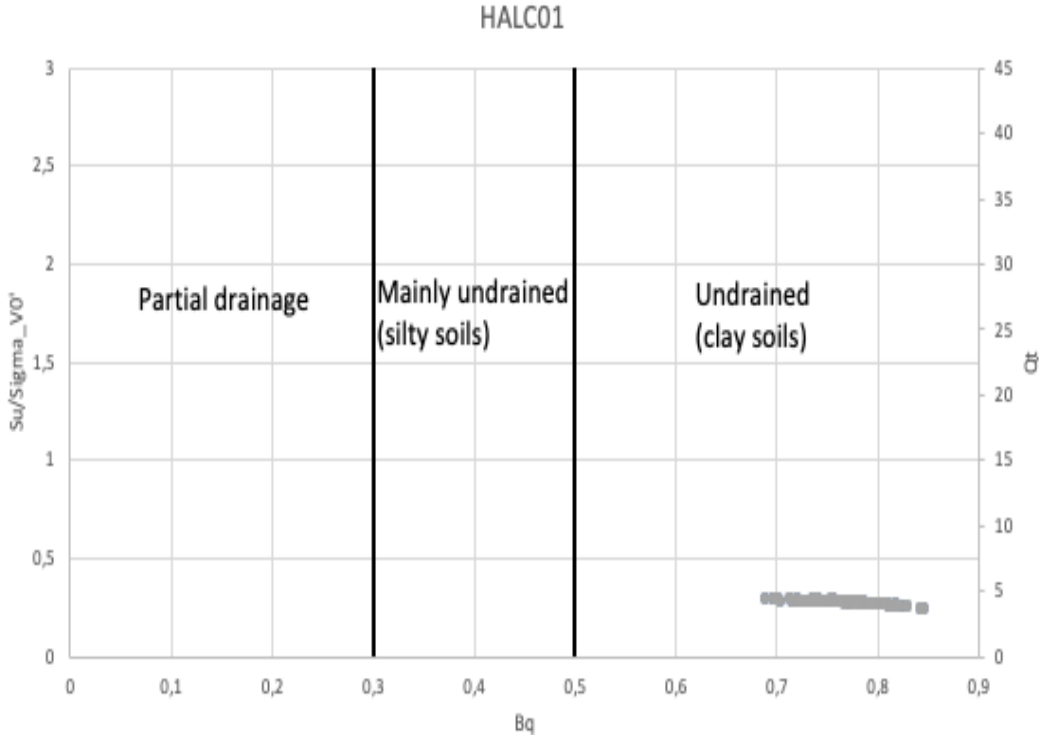
HALC12



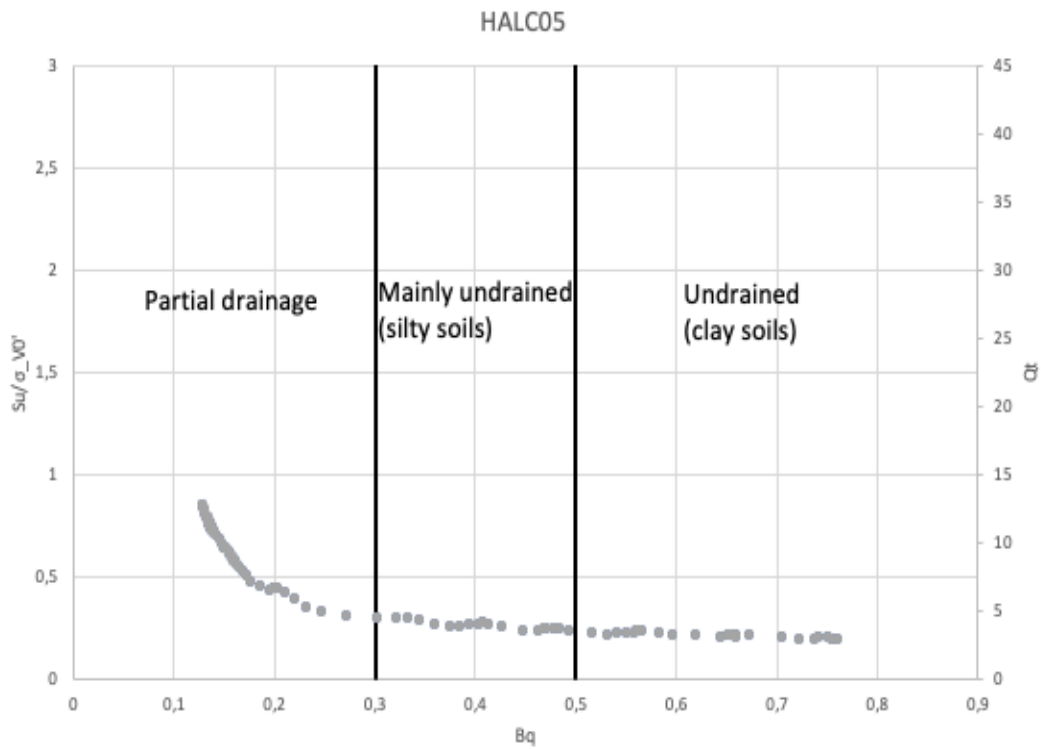
Appendix E

Drainage Conditions for Focus Interval 14.5-15.5 meters

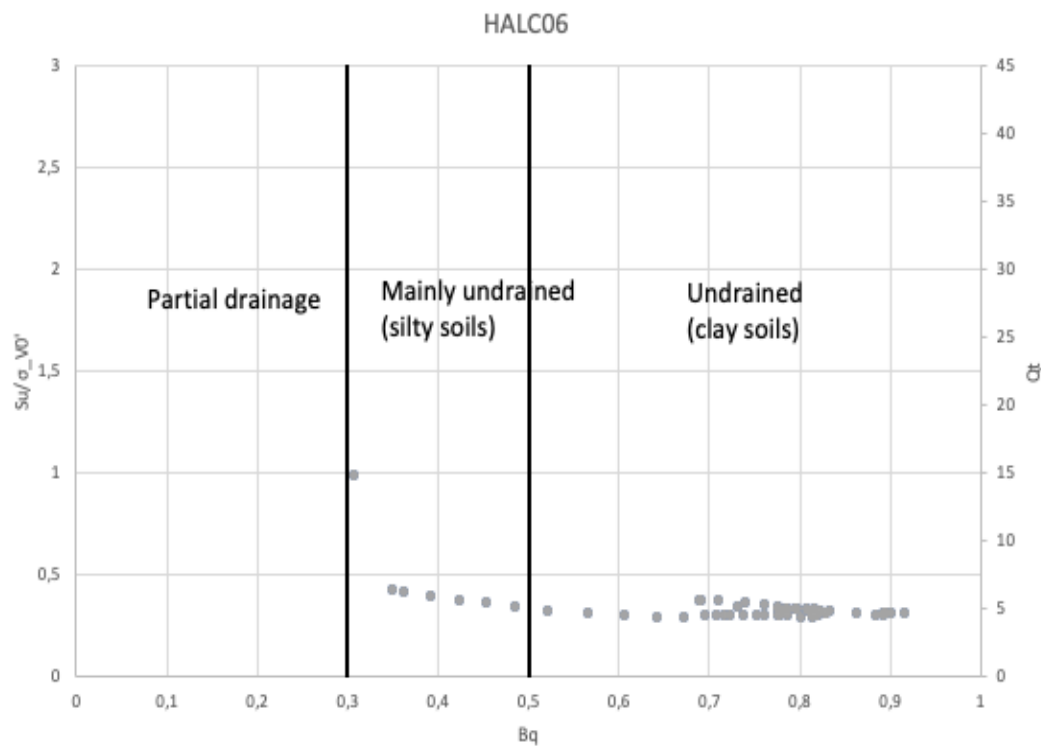
HALC01



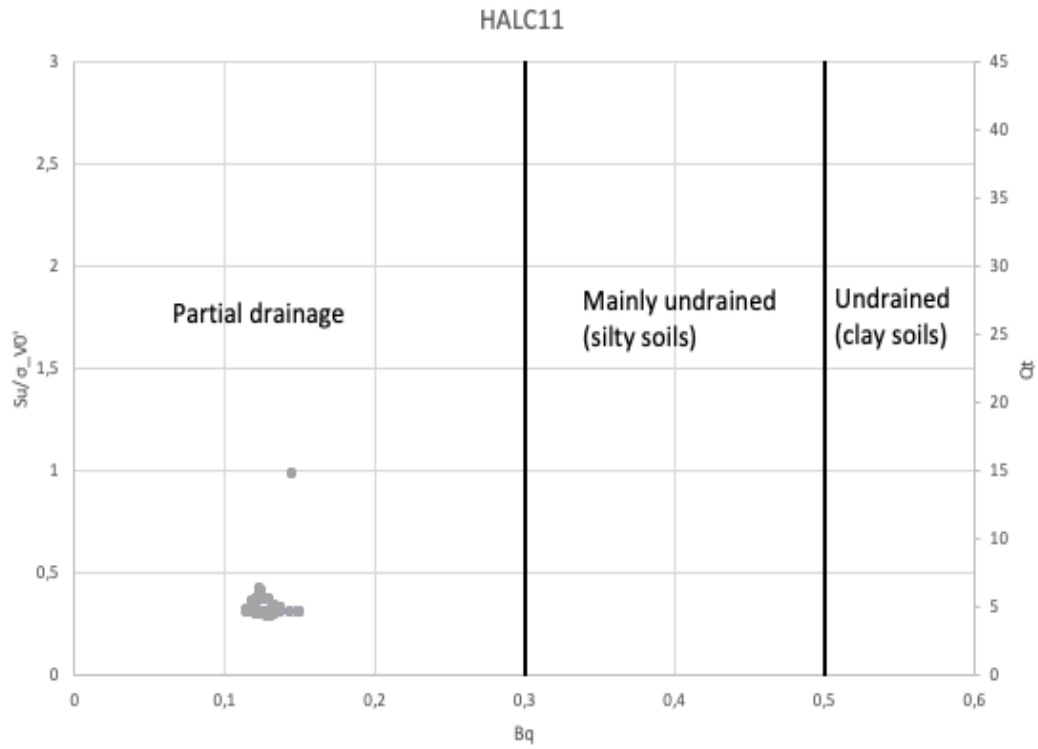
HALC05



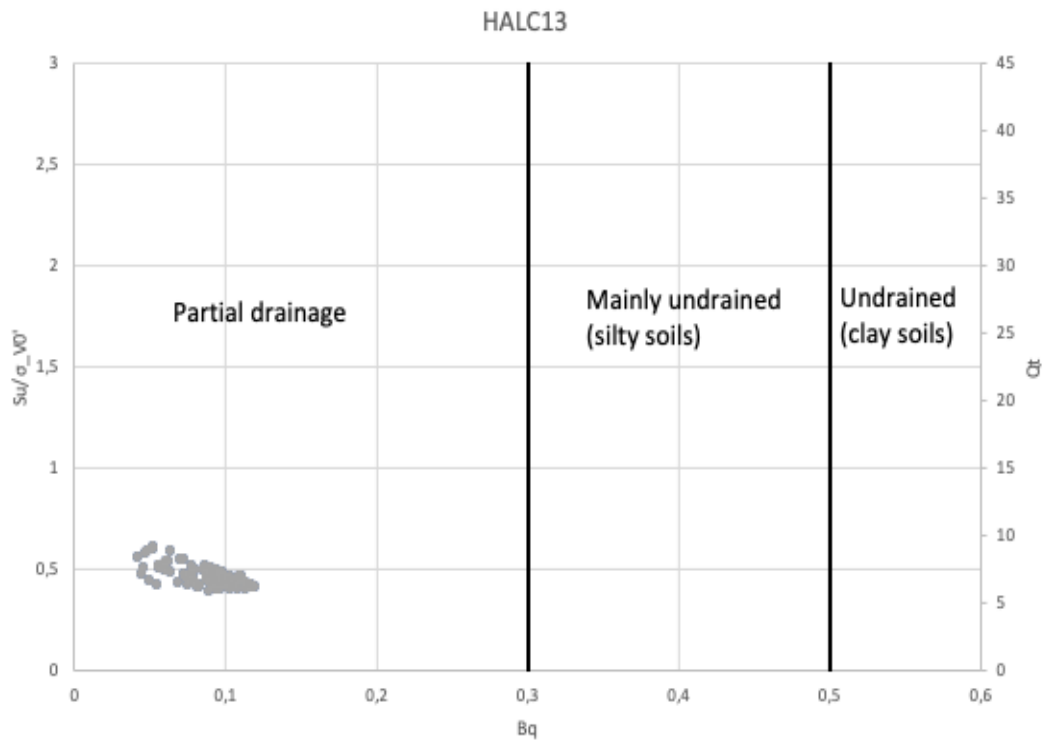
HALC06



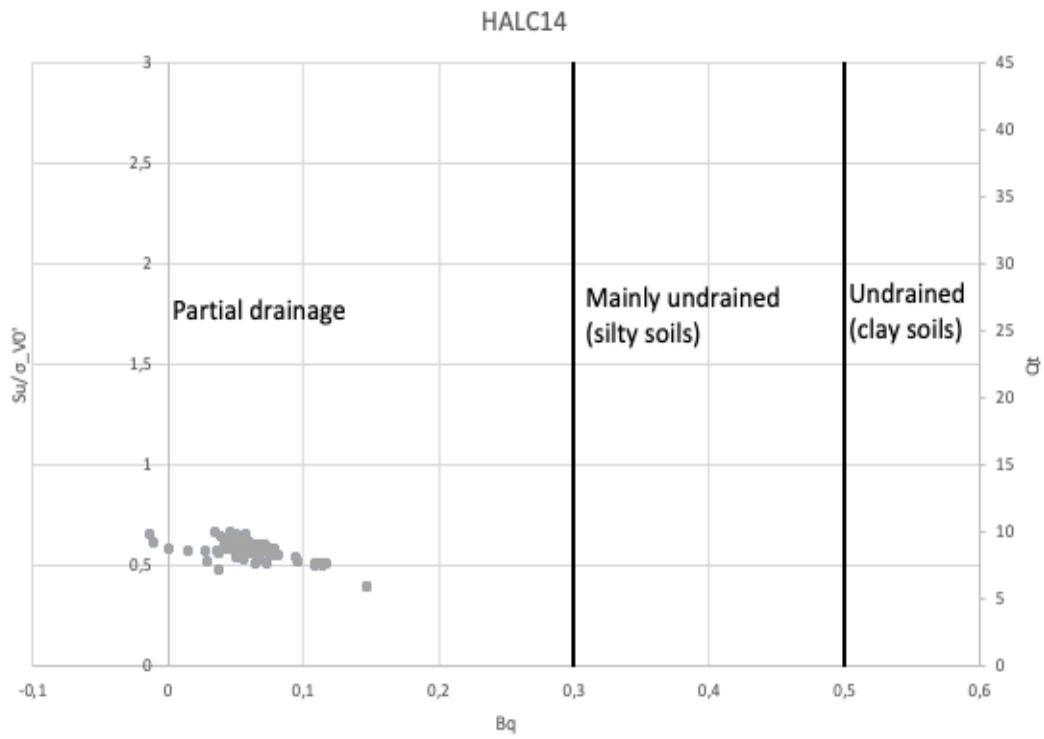
HALC11



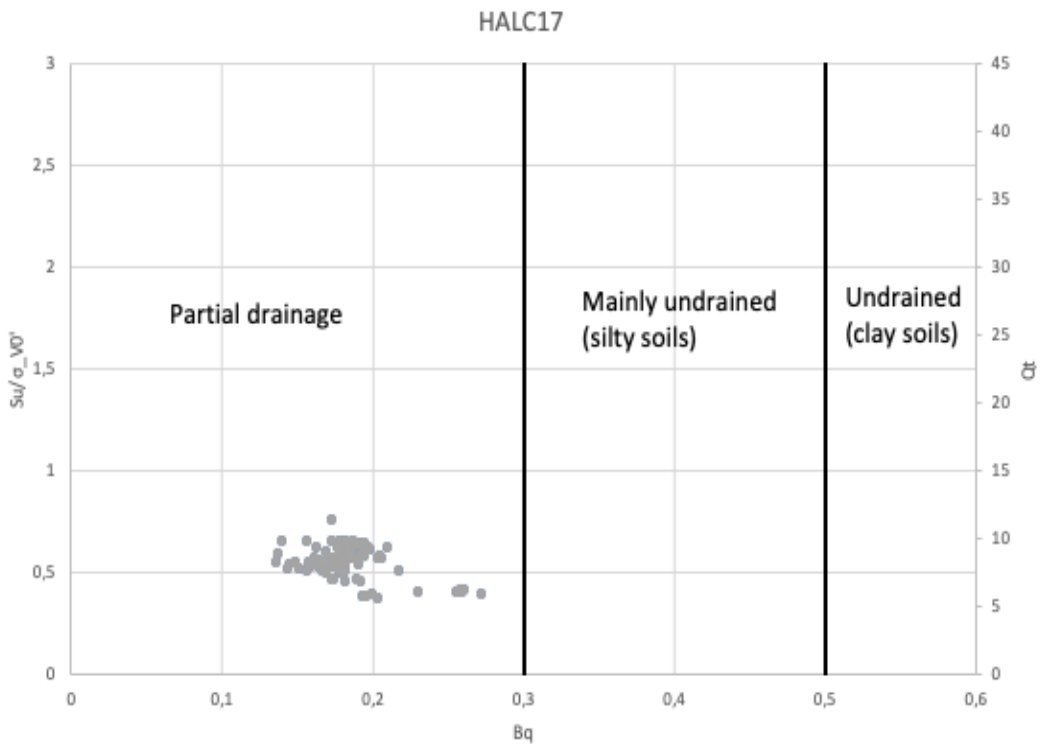
HALC13



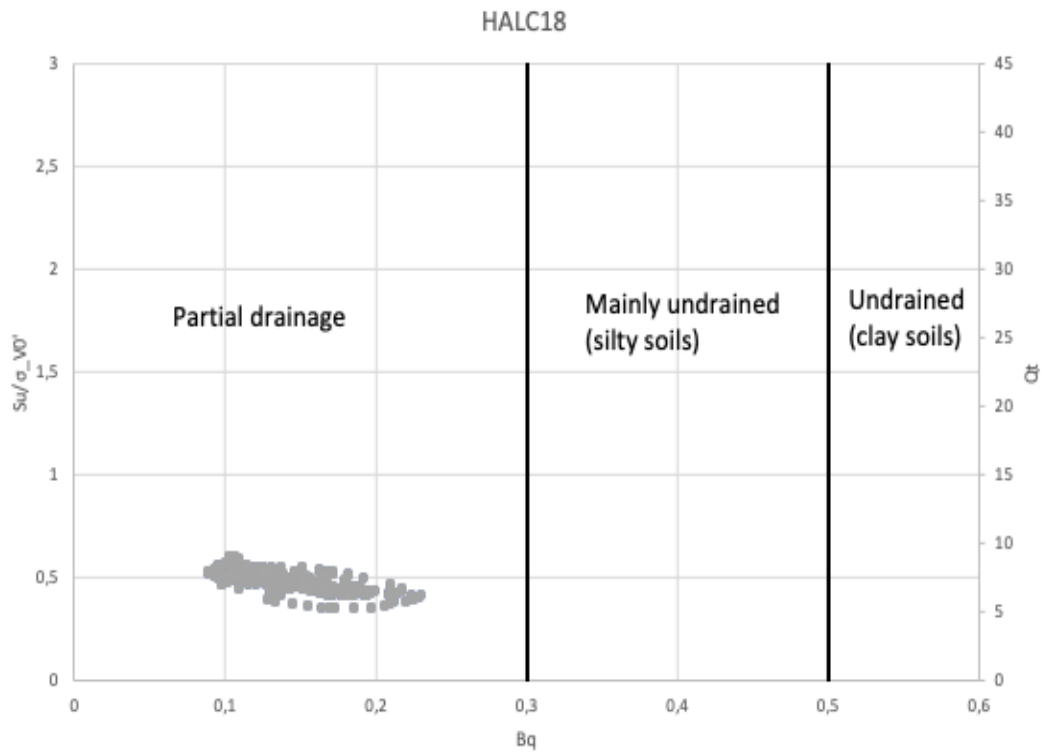
HALC14



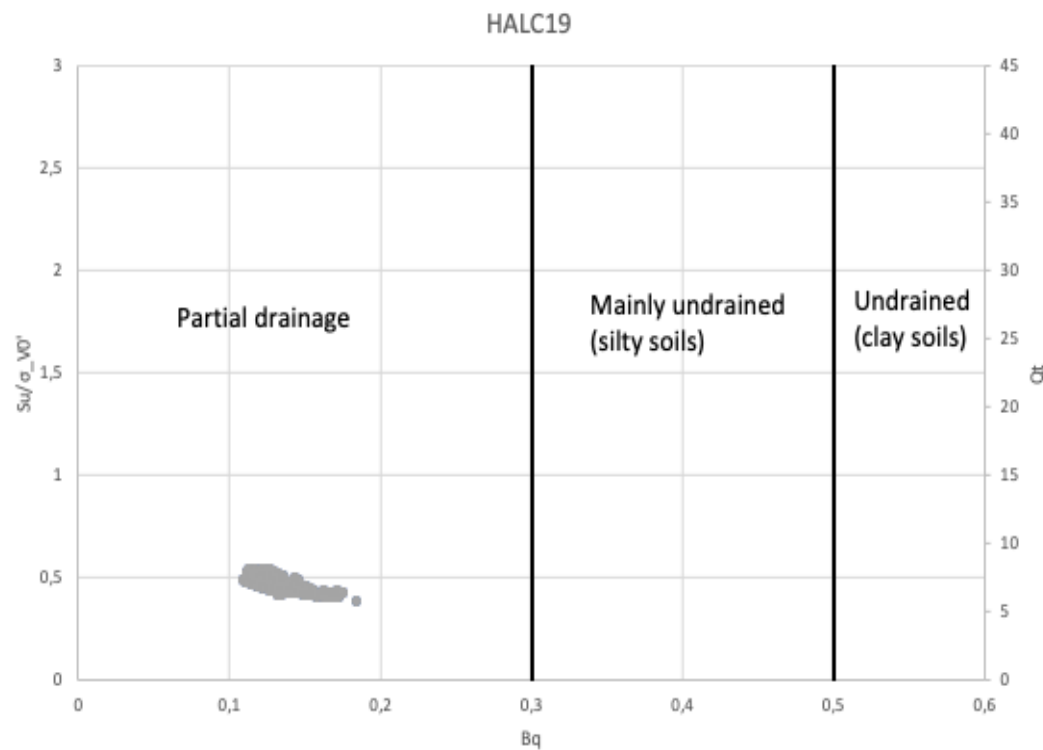
HALC17



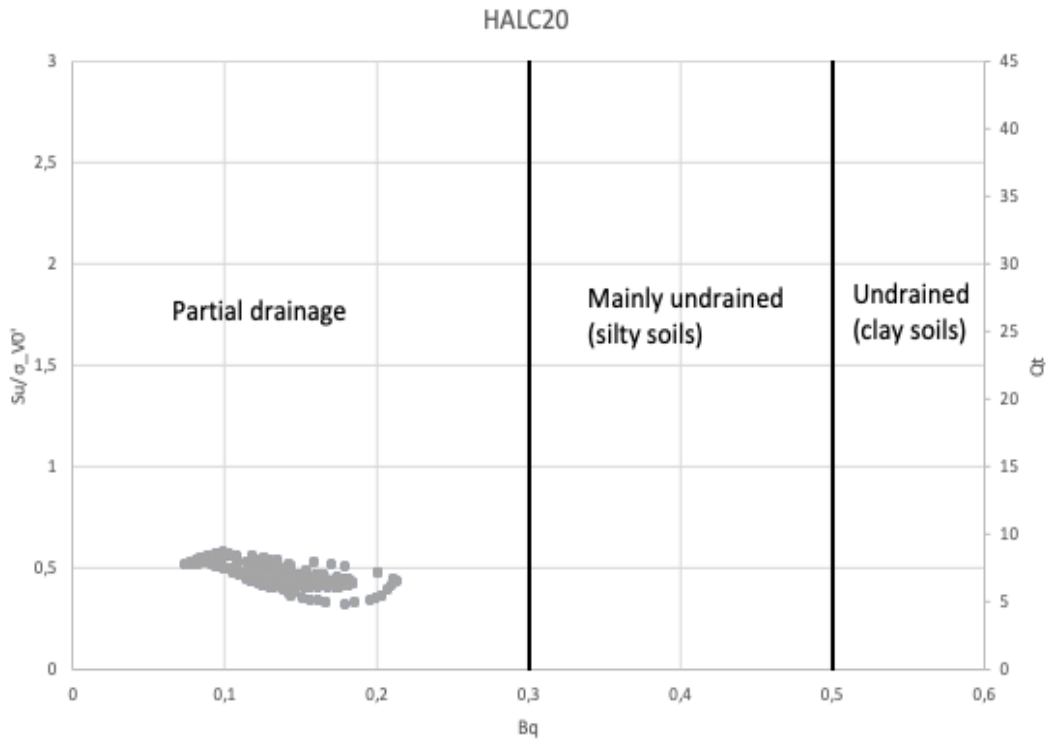
HALC18



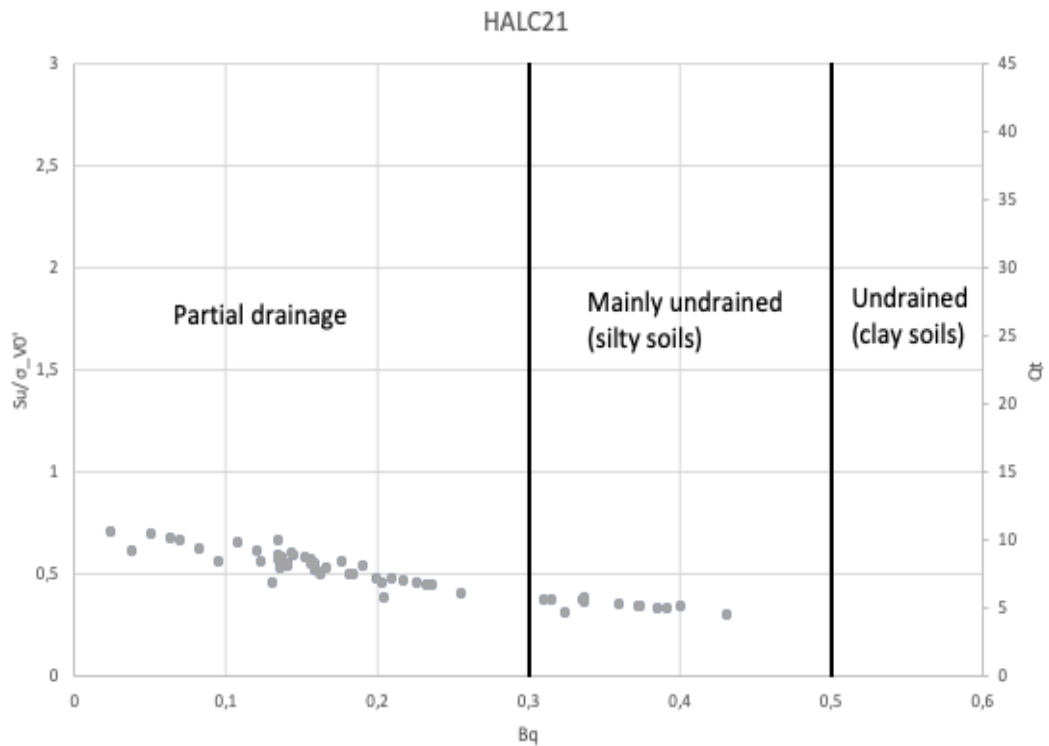
HALC19



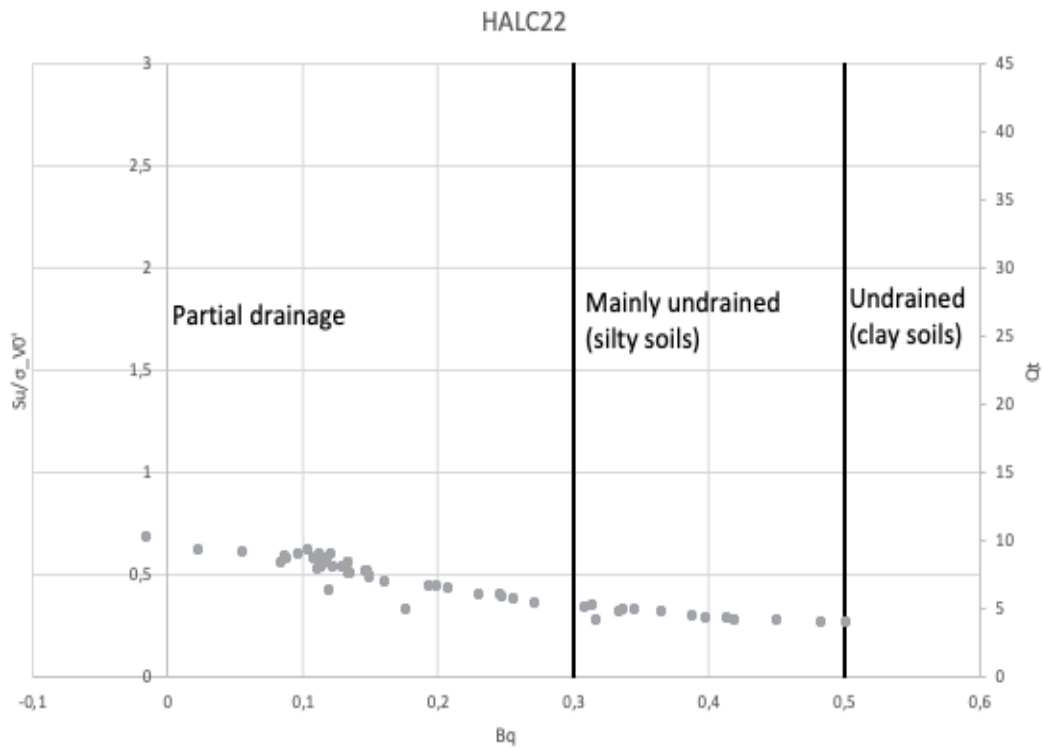
HALC20



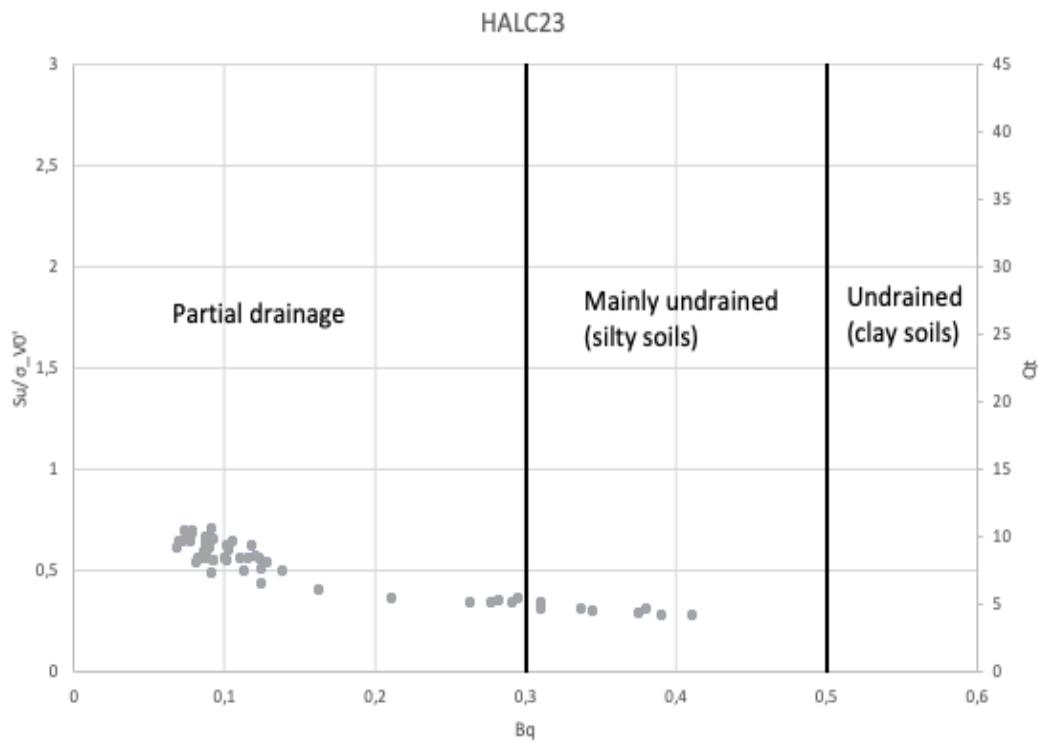
HALC21



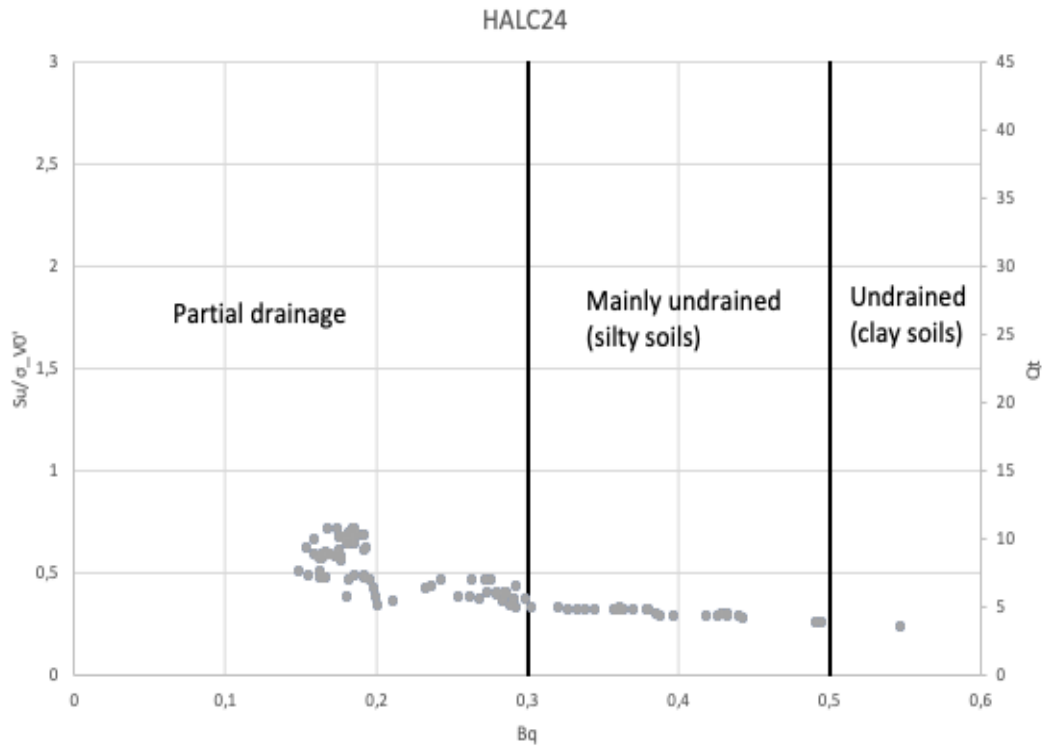
HALC22



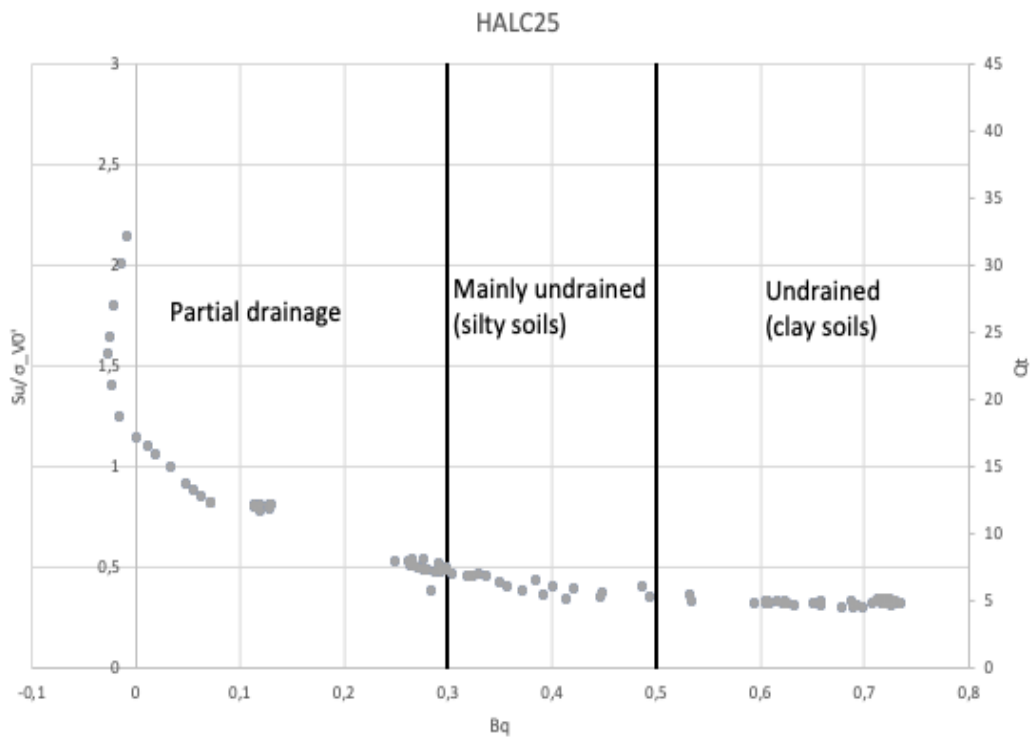
HALC23



HALC24



HALC25



Appendix F

Acronyms

CPTU, SCPT, RCPT Cone Penetration Test

SDMT Seismic flat dilatometer

CRS Constant Rate of Strain

CIUC-test Consolidated Isotropic Undrained Compression test